Univerzita Karlova v Praze
Přírodovědecká fakulta

Studijní program: Anorganická chemie

Mgr. Tomáš David

Geminální bis(fosfináty)
Geminal bis(phosphinates)

Dizertační práce

Školitel: prof. RNDr. Ivan Lukeš, CSc.

Praha, 2014

Prohlášení:

Prohlašuji, že jsem závěrečnou práci zpracoval samostatně a že jsem uvedl všechny použité informační zdroje a literaturu. Tato práce ani její podstatná část nebyla předložena k získání jiného nebo stejného akademického titulu.

V Praze, 25. 06. 2014

.....

Mgr. TOMÁŠ DAVID

(*autor*)

Table of content

1. Abstract

Slow complexation is one of the major limitations of current macrocyclic chelators utilized in nuclear medicine for complexation of metal radionuclides. This property can be improved by ligand design. Among metal radioisotopes, the copper ones (*e.g.* ^{60}Cu, ^{61}Cu, ^{62}Cu, ^{64}Cu and ^{67}Cu) have become commonly available in recent years and cyclam-derived ligands are the most suitable ligands for Cu^{2+} complexation. To alter the complexation rate, bis(phosphinic acid) group is promising unit as it is able to complex metal ions in acidic solutions. However, geminal bis(phosphinates) represent poorly studied group of compounds and, thus, it is challenging to uncover their properties.

Several *simple* amino-bis(phosphinates) were synthesized and its acid-base and coordination properties were studied. Unlike structurally similar geminal bis(phosphonates), the title compounds showed negligible adsorption onto hydroxyapatite (commonly used model of bone tissue). The obtained knowledge dealing with geminal bis(phosphinates) was utilized in synthesis of two novel cyclam derivatives. The ligands (bearing either one geminal bis(phosphinate) or one geminal phosphino-phosphonate pendant arm) were synthesized by highly efficient procedure. The corresponding Cu^{2+} complexes are formed with very high rates and show high thermodynamic stability. The results are supported by X-ray structures of complexes of both simple and macrocyclic ligands obtained at various pH.

Rare combination of simple ligand synthesis, very fast Cu^{2+} complex formation, high thermodynamic stability, extraordinary kinetic inertness and low bone tissue affinity predestinates these cyclam derivatives to be used as chelators for copper radioisotopes in nuclear medicine.

2. Abstrakt

Jedním z hlavních omezení makrocyklických ligandů aplikovaných v nukleární medicíně je pomalá rychlost komplexace kovových radionuklidů. Tento nedostatek lze ovlivnit vhodným návrhem ligandu. V poslední době se, zejména díky zvyšující se dostupnosti, studují radioizotopy mědi (^{60}Cu, ^{61}Cu, ^{62}Cu, ^{64}Cu a ^{67}Cu), pro jejichž komplexaci jsou vhodné ligandy odvozené od cyklamu. Urychlení komplexace je možné připojením vhodných pendantních ramen, jako je geminální bis(fosfinátová) skupina, jež je schopna velmi rychle komplexovat kovové ionty již při velmi nízkém pH. Tento strukturní motiv byl doposud jen velmi málo prozkoumán, je tedy výzvou odhalit vlastnosti této skupiny organofosforových sloučenin.

Bylo připraveno několik geminálních amino-bis(fosfinátů) a dále byly studovány jejich acidobazické a koordinační vlastnosti. Na rozdíl od strukturně podobných geminálních bis(fosfonátů) nevykazovaly studované sloučeniny afinitu k hydroxyapatitu, běžně používanému modelu kostní tkáně. Získané poznatky byly využity k návrhu a přípravě dvou nových makrocyklických derivátů odvozených od cyklamu. Ligandy (nesoucí jen jedno geminální bis(fosfinátové) nebo geminální fosfino-fosfonátové pendantní rameno) byly připraveny vysoce efektivním postupem. Jejich měďnaté komplexy vznikají extrémně rychle a jsou vysoce termodynamicky stabilní i kineticky inertní. Získané výsledky jsou podpořeny RTG analýzou monokrystalů měďnatých komplexů jednoduchých i makrocyklických ligandů získaných při různém pH.

Vzácná kombinace jednoduché syntézy, velmi rychlé komplexace měďnatých iontů, vysoké termodynamické stability i kinetické inertnosti komplexů, a také jejich nízké afinity ke kostní tkáni, předurčuje tyto cyklamové ligandy k aplikaci v nukleární medicíně.

3. Introduction

3.1. Preface

Nuclear medicine is an interdisciplinary field utilizing the application of radioactive substances in the diagnosis or treatment of diseases. Radionuclide-containing drugs (*i.e. radiopharmaceuticals* or *tracers*) are used routinely in nuclear medicine departments worldwide. Recent intensive development of diagnostic methods in nuclear medicine together with better understanding of molecular biology principles demand for new and more sophisticated radiopharmaceuticals. Lack of them is remarkable particularly in positron emission tomography (PET) where radiopharmaceuticals labelled with ^{18}F are predominantly used. This isotope allows only limited spectrum of application mainly due to its short half-live. The growing availability of new radionuclides (*e.g.* ^{64}Cu, ^{68}Ga and ^{86}Y) prompts to search ligands suitable for those metals applicable in PET in the future.

3.2. Diagnostic methods in nuclear medicine

The most common diagnostic method in nuclear medicine is planar scintigraphy. Activity of γ-rays from patient body is measured after application of radiopharmaceutical. The resulting 2D image is corresponding to the distribution of the radiopharmaceutical in the body. The method can be used in dynamic form as well (*i.e.* making several scans one after another) to observe changes in distribution of the radiopharmaceutical in time. Planar scintigraphy is used for diagnosis of heart, liver, thyroid or kidney diseases. A limitation of this technique is that it produces images of three-dimensional activity distribution in two-dimensional displays. This can be solved by obtaining images from different angles, but this is complicated by the complex surroundings around the organs of interest.[1]

Tomographic techniques are currently used to delineate the depth of the object of imaging. Computed tomography is based on rigorous mathematical algorithms which allow reconstruction of the 3D image from distinct focal planes (slices). There are two types of computed tomography used in nuclear medicine – single-photon emission tomography (SPECT) and PET which differs in the source of ionizing radiation and detection. Radiopharmaceuticals used in SPECT are based on γ-emitting radionuclides (such as ^{99m}Tc, ^{123}I, ^{67}Ga, ^{111}In), while those used in PET are based on β^+-emitting radionuclides (such as ^{11}C, ^{13}N, ^{15}O, ^{18}F, ^{82}Rb).[1]

3.3. PET

The PET uses neutron deficient radionuclides emitting positron particles (β^+) during radioactive decay. Those particles quickly loose its kinetic energy by interaction with surroundings and travel distance up to several millimetres in the patient's body (depending on used

radionuclide). Positron can then form a metastable positronium atom with electron from the surroundings, which undergoes rapid annihilation within picoseconds. Two γ-photons (with energy 511 keV) are created by this process and they travel in almost opposite direction (180 ± 0.5 °) from each other. These pairs of coincident γ-photons can be detected by system of γ-cameras localized around the patient. The data collected over many angles around the body axis of patient are then used to reconstruct the 3D image of the activity distribution in the organs of interest.[2]

PET is powerful imaging technique – it is being used for initial diagnosis, assessing disease extension and prognosis, planning and monitoring treatment and detecting recurrent disease. In this respect, [^{18}F]fluoro-2-deoxy-D-glucose (^{18}**FDG**) is by far the most commonly used PET agent.[3] The examination with ^{18}**FDG** is based on the preferential uptake of the radiopharmaceutical by tumors, which frequently have a high glucose metabolic activity.[4] Isotope ^{18}F has nearly ideal properties for PET – suitable half-life ($t_{½}$ = 110 min), low energy of emitted β^+ particles (635 keV, 97 % abundance) and lack of side emissions. Peptides and other small molecules (*i.e.* ^{18}**FDG**) are good carriers of ^{18}F isotope since they rapidly enter the extracellular space from blood and then they are quickly excluded from the body. Preparation of such conjugates is, however, often lengthy procedure (in contrast with the short half-life) with the total time for preparation of radiopharmaceutical ranging between 1 – 3 h.[5] Moreover, production of ^{18}F in cyclotrons is considered as a very expensive.[6] There are two possible approaches how to deal with these obstacles – searching for more effective ways of radiolabeling with ^{18}F or endeavour of utilizing other suitable isotopes to clinical praxis.

3.4. Metal radioisotopes

Recently, there is a considerable interest in non-traditional metal radioisotopes, mainly due to their increased production and availability. Among others (^{94m}Tc, ^{66}Ga, ^{68}Ga, ^{86}Y), various radioisotopes of copper (^{60}Cu, ^{61}Cu, ^{62}Cu, ^{64}Cu and ^{67}Cu) with different properties are predetermined for use in nuclear medicine.[7] The use of metal nuclides, in general, brings one advantage over covalently bound conjugates with traditionally used radioisotopes (such as ^{18}F). In this case, suitable ligand for the metal radionuclide plays role of the carrier and the radiolabelling process is, therefore, one-step formation of a complex. Unlike most of the organic reactions, coordination reactions are usually fast which can eventually lead to minimizing of the undesired loss of activity during radiopharmaceutical preparation.

Radionuclide ^{64}Cu is an attractive radiometal for use in several areas of nuclear medicine. It has suitable half-life ($t_{½}$ = 12.7 h) for both short-term and long-term examinations and possesses two beneficial decay modes (β^+ and β^-). On one hand, the β^+ decay mode (656 keV, 17.8 % abundance) can provide high-quality PET images and, at the same time, relatively low dose to patients and radiochemistry personnel. On the other hand, the β^- decay mode (573 keV, 39.6 % abundance) makes it potential candidate for therapy. Therefore, ^{64}Cu holds admirable

promise for combination of both diagnosis and therapy.[8] Production of ^{64}Cu can be effectively done by both reactor- and accelerator-based methods. The high-specific activity ^{64}Cu can be prepared in reactor by ^{64}Zn(n,p)^{64}Cu reaction.[9] Recently, production of no-carrier-added ^{64}Cu utilizing ^{64}Ni(p,n)^{64}Cu reaction in cyclotron has been well-estabilished.[10],[11]

The role of a ligand as a carrier for metal radioisotopes is accompanied with several requirements. On one hand, the ligand has to form thermodynamically stable and kinetically inert complexes with the isotope of interest. This slows down dissociation of the complex and subsequent undesired non-specific deposition of free metal ions in the tissue. For *in vivo* application, it turns out that the kinetic inertness is perhaps more relevant than the thermodynamic stability. On the other hand, the ligand should also complex the metal ion as fast as possible (for above mentioned reasons) and as selectively as possible. Furthermore, the complex has to be resistant to *in vivo* transmetalation (*i.e.* exchange of metal ions in the complex) and to *in vivo* transchelatation (*i.e.* exchange of ligands). These properties are important factors when evaluating the possible radiopharmaceutical application and they are determined mainly by the structure of the ligand. Moreover, the ligand usually has to carry targeting groups, which would cause specific uptake of the complex in areas of interest.[12] This can be achieved by attachement of suitable molecular fragments (*i.e.* antibodies, proteins, functional groups) to the ligand.

To fulfil all above mentioned conditions, an intimate interplay of both metal coordination chemistry and ligand design is required. Polydentate ligands currently used in nuclear medicine can be divided into two groups – acyclic (or *open-chain*) ligands and macrocyclic ligands. Complexes with acyclic ligands (structures of two representatives, H_4**EDTA** and H_5**DTPA** are depicted on **Figure 1**) usually possess sufficient thermodynamic stability and the complexes are mostly formed fast, but their huge downside is lack of *in vivo* stability (such complexes are vulnerable to *in vivo* transchelatation).

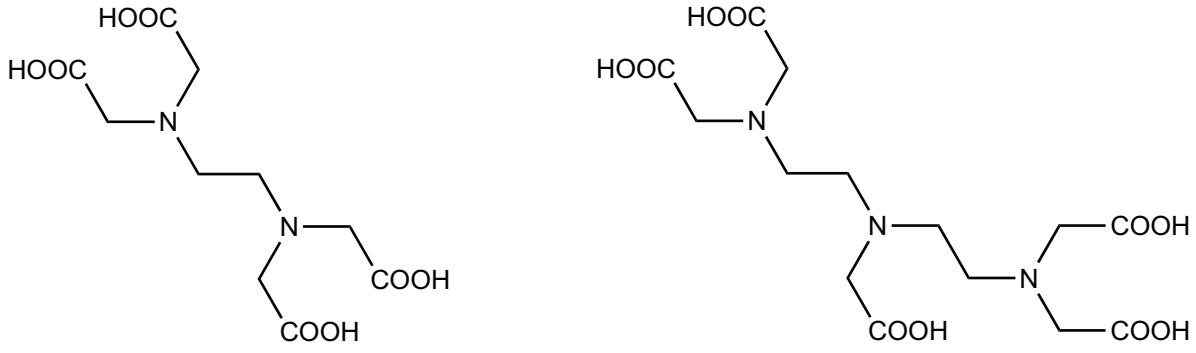

H_4**EDTA** H_5**DTPA**

Figure 1. Two examples of polydentate acyclic ligands – H_4**EDTA** and H_5**DTPA**.

As opposed, complexes with macrocyclic ligands (structures of two picked representatives, **Cyclam** and H_4**TETA**, are depicted on **Figure 2**) possess high *in vivo* stability as the result of combined very high thermodynamic stability and sufficient kinetic inertness. But while the complexes are hard to destroy once formed, the drawback is that their formation is often sluggish. Nevertheless, the use of acyclic ligands in various fields of medicine has been

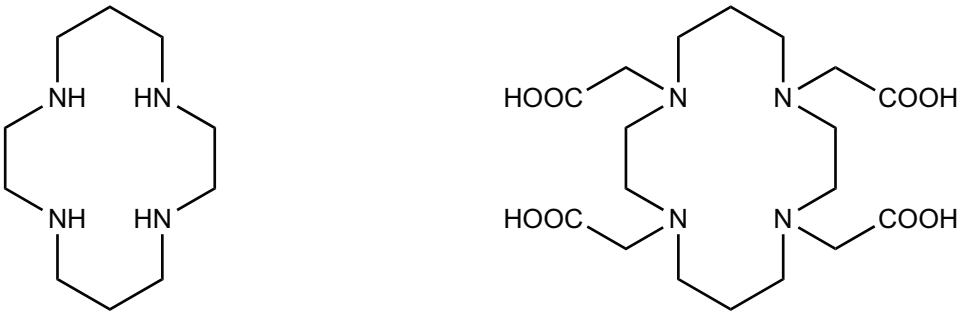

Cyclam H_4**TETA**

Figure 2. Two examples of polydentate macrocyclic ligands – **Cyclam** and H_4**TETA**.

decreasing since the discovery of acute nephrotoxicity of several commercially available gadolinium-based MRI agents.[13] Therefore, macrocyclic ligands are now being recognized as the only reliable carriers for a wide range of metal ions for *in vivo* application. The more detailed compendium of macrocyclic ligands is beyond the scope of this work, due to the immense amount of data. Some excellent reviews can, however, bring some insight to the subject matter, bearing in mind the main focus on ligands suitable for Cu^{2+} ions.[12],[14],[15]

3.5. Geminal bis(phosphonates)

Despite the enormous amount of compounds investigated as potential ligands for metal radioisotopes applicable in PET and SPECT, the ability of macrocyclic ligands to complex radionuclides rapidly remains still a challenging obstacle to overcome. Complexation rate is, in general, directly proportional to the concentration of components. Therefore, the ultra-low concentrations used in nuclear medicine demand for ligands capable of very fast complexation.

Geminal bis(phosphonates) are one of the most studied family of organophosphorus compounds (**Figure 3**). They are formal analogues of endogenous pyrophosphate H_4**PP$_I$** (**Figure 3**) and possess very high affinity to hydroxyapatite which is the main inorganic component of bones.[16]–[18] This high affinity together with metabolic stability of the P—C—P fragment is the basis for important applications in treatment of diseases associated with disorder of calcium metabolism, including osteoporosis, Paget's disease and cancer.[16]–[20]

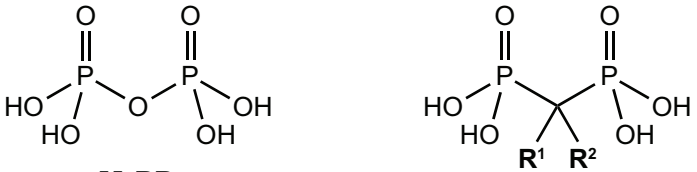

H_4**PP$_I$**

Figure 3. Pyrophosphate H_4**PP$_I$** and general formula of geminal bis(phosphonates).

During recent development of novel agents for molecular imaging, it was found that presence of geminal bis(phosphonate) can dramatically increase incorporation of the metal ion into the macrocyclic cavity.[21]–[23] The ability of geminal bis(phosphonate) pendant arm to accelerate complexation can be explained by formation of intermediate *out-of-cage* complex

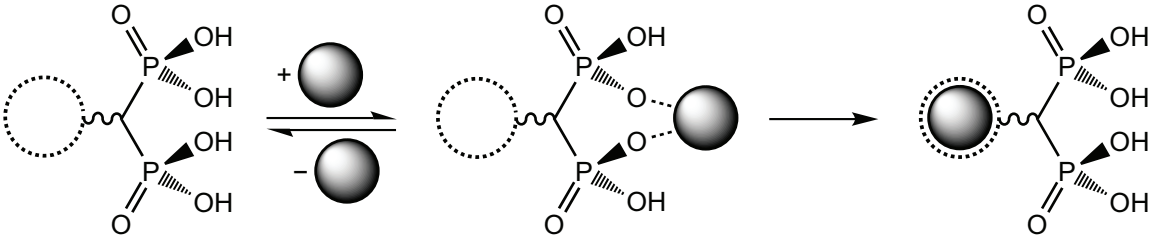

Figure 4. Schematic model of bis(phosphonate) pendant arm-assisted complexation of metal ion (●) into macrocyclic cavity (◌).

of bis(phosphonic) acid moiety and the metal ion which can either dissociate back or re-arrange to the desired product (*i.e. in-cage* complex, **Figure 4).**

3.6. Geminal bis(phosphinates)

The faster *in-cage* complexation induced by geminal bis(phosphonates) described in **Figure 4** cannot be, unfortunately, used for other than bone-associated applications due to extremely strong affinity of bis(phosphonates) and their complexes to calcified tissues.[16] However, this could be overcome by using geminal bis(phosphinates) (**Figure 5**) instead of geminal bis(phosphonates). The geminal bis(phosphinates) maintain the same P—C—P fragment and show low affinity to hydroxyapatite.[24] Due to structure analogous structure to geminal bis(phosphonates), similar coordination properties could be expected.

Despite their simple motif, geminal bis(phosphinates) attracted surprisingly less attention compared to geminal bis(phosphonates). Some of them have been prepared,[24–26,27–29] but only few papers dealing with their coordination behaviour has been published,[30,31] except two simple ligands, methylene-bis(phosphinic acid) H_2**MBPIN** and methylene-bis[(phenyl)phosphinic acid] H_2**BPHPIN** (**Figure 5**). Complexes of those ligands with various metal ions were studied in more detail.[32–48]

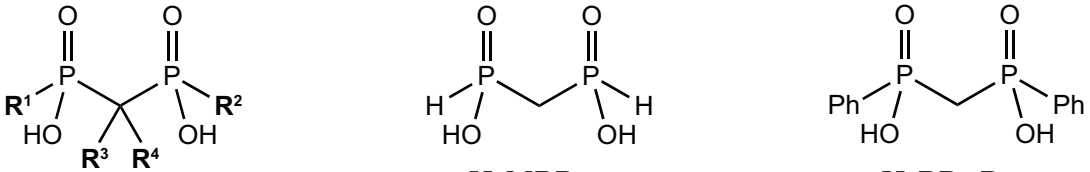

H_2**MBPIN** H_2**BPHPIN**

Figure 5. General formula of geminal bis(phosphinates) and structures of two ligands.

3.7. Aims of the work

Due to the missing fundamental knowledge about geminal bis(phosphinates), the aim of the first part of the project was to synthesize and study *simple* bis(phosphinates) H_2**L**^{1} – H_4**L**^{11} (**Figure 6**). The objective was to gather synthetic knowledge and investigate acid-base, coordination and adsorption properties of the title ligands. In the case of bis(phosphinates) bearing primary amine group (H_2**L**^{5} – H_4**L**^{11}), the aim was to determine which position of the amine

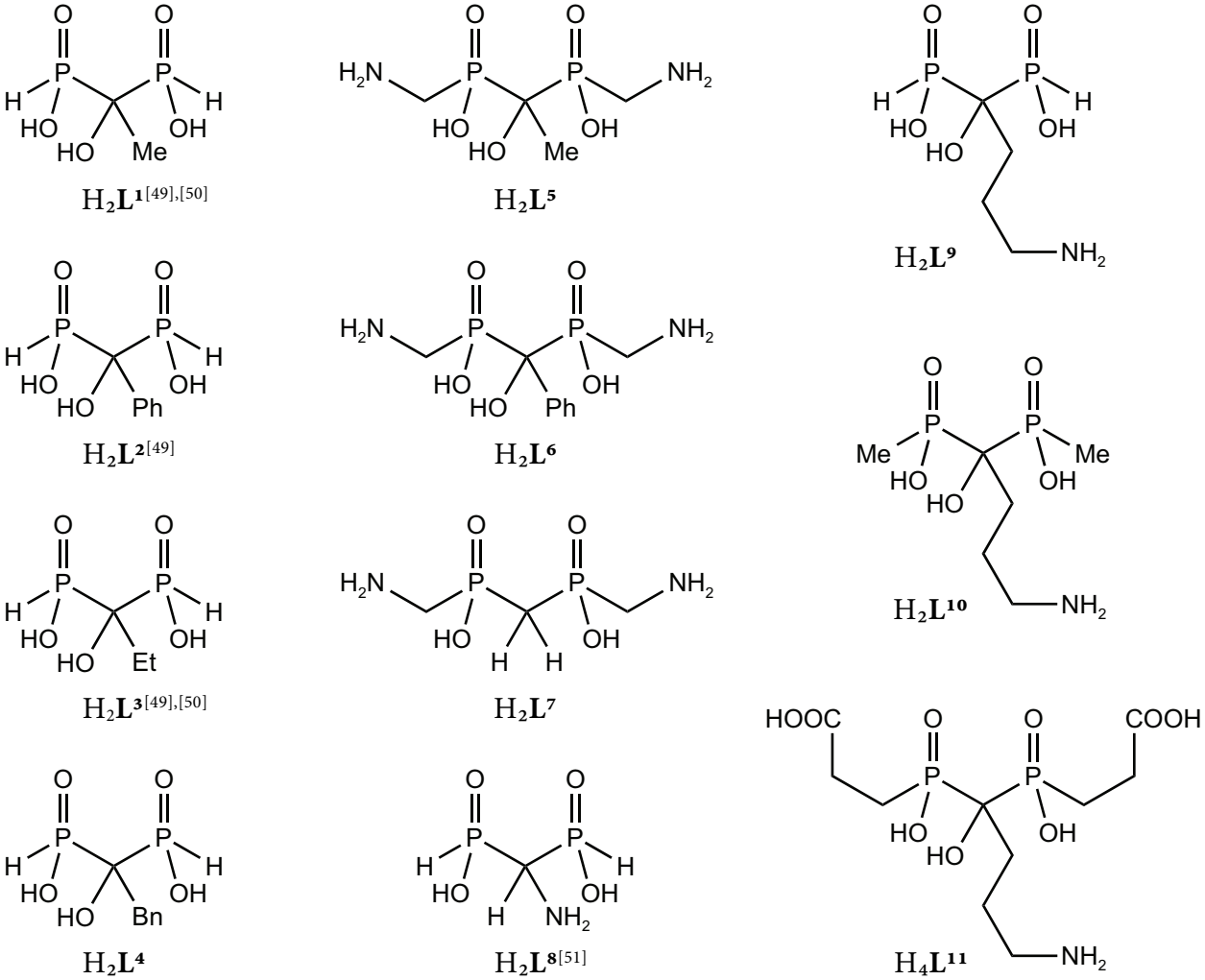

Figure 6. List of studied simple geminal bis(phosphinates) $H_2\mathbf{L^1}$ – $H_4\mathbf{L^{11}}$. The substituents on the carbon atom joining the two phosphinate moieties (*i.e.* —H and —NH_2 in the compound $H_2\mathbf{L^8}$) are called to be in the *central* position. Likewise, the substituents directly attached to the phosphorus atoms (*i.e.* two —CH_2—NH_2 fragments in compounds $H_2\mathbf{L^5}$ – $H_2\mathbf{L^7}$) are called to be in the *terminal* position throughout the text.

group is more suitable for attachment of macrocyclic ligand – on *terminal* end ($H_2\mathbf{L^5}$ – $H_2\mathbf{L^7}$) or in the *central* position ($H_2\mathbf{L^8}$ – $H_4\mathbf{L^{11}}$).

In the second part of the project, the goal was to employ the acquired knowledge to design and synthesize bis(phosphinate) derivatives of macrocyclic ligand 1,4,8,11-tetraazacyclotetradecane (**Cyclam**, **Figure 2**) which is known to selectively bind Cu^{2+} ions. The aim was to design compounds with combination of several important properties – fast complexation rate, high thermodynamic stability as well as sufficient kinetic inertness of its Cu^{2+} complexes together with negligible adsorption onto bone tissue. The combination of such properties in one compound would make those ligands superior candidates for application as PET agents or in other fields of nuclear medicine.

Ultimately, the results of this study focused on Cu^{2+} ions can be subsequently used in the design of new bis(phosphinate)-containing macrocyclic ligands suitable for other metal ions applied in nuclear medicine.

4. Simple bis(phosphinates)

4.1. Synthesis of ligands

The desired ligands $H_2\mathbf{L^1}$ – $H_4\mathbf{L^{11}}$ (except $H_2\mathbf{L^7}$ and $H_2\mathbf{L^8}$) were prepared by slightly modified conditions from literature.[49] Two molecules of *in situ* silylated phosphinate were reacted with an acyl chloride, followed by hydrolysis of silyl groups with ethanol (**Figure 7**). Those general conditions afforded appropriate derivatives containing hydroxy group in the *central* position with approximately 60 % overall yields.

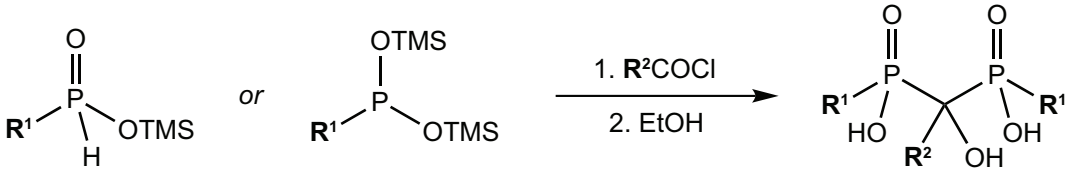

Figure 7. General synthetic scheme for preparation of derivatives containing hydroxy group in the *central* position.

Compound $H_2\mathbf{L^7}$ was prepared by different synthetic strategy with 71 % overall yield. Instead of joining two phosphinate moieties together as depicted on **Figure 7**, two-step derivatization of methylene-bis(phosphinic acid) was utilized (**Figure 8**).

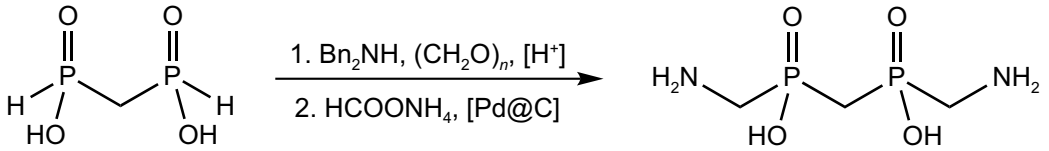

H_2**MBPin** $H_2\mathbf{L^7}$

Figure 8. Synthetic scheme for preparation of compound $H_2\mathbf{L^7}$ by Mannich-type reaction and subsequent removal of benzyl groups.

For preparation of compound $H_2\mathbf{L^8}$, reaction conditions similar to that on **Figure 7** were chosen, however, starting with formimidate instead of acyl chloride (**Figure 9**). The yield of this reaction was significantly lower (37 %) than those of the other ligands.

All compounds were fully characterized by conventional methods (NMR, MS, TLC, EA). In addition, nine different crystal structures of free ligands or their complexes were obtained by X-ray analysis. Two particular crystal structures of complexes with Cu^{2+} and Co^{2+}

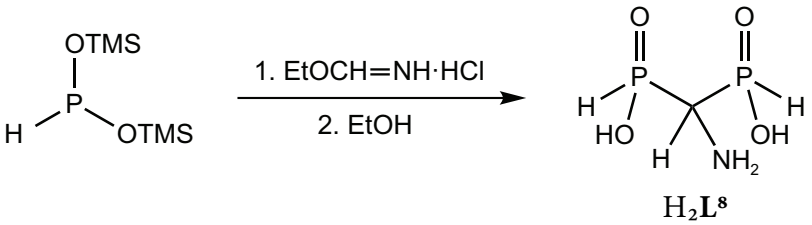

$H_2\mathbf{L^8}$

Figure 9. Synthetic scheme for preparation of compound $H_2\mathbf{L^8}$ by reaction of two molecules of bis(trimethylsilyl)phosphonite with ethyl formimidate followed by hydrolysis of silyl groups.

ions (**Figure 14** and **Figure 15**, respectively) are discussed below. Detailed experimental procedures as well as all crystal structures can be found in appendixes ($H_2\mathbf{L^1}$ – $H_2\mathbf{L^4}$ in *Appendix 1*, $H_2\mathbf{L^5}$ – $H_2\mathbf{L^7}$ in *Appendix 2* and $H_2\mathbf{L^8}$ – $H_4\mathbf{L^{11}}$ in *Appendix 3*).

4.2. Chemical stability

One of the first attempts to prepare ligands $H_2\mathbf{L^5}$ or $H_2\mathbf{L^6}$ revealed surprising fact – unlike geminal bis(phosphonates), aqueous solutions of geminal bis(phosphinates) are not ultimately stable. Attempts to attach *N*-protected *terminal* amine groups to compound $H_2\mathbf{L^1}$ or $H_2\mathbf{L^2}$ by Mannich-type reaction (which could finally yield compounds $H_2\mathbf{L^5}$ and $H_2\mathbf{L^6}$, **Figure 10**) were unsuccessful due to the decomposition of starting material. However, the desired ligands $H_2\mathbf{L^5}$ and $H_2\mathbf{L^6}$ were later prepared by different synthetic strategy (**Figure 7**) and showed no decomposition as opposed to ligands $H_2\mathbf{L^1}$ and $H_2\mathbf{L^2}$.

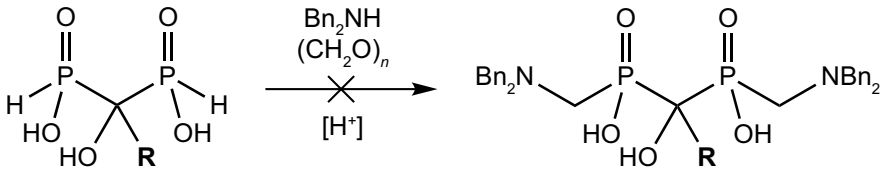

$H_2\mathbf{L^1}$ or $H_2\mathbf{L^2}$

Figure 10. Unsuccessful synthesis of $H_2\mathbf{L^5}$ (**R** = Me) and $H_2\mathbf{L^6}$ (**R** = Ph) precursors by Mannich-type reaction.

The chemical stability of all prepared compounds ($H_2\mathbf{L^1}$ – $H_4\mathbf{L^{11}}$) was, therefore, closely investigated afterwards. Ligands were incubated at 80 °C at various pH for several weeks. It was found that chemical structure of bis(phosphinates) plays dominant role in compound stability – only compounds with hydrogen atom directly bound to phosphorus atom (with P—H bond) were found to be unstable ($H_2\mathbf{L^1}$ – $H_2\mathbf{L^4}$, $H_2\mathbf{L^8}$ and $H_2\mathbf{L^9}$). The decomposition occurs in strongly acidic media (in the case of ligand $H_2\mathbf{L^2}$ also in strongly alkaline media). In neutral or weakly alkaline region, the decomposition was very slow or not occurring at all (which allowed the isolation of the title compounds).

The products of decomposition were succesfully identified and isolated. This revealed the relationship between chemical structure of geminal bis(phosphinate) and its chemical stability. Formally, the reaction is hydrolysis of P—C bond (**Figure 11**).

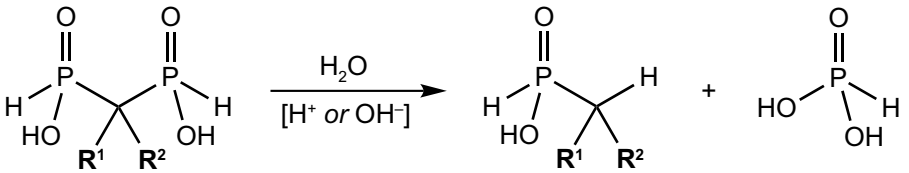

$H_2\mathbf{L^1}$ – $H_2\mathbf{L^4}$, $H_2\mathbf{L^8}$ and $H_2\mathbf{L^9}$

Figure 11. Decomposition reaction of geminal bis(phosphinates) with P—H bond yielding correspoding phosphinates and phosphorous acid (except $\mathbf{R^1}$ = $\mathbf{R^2}$ = H).

Since the compound H_2**MBPin** (**Figure 5)** also containing P—H bonds was fully stable at all examined pH, we concluded that the decomposition occurs only in the case of geminal bis(phosphinates) with P—H bond and that the decomposition rate is directly proportional to sum of electron withdrawing effects of substituents on the *central* carbon atom. Ultimately, this allows reasonable prediction of chemical stability of geminal bis(phosphinates), which could facilitate their future study. This knowledge was utilized in design of macrocyclic derivatives. More details about mechanism of decomposition and its reaction rates as well as about the products of decomposition can be found in appendixes (H_2**L**^{1} – H_2**L**^{4} in *Appendix 1*, and H_2**L**^{8} – H_2**L**^{9} in *Appendix 3*).

4.3. Acid-base and coordination properties

Solution behaviour of amino-bis(phosphinates) H_2**L**^{5} – H_2**L**^{7} as well as H_2**L**^{10} and H_4**L**^{11} was studied by potentiometric titrations. This afforded dissociation constants of amine and phosphinate groups. Due to the low stability of compounds H_2**L**^{8} and H_2**L**^{9} (discussed above), NMR titrations study were performed to obtain at least partial information about acid-base properties. Basicity of amine groups is the crucial factor for coordination behaviour of the ligands. Protonation constants (logK_a) of the amine groups of compounds H_2**L**^{5} – H_4**L**^{11} are summarized in **Table 1**. Detailed acid-base properties can be found in appendixes (H_2**L**^{5} – H_2**L**^{7} in *Appendix 2* and H_2**L**^{10} – H_4**L**^{11} in *Appendix 3*).

Table 1. Consecutive protonation constants (logK_a(**L**) and logK_a(H**L**)) of amine groups of ligands H_2**L**^{5} – H_4**L**^{11} acompanied by data of related compounds.[52]

	H_2**L**^{5}	H_2**L**^{6}	H_2**L**^{7}	H_2**L**^{8}	H_2**L**^{9}	H_2**L**^{10}	H_4**L**^{11}	H_4**Meth**	H_4**Ale**
logK_a(**L**)	10.0[a]	9.84[a]	9.49[a]	6.79[b]	10.8[b]	10.8[a]	11.1[a]	11.4[52]	12.7[52]
logK_a(H**L**)	8.89[a]	8.55[a]	8.80[a]	—	—	—	—	—	—

[a] Determined by potentiometric titrations. [b] Determined by NMR titrations.

Terminal amino groups in compounds H_2**L**^{5} – H_2**L**^{7} show similar protonation constants indicating that substituents on *central* carbon atom does not affects basicity of this amine groups significantly. The logK_a values are surprisingly high if compared with simple aminomethylphosphinic acids and comparable to those of phosphonic amino acid (comparision can be found in *Appendix 2*). The high basicity of the nitrogen atoms could be ascribed to the presence of intramolecular hydrogen bonds similar to those found in the solid state (*Appendix 2*). Even higher logK_a values of amine group in compounds H_2**L**^{9} – H_4**L**^{11} are result of the long distance between the amine group and the bis(phosphinate) moiety. Nevertheless, basicity of those ligands are lower than that of analogical bis(phosphonate) H_4**Ale** (**Figure 12**). It could be explained by lower charge of the fully deprotonated bis(phosphinate) group in comparison with bis(phosphonates).[52] The same applies for low logK_a value of amine group in compound H_2**L**^{8} if compared with analogous bis(phosphonate) H_4**Meth** (**Figure 12**).[52]

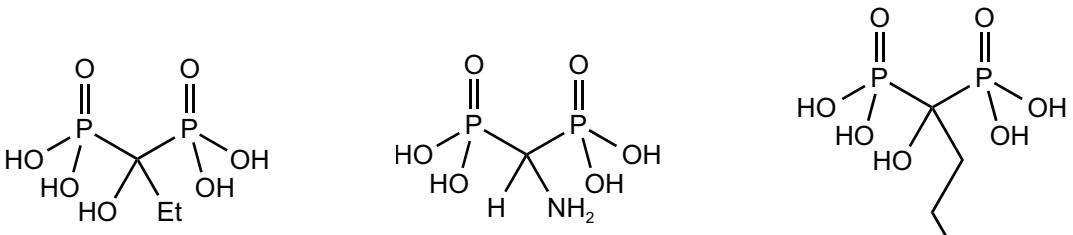

Figure 12. Structure of geminal bis(phosphonates) disscussed in the text.

Stability constants of complexes of compounds $H_2\mathbf{L^5}$ – $H_2\mathbf{L^7}$, $H_2\mathbf{L^{10}}$ and $H_4\mathbf{L^{11}}$ with selected divalent ions (Cu^{2+}, Zn^{2+}, Ni^{2+} and Co^{2+}) were determined by potentiometric titrations. Excerpt from obtained results (stability constants of 1:1 complexes with Cu^{2+} ions, denoted $\log K_{ML}$) are presented in **Table 2**. Stability constants with other studied metal ions as well as distribution diagrams can be found in appendixes ($H_2\mathbf{L^5}$ – $H_2\mathbf{L^7}$ in *Appendix 2* and $H_2\mathbf{L^{10}}$ – $H_4\mathbf{L^{11}}$ in *Appendix 3*).

Table 2. Stability constants ($\log K_{ML}$) of Cu^{2+}–ligand (1:1) complexes $H_2\mathbf{L^5}$ – $H_2\mathbf{L^7}$,$H_2\mathbf{L^{10}}$ and $H_4\mathbf{L^{11}}$ acompanied by data of related compounds.[52]–[55]

	$H_2\mathbf{L^5}$	$H_2\mathbf{L^6}$	$H_2\mathbf{L^7}$	$H_2\mathbf{L^{10}}$	$H_4\mathbf{L^{11}}$	H**AmPin**	H**Am$_2$Pin**	H_2**GlyP**	H_4**Ale**
$\log K_{ML}$	10.8	11.1	9.87	8.12	9.25	4.84[53]	7.64[54]	8.12[55]	15.1[52]

Generally, the geminal bis(phosphinates) were found to complex Cu^{2+} ions even under strongly acidic conditions (*i.e.* pH = 1) where only phosphinate groups are coordinated to the central ion while amine groups are protonated and remain uncoordinated. At neutral pH, amine groups are deprotonated and simultaneously coordinated. The presence of two highly basic nitrogen atoms and two phosphinate groups in compounds $H_2\mathbf{L^5}$ – $H_2\mathbf{L^7}$ results in higher stability constants of the complexes if compared with aminomethylphosphinic acids H**AmPin** and H**Am$_2$Pin** and aminomethylphosphonic acid H_2**GlyP** (**Figure 13**).[53]–[55] The stability constants are higher than those of compounds $H_2\mathbf{L^{10}}$ and $H_4\mathbf{L^{11}}$ with lower basicity leading to much lower values of stability constants if compared with their bis(phosphonate) analogue H_4**Ale** (**Figure 12**).[52] The low chemical stability of ligand $H_2\mathbf{L^8}$ (with amine group directly attached to the central carbon atom) disallowed study of its coordination properties. However, the low basicity of the ligand together with low chemical stability indicates unsuitability of this ligand for complexation of Cu^{2+} ions.

Coordination behaviour of ligands with two *terminal* amine groups ($H_2\mathbf{L^5}$ – $H_2\mathbf{L^7}$) is, however, not uniform among the compounds. While the ligands $H_2\mathbf{L^5}$ and $H_2\mathbf{L^6}$ form dark

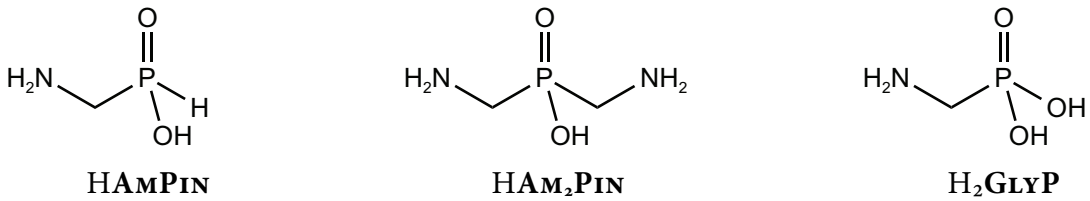

Figure 13. Structure of $H_2N—CH_2—P$ fragment-containing compounds discussed in the text.

green solutions with Cu^{2+} ions at pH above 6, ligand $H_2\mathbf{L^7}$ forms only light blue poorly soluble Cu^{2+} complexes. Analysis of electronic spectra of those solutions revealed that presence of the hydroxy group in the *central* position in ligands $H_2\mathbf{L^5}$ and $H_2\mathbf{L^6}$ results in significantly different coordination behaviour of the Cu^{2+} complexes at neutral pH and above (compared with $H_2\mathbf{L^7}$). The shift of the CT-bands to visible region indicates coordination of alcoholate groups in the solution. This was proven by single-crystal X-ray analysis of Cu^{2+}–$H_2\mathbf{L^6}$ complex grown at pH = 10 which revealed formation of unusual dimeric complex with two μ_2-bridging alcoholate oxygen atoms (**Figure 14**). For both ligands $H_2\mathbf{L^5}$ and $H_2\mathbf{L^6}$, the dinuclear complexes were also further identified as major signals in the HRMS spectra of their solutions (more details can be found in *Appendix 2*).

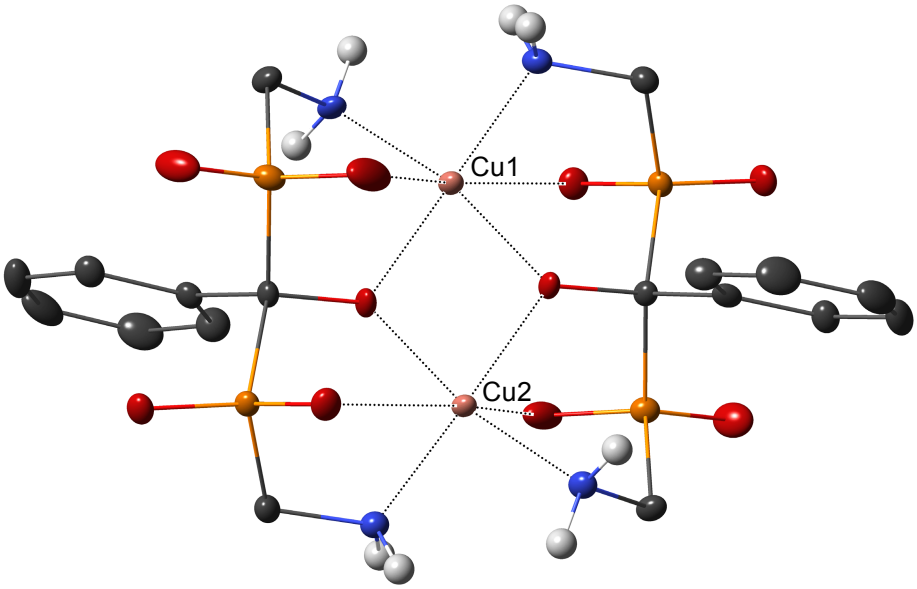

Figure 14. One of $[Cu_2(H_{-1}\mathbf{L^6})_2]^{2-}$ units (carbon-bound hydrogen atoms were omitted for the sake of clarity) found in the crystal structure of $(Hgua)_4[Cu_2(H_{-1}\mathbf{L^6})_2]CO_3{\cdot}10H_2O$.

Even more surprising was cubane-like structure found by single-crystal X-ray analysis of Co^{2+}–$H_2\mathbf{L^5}$ complex grown at pH = 8 (**Figure 15**). The structure with three μ_3-bridging alcoholate oxygen atoms indicates tendency of ligands $H_2\mathbf{L^5}$ and $H_2\mathbf{L^6}$ to form polynuclear complexes with selected metal ions.

The higher stability of Cu^{2+} complexes of ligands with amine groups attached to the *terminal* position compared to the *central* position as well as the role of the hydroxyl group in the *central* position were taken into considerations during the design of macrocyclic derivatives.

4.4. Adsorption properties

To evaluate adsorption properties, experiment with ligand $H_2\mathbf{L^3}$ was conducted (this derivative was deliberately chosen as it contains an aromatic group that allows quantification by UV-Vis spectroscopy). Suspension of hydroxyapatite (**HA**) was used as model of bone tissue. Solution of the compound in TRIS buffer (pH = 7.4) was treated with various amounts

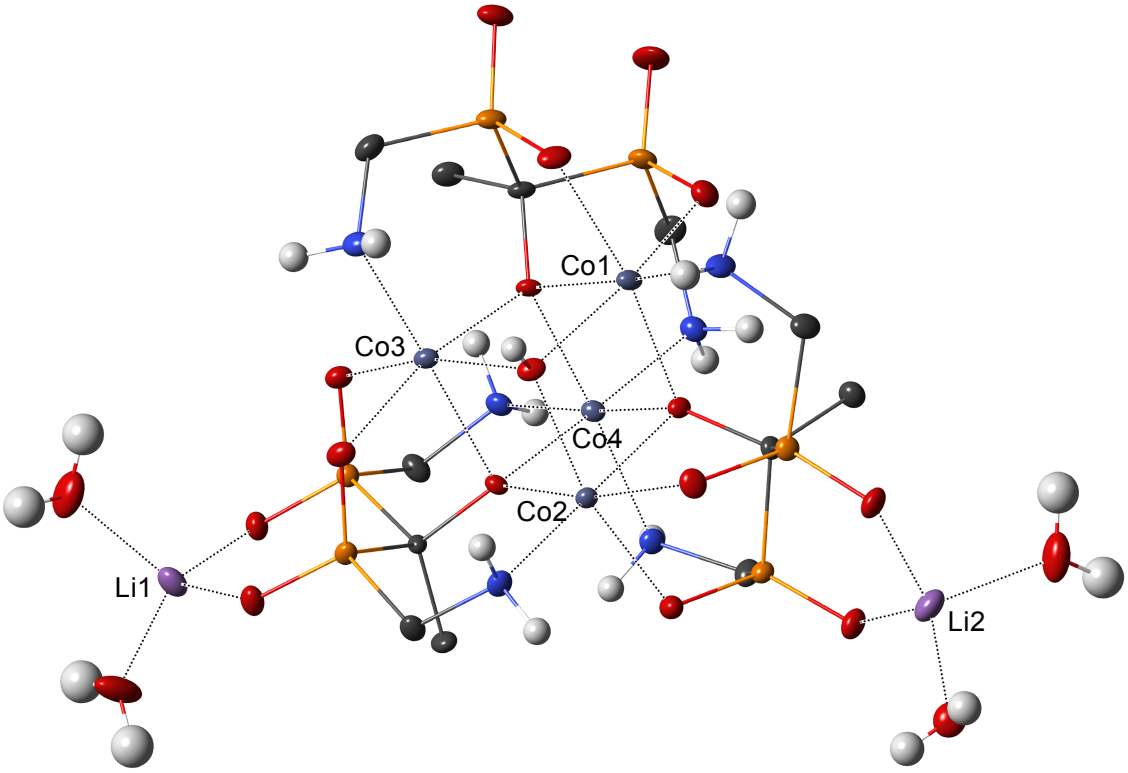

Figure 15. Crystals structure of cubane-like unit $[Co_4(H_{-1}\mathbf{L^5})_3(OH)\{Li(H_2O)_2\}_2]$ with three μ_3-bridging alcoholate groups (carbon-bound hydrogen atoms were omitted for the sake of clarity) found in the crystal structure of $Li_2[Co_4(H_{-1}\mathbf{L^5})_3(OH)]\cdot 17.5H_2O$.

of **HA**. The results were compared with the sorption curve of similar bis(phosphonate) H_4**Hedp** (**Figure 12**) that was simulated on basis of previously published data.[56] Obtained results proved negligible adsorption of the bis(phosphinate) $H_2\mathbf{L^3}$ onto **HA** (**Table 3**). More details about the adsorption experiment can be found in *Appendix 1*.

Table 3. Comparison of adsorption of bis(phosphinate) $H_2\mathbf{L^3}$ and related bis(phosphonate) H_4**Hedp** onto hydroxyapatite (**HA**) expressed as a percentage of the initial concentration remaining in supernatant at different amount of added **HA**.

	Percentage of non-adsorbed ligand			
	50 mg **HA**	100 mg **HA**	150 mg **HA**	200 mg **HA**
$H_2\mathbf{L^3}$	~ 93 %	~ 87 %	~ 85 %	~ 84 %
H_4**Hedp**	~ 52 %	~ 8 %	< 1 %	< 1 %

5. Macrocyclic bis(phosphinates)

5.1. Design of ligands

Knowledge about bis(phosphinates) $H_2\mathbf{L^1}$ – $H_4\mathbf{L^{11}}$ was utilized in design of macrocyclic derivatives based on **Cyclam** backbone (**Figure 2**) which possesses high selectivity towards Cu^{2+} ions. The most important factor in consideration of the particular ligand structure was fast complexation rate. To enhance complexation rate of Cu^{2+} ions into macrocyclic

cavity by bis(phosphinate) pendant arm, it was assumed that both of these coordination sites had to be as close as possible to each other for the process to be effective. The closest possible connection of bis(phosphinate) unit to amine group of the macrocyclic core is through one carbon atom. There are two possible ways of such attachment – through formation of either *terminal* or *central* N—C—P bridge, as illustrated on **Figure 16**.

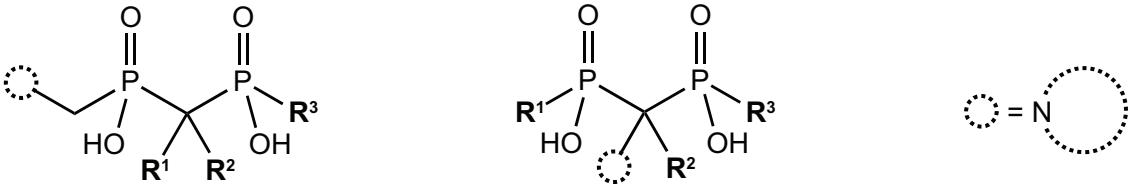

terminal attachment *central* attachment

Figure 16. Schematic illustration of two different ways of shortest possible connection of bis(phosphinate) unit to a general secondary amine-containing macrocyclic core (◌) through formation of either *terminal* or *central* N—C—P bridge.

It was examplified on ligands $H_2\mathbf{L^5}$ – $H_2\mathbf{L^7}$ (see above) that the *terminal* approach is more suitable for connection to the cyclam core due the high chemical stability, synthetic availability and high thermodynamical stability of Cu^{2+} complexes of ligands with this arrangement. Contrary, the *central* position was not found to be very suitable for such purpose. Only one representative ($H_2\mathbf{L^8}$) was successfully prepared, other synthetic attempts did not yield desired compounds. Ligand $H_2\mathbf{L^8}$ was found to be chemically unstable, which tied down its further study. In addition, due to the very low basicity of the amine group, this arrangement is not expected to form stable complexes with Cu^{2+} ions. While the other ligands with primary amino group in the *central* position ($H_2\mathbf{L^9}$ – $H_4\mathbf{L^{11}}$) possess sufficient thermodynamical stability of its Cu^{2+} complexes, the distance between the amino group and the bis(phosphinate) is probably too long for significant enhancement of complexation rate into macrocyclic cavity. The *terminal* attachment of cyclam core to the bis(phosphinate) moiety was, therefore, chosen for the ligand build-up.

The next step in the design was decision about nature of substituents in the *central* position of such arrangement – more specifically presence or absence of hydroxyl group directly attached to the *central* carbon atom as illustrated on **Figure 17**. Ligands $H_2\mathbf{L^5}$ and $H_2\mathbf{L^6}$ with such group were found to form thermodynamically more stable complexes with Cu^{2+} ions than ligand $H_2\mathbf{L^7}$ without that group. But while bridging character of the alcoholate oxygen atoms plays dominant role in coordination behaviour of the whole bis(phosphinate) moiety, it is hard to predict whether it will influence complexation rate into macrocyclic cavity in a possitive or negative way. In addition, the synthesis of the final products with hydroxyl group in the *central* postion might be non-trivial, since the firstly-thought useful precursors ($H_2\mathbf{L^1}$ – $H_2\mathbf{L^4}$) were found to be chemically unstable and, therefore, not suitable for further derivatization.

Simple and synthetically available methylene-bis(phosphinate) fragment was thus chosen for the ligand build-up (as in the case of ligand $H_2\mathbf{L^7}$). Consequently, the influence

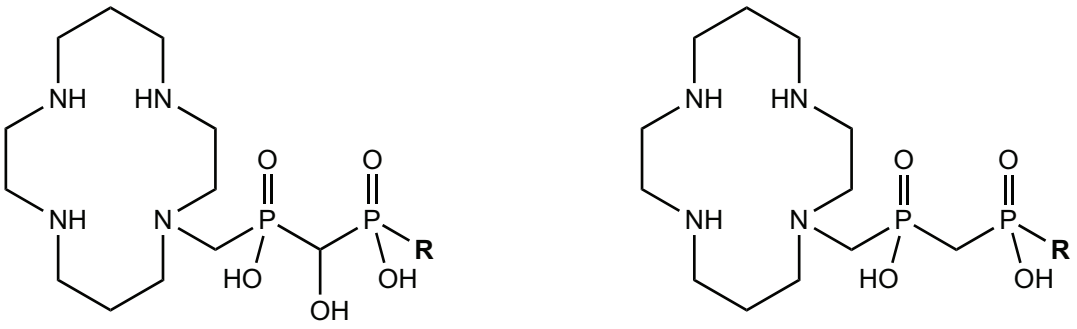

presence of α-hydroxy group absence of α-hydroxy group

Figure 17. Two hypothetical structural alternatives of cyclam-based ligands with attached bis(phosphinate) pendant arm (through *terminal* end) with either presence or absence of hydroxyl group in the *central* position (α-hydroxy group).

of other substituents in *central* position (*e.g.* —OH) to the overall complexation rate can be studied in the future and easily compared to this structurally simplest approach. The combination of above mentioned parameters ultimately led to two novel ligands based on cyclam backbone with either one geminal bis(phosphinate) pendant arm ($H_2\mathbf{L}^{\mathbf{BPin}}$, **Figure 18**) or one mixed geminal phosphino-phosphonate pendant arm ($H_3\mathbf{L}^{\mathbf{PP}}$, **Figure 18)**.

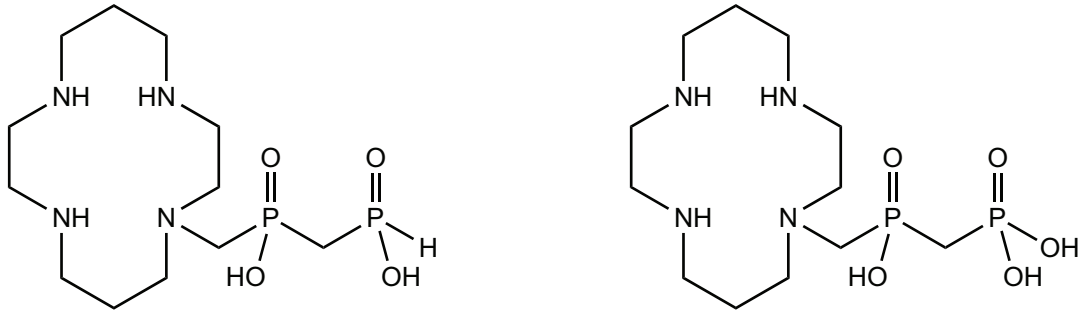

$H_2\mathbf{L}^{\mathbf{BPin}}$ $H_3\mathbf{L}^{\mathbf{PP}}$

Figure 18. Studied derivatives based on **Cyclam** backbone with attached bis(phosphinate) ($H_2\mathbf{L}^{\mathbf{BPin}}$) or phosphino-phosphonate ($H_3\mathbf{L}^{\mathbf{PP}}$) pendant arm.

Both compounds $H_2\mathbf{L}^{\mathbf{BPin}}$ and $H_3\mathbf{L}^{\mathbf{PP}}$ were thought to be resistant to the hydrolysis of the phosphorus-containing pendant arm and at least the compound $H_2\mathbf{L}^{\mathbf{BPin}}$ was thought to be easily synthesizable by Mannich-type reaction (in a similar fashion as already prepared ligand $H_2\mathbf{L}^{7}$, **Figure 8**). Moreover, the presence of the *terminal* P—H bond in ligand $H_2\mathbf{L}^{\mathbf{BPin}}$ can be further used for derivatization towards bifunctional derivatives.

The ligand $H_3\mathbf{L}^{\mathbf{PP}}$ is unique as it contains geminal phosphino-phosphonate fragment, which has been only very rarely seen at any compound described in the literature. This group structurally lays between the geminal bis(phosphinates) with low affinity to **HA** on one end and geminal bis(phosphonates) with high affinity to **HA** on the other end. Therefore, it is challenging goal to uncover its influence on coordination and adsorption properties of ligand $H_3\mathbf{L}^{\mathbf{PP}}$ (mainly, in comparision with ligand $H_2\mathbf{L}^{\mathbf{BPin}}$). Nevertheless, both ligands represent the first compounds of this kind – no such type of derivatives has been described in the literature yet.

5.2. Synthesis of the ligands

The ligand $H_2\mathbf{L}^{BPin}$ was successfully prepared by one-step Mannich-type reaction of H_2**MBPin**, paraformaldehyde and **Cyclam** (**Figure 19**). The reaction afforded product in good yield (70 %) without utilization of any protection group. Both **Cyclam** and H_2**MBPin** were used in excess to get smooth course of the reaction and they were successfully regenerated during isolation of the compound $H_2\mathbf{L}^{BPin}$ on ion-exchange resins (no other lenghty chromatography was required for isolation of $H_2\mathbf{L}^{BPin}$).

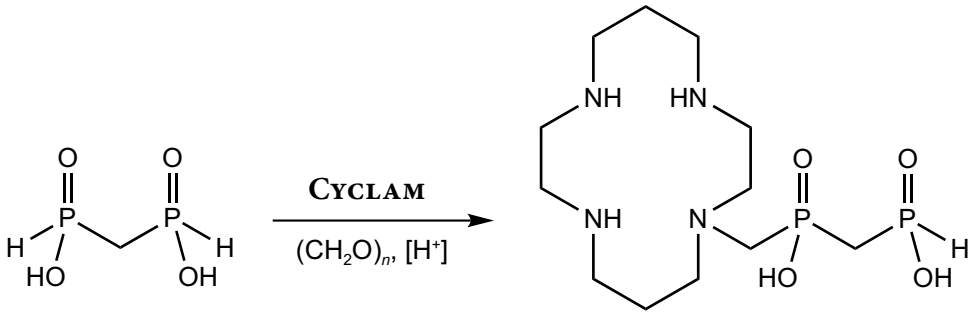

Figure 19. Synthesis of ligand $H_2\mathbf{L}^{BPin}$ from H_2**MBPin** using one-step Mannich-type reaction.

Ligand $H_3\mathbf{L}^{PP}$ was prepared by another one-step reaction – oxidation of P—H bond on the *terminal* end of the $H_2\mathbf{L}^{BPin}$ pendant arm. After several unsuccessful attempts with commonly used oxidation agents (*e.g.* H_2O_2 or I_2/pyridine), the mild oxidation using $HgCl_2$ followed by Hg removal using H_2S (**Figure 20**) afforded ligand $H_3\mathbf{L}^{PP}$ in excellent yield (86 %). More details about the synthesis can be found in *Appendix 4*.

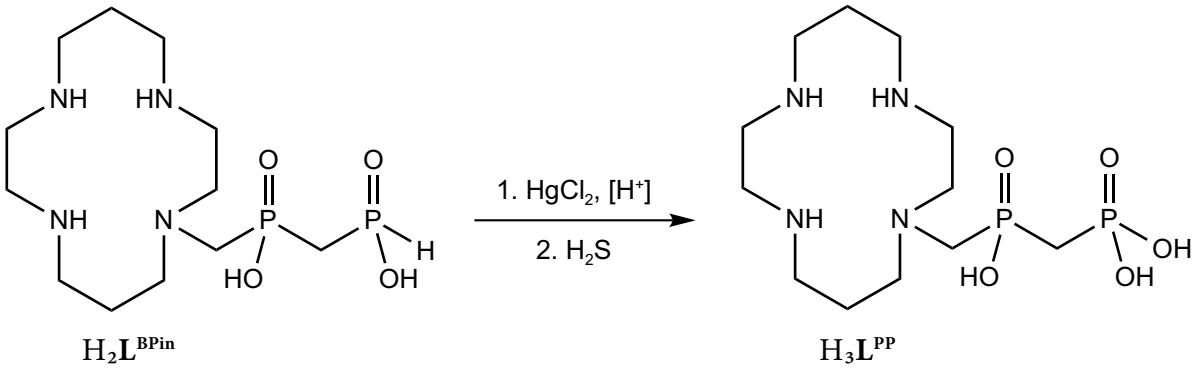

Figure 20. Synthesis of ligand $H_3\mathbf{L}^{PP}$ from $H_2\mathbf{L}^{BPin}$ by mild oxidation using Hg^{2+} ions.

5.3. Coordination properties

Generally, complexes of cyclam-based ligands with divalent metal ions adopts various geometries that are mainly given by configuration on the coordinated ring nitrogen atoms and are usually classified as described in the literature.[57] Some of the conformers are presented in **Figure 21**. Depending on overall coordination environment of the central metal ion (*i.e.* coordination of pendant arms or other ligands), the given conformers of the complexes can

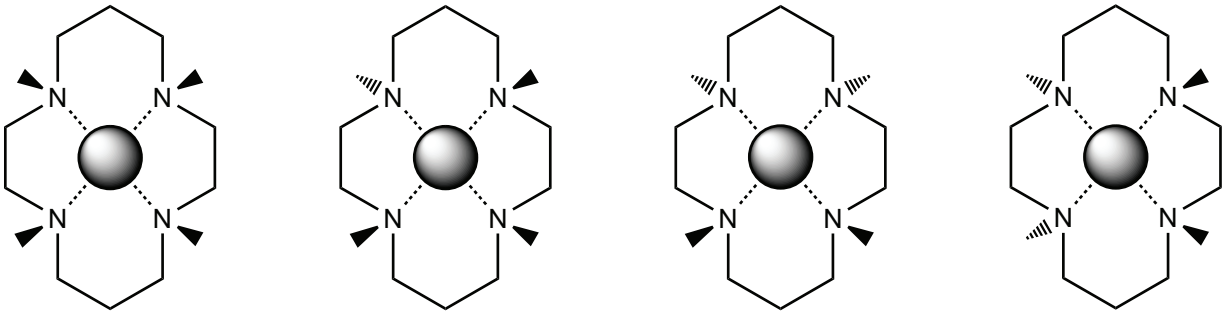

Figure 21. Nomenclature of common conformers found in complexes of cyclam-based ligands with divalent metal ions. The Cu^{2+} complexes mostly adopt *cis*-**I** or *trans*-**III** configurations. The torsion of the cyclam core itself as well as the other possible coordination modes of the central metal ion (●) is ommitted for the sake of clarity.

further adopt *cis* or *trans* configuration. Among them, two isomers are the most common in the case of Cu^{2+} complexes – *cis*-**I** and *trans*-**III**.[58] The isomer *cis*-**I** has all nitrogen substituents (and, usually, the central metal ion as well) pointing above the N_4 plane. Contrary, the isomer *trans*-**III** has pair of nitrogen substituents pointing above and another pair pointing below the N_4 plane and the central metal ion is usually in the N_4 plane.

The structurally most similar derivatives to $H_2\mathbf{L}^{\mathbf{BPin}}$ and $H_3\mathbf{L}^{\mathbf{PP}}$ are cyclam-based ligands with methylphosphonate pendant arm(s) H_2**TEP**, $H_4\mathbf{TE_2P^{1,8}}$ and $H_4\mathbf{ME_2TE_2P^{1,8}}$ (**Figure 22**). Upon exposure to Cu^{2+} ions, all three ligands form blue *cis*-**I** isomer. This complex is the kinetic product and is formed at room temperature. At higher temperatures, extremely kinetically inert violet *trans*-**III** isomer is formed as the thermodynamically most stable complex. The structures of *trans*-**III**-[Cu(**TEP**)], *cis*-**I**-[Cu($H_2\mathbf{TE_2P^{1,8}}$)], *trans*-**III**-[Cu($H_2\mathbf{TE_2P^{1,8}}$)] and *cis*-**I**-[Cu($H_2\mathbf{ME_2TE_2P^{1,8}}$)] were unambiguously determined by X-ray diffraction.[59]–[62]

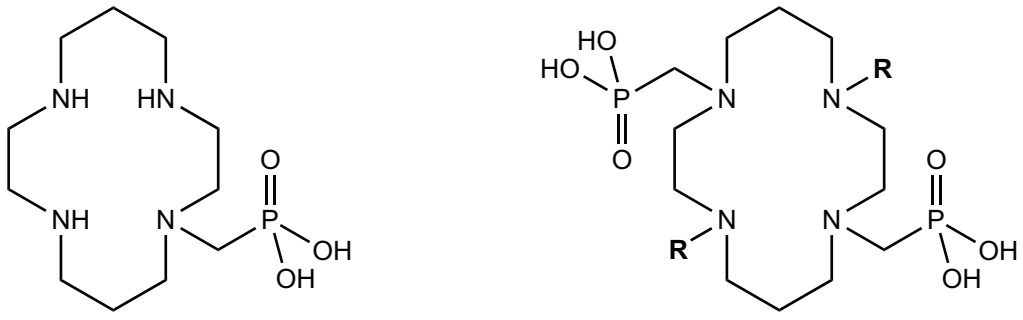

Figure 22. Structure of related cyclam-based ligands with methylphosphonate pendant arm(s) discussed in the text.

Both title ligands, $H_2\mathbf{L}^{\mathbf{BPin}}$ and $H_2\mathbf{L}^{\mathbf{PP}}$, show similar coordination behavior. Upon mixing with Cu^{2+} ions, they form deep blue complexes corresponding to the expected *cis*-**I** isomers. The formation process is, however, more complicated than that during formation of *cis*-**I** isomers of ligands $H_4\mathbf{TE_2P^{1,8}}$ and $H_4\mathbf{ME_2TE_2P^{1,8}}$ (described in the next chapters). Treatment of the *cis*-**I**

complexes of $H_2\mathbf{L}^{\mathbf{BPin}}$ and $H_2\mathbf{L}^{\mathbf{PP}}$ at high temperature or in strongly alkaline solutions (pH > 12) at room temperature led to expected isomerisation to violet *trans*-**III** isomer but the conversion was surprisingly never quantitative. However, the resulting mixture of *cis*-**I** and *trans*-**III** complexes was efficiently separated by column chromatography. Thus, it was possible to isolate and characterize all four different species (*cis*-**I** and *trans*-**III** isomers of both ligands, $H_2\mathbf{L}^{\mathbf{BPin}}$ and $H_3\mathbf{L}^{\mathbf{PP}}$). Additionaly, structure of *trans*-**III**-[Cu(H$\mathbf{L}^{\mathbf{PP}}$)] was unambiguously determined by X-ray analysis **(Figure 23**). In the structure, the phosphinate moiety is weakly coordinated to the pentacoordinated central atom while the terminal phosphonate group cannot reach the central atom due to steric reasons.

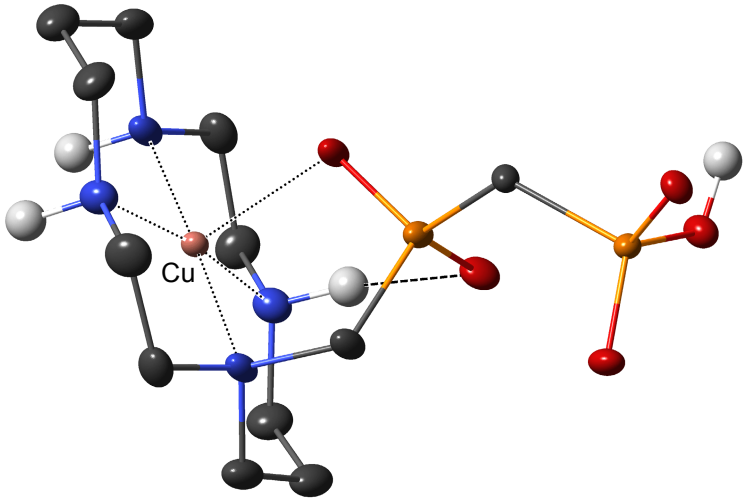

Figure 23. [Cu(H$\mathbf{L}^{\mathbf{PP}}$)] unit (carbon-bound hydrogen atoms were omitted for the sake of clarity) with one strong intramolecular hydrogen bond (*dashed*) found in the crystal structure of *trans*-**III**-[Cu(H$\mathbf{L}^{\mathbf{PP}}$)]·5H_2O.

Despite great effort, no single crystals of *cis*-**I** isomer suitable for X-ray analysis were successfully grown (experiments resulted mostly in formation of a blue oil). Nevertheless, the terminal phosphinate (in the case of *cis*-**I**-[Cu($\mathbf{L}^{\mathbf{BPin}}$)]) or terminal phosphonate (in the case of *cis*-**I**-[Cu(H$\mathbf{L}^{\mathbf{PP}}$)]) group cannot be coordinated to the central Cu^{2+} ion under any circumstances due to the same steric reasons as in the case of *trans*-**III** isomers. More details about the discussed crystal structure as well as details about synthesis of particular isomers and its spectral properties can be found in *Appendix 4*.

5.4. Thermodynamic properties

Acid-base properties of the ligands $H_2\mathbf{L}^{\mathbf{BPin}}$ and $H_3\mathbf{L}^{\mathbf{PP}}$ and thermodynamic stability of their complexes with selected divalent ions (Cu^{2+}, Zn^{2+} and Ni^{2+}) were studied by potentiometry. Excerpt from obtained results (stability constants of 1:1 Cu^{2+}–ligand complexes, denoted as $\log K_{ML}$) is presented in **Table 4**. Stability constants with other studied metal ions and distribution diagrams can be found in *Appendix 4*. The results show that both ligands $H_2\mathbf{L}^{\mathbf{BPin}}$ and $H_3\mathbf{L}^{\mathbf{PP}}$ exhibit very high stability of Cu^{2+} complexes, similar to those of **Cyclam** and other

Table 4. Stability constants ($\log K_{ML}$) of 1:1 Cu^{2+} complexes of ligands $H_2\mathbf{L}^{\mathbf{BPin}}$ and $H_3\mathbf{L}^{\mathbf{PP}}$ acompanied by data of related compounds.[59]–[64]

	$H_2\mathbf{L}^{\mathbf{BPin}}$	$H_3\mathbf{L}^{\mathbf{PP}}$	**Cyclam**	H_2**TEP**	H_4**TE$_2$P**^{1,8}	H_4**Me$_2$TE$_2$P**^{1,8}
$\log K_{ML}$	25.8[a]	27.7[a]	27.2[b,63]; 28.0[b,64]	27.3[a,59]	25.4[a,60]; 26.5[b,60]	24.0[a,61]

[a] Corresponds to isomer *cis*-**I**. [b] Corresponds to isomer *trans*-**III**.

related compounds with methylphosphonate pendant arm(s). The obtained values correspond to formation of *cis*-**I** isomers, values corresponding to the *trans*-**III** isomers cannot be obtained due to the non-quantitative formation of the species (discussed below). Furthermore, stability constants with Ni^{2+} and Zn^{2+} ions are significantly lower (obtained values can be found in *Appendix 4*). This is in good agreement with Irwing-Williams series.[65] The high selectivity of ligands $H_2\mathbf{L}^{\mathbf{BPin}}$ and $H_3\mathbf{L}^{\mathbf{PP}}$ towards Cu^{2+} ions is important for the complexation of copper radionuclides, since Ni^{2+} and Zn^{2+} are common impurities.

5.5. Formation kinetics

Formation kinetics of Cu^{2+} complexes of ligands $H_2\mathbf{L}^{\mathbf{BPin}}$ and $H_3\mathbf{L}^{\mathbf{PP}}$ is of uttermost importance from the perspective of application in nuclear medicine. The formation of Cu^{2+} complexes was found to be too fast for its study using conventional techniques and, therefore, the stopped-flow technique was employed. The proposed mechanism of *cis*-**I** isomers formation consists from three consecutive steps and is presented on **Figure 24**.

Upon mixing of ligands $H_2\mathbf{L}^{\mathbf{BPin}}$ and $H_3\mathbf{L}^{\mathbf{PP}}$ with Cu^{2+} ions, the metal ion is immediately captured by the pendant arm forming an intermediate where the macrocyclic cavity remains protonated and does not participate in the coordination yet. This kind of intermediate is usually denoted as an *out-of-cage*‡ complex. The kinetic data points to a presence of the *out-of-cage*‡ species in the overall formation mechanism as previously reported for complexations of Ln^{3+} ions by DOTA-like ligands.[66],[67]

In the next step, the *out-of-cage*‡ intermediate quickly re-arranges to another intermediate which is more likely to be *cis*-**II**‡ complex (details can be found in *Appendix 4*). Rate of this reaction is strongly dependent on pH – with increasing concentration of OH^- ion, the reaction proceeds faster. While the precise structure of the intermediate cannot be simply estimated as in the case of the *out-of-cage*‡ complex due to its short half-life and fast spontaneous isomerisation to the final *cis*-**I** product, there is a spectral evidence ($\lambda_{max} \approx 590$ nm) that the Cu^{2+} ion is chelated by all four ring nitrogen atoms (*i.e.* it is *in-cage* complex). Moreover, there is just small difference in the shape of the UV-Vis spectra of this intermediate and the final *cis*-**I** isomer (*i.e.* λ_{max} (*cis*-**II**‡) $\approx \lambda_{max}$ (*cis*-**I**) ≈ 590 nm) indicating very similar geometry of both species. Thus, we can conclude that both of them are similar complexes differing just in the geometry on ring nitrogen atoms. Among several possible *cis*-**II**‡ isomers (differing at the position of the one substituent which is pointing at opposite direction than the other three substituents as implies from **Figure 21**) the most probable variant is depicted on **Figure 24**.

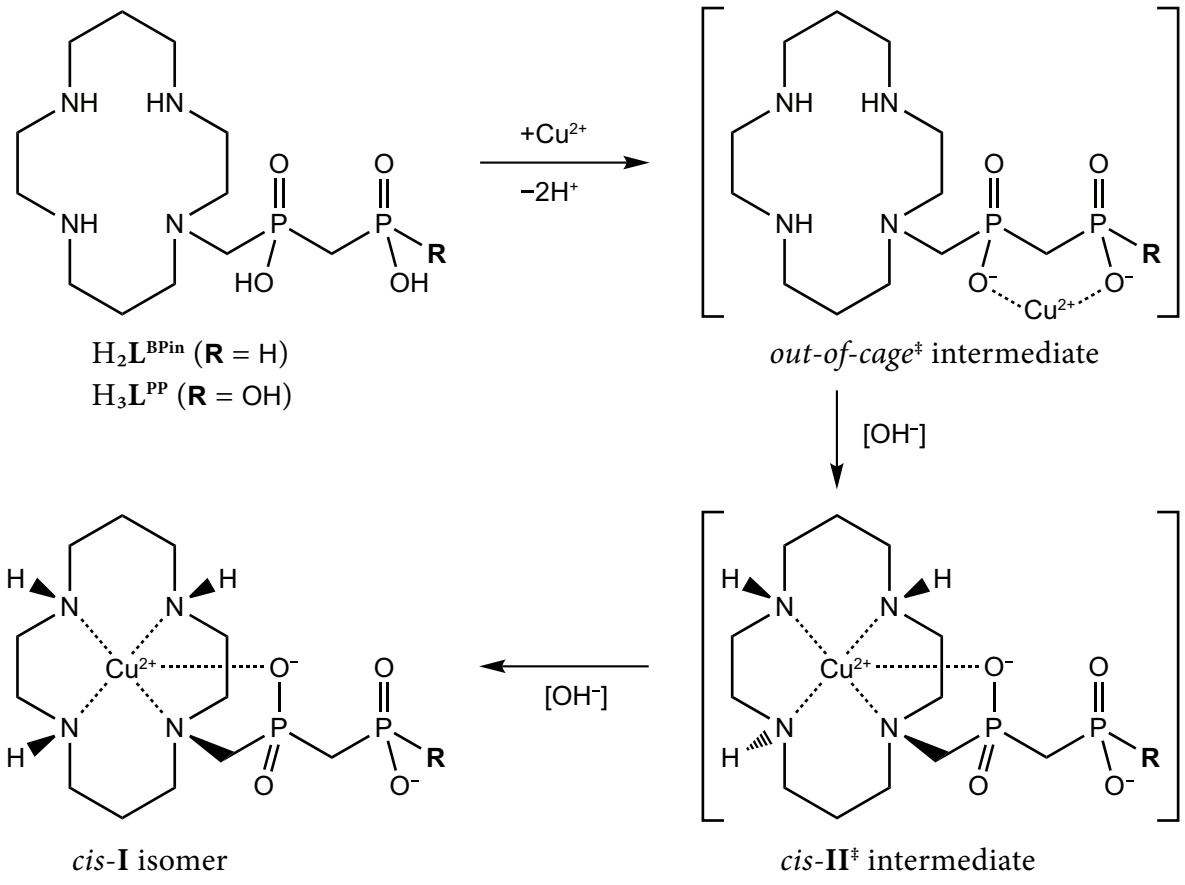

Figure 24. Proposed overall mechanism of *cis*-**I**-[Cu$\mathbf{L}^{\mathbf{BPin}}$] and *cis*-**I**-[CuH$\mathbf{L}^{\mathbf{PP}}$] formation.

In the last step, complex *cis*-**II**‡ undergoes spontaneous isomerisation to the final product – isomer *cis*-**I**. This reaction is also pH dependent. The reaction occurs even at highly acidic conditions and is only roughly one order of magnitude slower than formation of the *cis*-**II**‡ isomer. The overall formation mechanism of *cis*-**I**-[Cu($\mathbf{L}^{\mathbf{BPin}}$)] and *cis*-**I**-[Cu(H$\mathbf{L}^{\mathbf{PP}}$)] species is very different from that of *cis*-**I**-[Cu($H_2\mathbf{TE_2P}^{\mathbf{1,8}}$)] where only the final product was observed during formation (identified as isomer *cis*-**I** by X-ray analysis) and the *out-of-cage*‡ reaction intermediate was not observed at all.[60] This indicates that arrangement of phosphonate- or phosphinate ligands based on cyclam backbone has significant influence on formation of *in-cage* Cu^{2+} complexes (*i.e.* species where metal ion is bound in the macrocyclic cavity).

Nevertheless, for the purpose of application in nuclear medicine, the exact structure of the complexes is not of significant importance. Instead, the crucial factor is time necessary for the formation of species with considerably high thermodynamical stability and sufficient *in vivo* kinetic inertness (*i.e. in-cage* complexes). On one hand, direct comparison of the formation rates of studied ligands $H_2\mathbf{L}^{\mathbf{BPin}}$ and $H_3\mathbf{L}^{\mathbf{PP}}$ with previously reported cyclam derivatives with carboxylate-, phosphinate- or phosphonate-containing pendant arm(s) is difficult – not only it is impeded by different mechanisms of complexation but also by the inevitable differences in acid-base properties of the ligands and in experimental conditions used in the kinetic studies (*e.g.* in absolute concentrations of the reactants and their stoichiometry, temperature, ionic strength, type of electrolyte, type of buffer used, pH). On the other hand, the formation of the firstly-formed *in-cage* Cu^{2+} complexes of both ligands $H_2\mathbf{L}^{\mathbf{BPin}}$ and $H_3\mathbf{L}^{\mathbf{PP}}$ (*i.e.* isomers

cis-**II**‡) was found to be much faster (under similar conditions) than those of *in-cage* Cu^{2+} complex of ligand H_4**TE$_2$P**^{1,8} (*i.e.* isomer *cis*-**I**) which was considered one of the fastest Cu^{2+} complex-forming cyclam derivatives described up to date (unfortunetely, no quantitative comparision is possible due to the above mentioned reasons). This huge increase in the formation rate observed for ligands H_2**L**^{BPin} and H_3**L**^{PP} (slightly higher for H_3**L**^{PP} than for H_2**L**^{BPin}) is, therefore, an experimental proof of desired accelerated complexation of Cu^{2+} ions into the macrocyclic cavity in the presence of bis(phosphinate) or phosphino-phosphonate pendant arms. For illustration, the formation is so fast that, at pH around 6 (commonly used for Cu^{2+} radiolabelling), the *cis*-**II**‡ *in-cage* complexes are fully formed in the scale of tens of milliseconds in the metal concentrations as low as tenths millimolar. This is a good reason to suppose fast complexation of copper radionuclides by ligands H_2**L**^{BPin} and H_3**L**^{PP} even at the ultra-low concentrations routinely used for radiolabelling (*i.e.* nanomolar scale). More details about the formation of Cu^{2+} complexes can be found in *Appendix 4*.

5.6. Isomerization kinetics

As mentioned above, violet *trans*-**III**-[Cu(**L**^{BPin})] and *trans*-**III**-[Cu(H**L**^{PP})] species ($\lambda_{max} \approx 535$ nm) are formed from the corresponding *cis*-**I** isomers at high temperatures or under strongly alkaline conditions (pH > 12) at room temperature. The harsh formation conditions leave the *trans*-**III** isomers irrelevant from the perspective of nuclear medicine. However, the isomerisation process is unique among similar cyclam-based ligands. The *trans*-**III** isomer is usually the final, thermodynamical, product of the Cu^{2+} complex formation, and it mostly exhibits extremely high kinetic inertness. In the case of ligands H_2**L**^{BPin} and H_3**L**^{PP}, the formation of those isomers has, surprisingly, never been quantitative process. This indicates that species *cis*-**I** and *trans*-**III** are in an equilibrium (**Figure 25**). This phenomenon has not been yet observed for Cu^{2+} complexes of cyclam-based ligand.

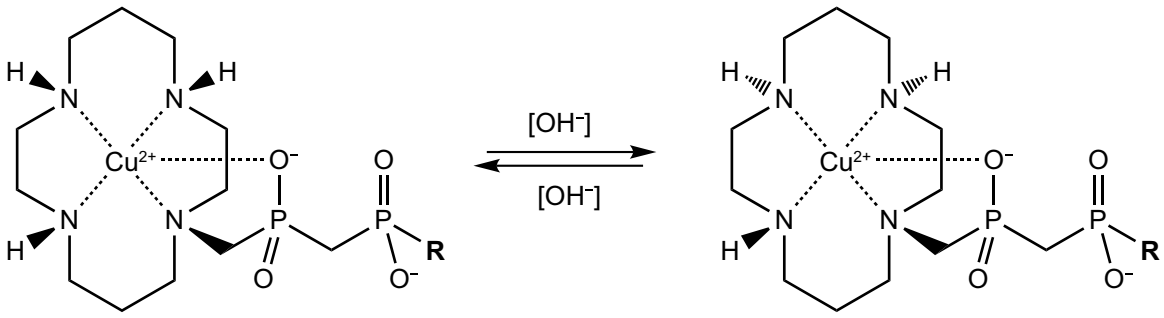

cis-**I** isomer *trans*-**III** isomer

Figure 25. The observed equilibrium between *cis*-**I** and *trans*-**III** isomers of ligands H_2**L**^{BPin} (**R** = H) and H_3**L**^{PP} (**R** = OH).

The *cis*-**I** $\rightleftharpoons$ *trans*-**III** interconversion process was studied for both ligands H_2**L**^{BPin} and H_3**L**^{PP} starting from both pure isolated *cis*-**I** and *trans*-**III** isomers. The interconversion is extremely slow process below pH 12 at room temperature; it allows isolation of all species.

Experiments conducted from all four isolated species above pH 12 at room temperature gave fully consistent results (*i.e.* resulted in mixture of *cis*-**I** and *trans*-**III** isomers with ratio ≈ 1:4 in all cases) which proove correctness of the chosen model. It was found that the isomerization is a base-catalysed process which proceeds faster for complexes of $H_2\mathbf{L}^{\mathbf{BPin}}$. The slower interconversion rate observed for complexes of $H_3\mathbf{L}^{\mathbf{PP}}$ can be explained by higher repulsion between OH^- ions and negatively charged complexes. The *cis*-**I** ⇌ *trans*-**III** isomerisation occurs also in strongly acidic solutions but it is difficult to study the process in details due to the simultaneous dissociation of the complexes. More details about the interconversion of the Cu^{2+} complexes can be found in *Appendix 4*.

5.7. Dissociation kinetics

The *in vivo* kinetic inertness is a crucial parameter for application of the complexes in nuclear medicine. Kinetic inertness of the isomer *cis*-**II**‡ is (despite the importance of this isomer formation rate), however, not relevant from the perspective of nuclear medicine, due to quick re-arrangement to isomer *cis*-**I** (*i.e.* the *cis*-**II**‡ isomer will probably isomerize to *cis*-**I** prior to the eventual dissociation). Thus, it is kinetic inertness of the *cis*-**I** (which does not undergo any isomerisation under physiological conditions) species that is the most relevant from the perspective of nuclear medicine. Determination of *in vivo* kinetic inertness is usually preceeded by evaluation of *in vitro* kinetic inertness under defined conditions (easier to perform and also to compare with other compounds). Therefore, *in vitro* kinetic inertness of *cis*-**I**-[Cu($\mathbf{L}^{\mathbf{BPin}}$)] and *cis*-**I**-[Cu(H$\mathbf{L}^{\mathbf{PP}}$)] were evaluated and the results are summarized in **Table 5**.

Table 5. *In vitro* kinetic inertness of Cu^{2+} *cis*-**I** complexes of ligands $H_2\mathbf{L}^{\mathbf{BPin}}$ and $H_3\mathbf{L}^{\mathbf{PP}}$ expressed as half-life ($t_{½}$) in acidic media ([H^+] = 1.0 M, I = 5.0 M, T = 25 °C) and accompanied by the data of related complexes.[60]-[61]

	cis-**I**-[Cu($\mathbf{L}^{\mathbf{BPin}}$)]	*cis*-**I**-[Cu(H$\mathbf{L}^{\mathbf{PP}}$)]	*cis*-**I**-[Cu($H_2\mathbf{TE_2P}^{\mathbf{1,8}}$)]	*cis*-**I**-[Cu($H_2\mathbf{ME_2TE_2P}^{\mathbf{1,8}}$)]
$t_{½}$	– [a]	2.7 ± 0.2 h	19.7 min[60]	1.7 min[61]

[a] cannot be precisely determined due to the oxidation of the ligand P—H bond under this reaction conditions.

Under the examined acidic conditions, *cis*-**I** ⇌ *trans*-**III** also takes place. Nevertheless, since both the isomerisation to *trans*-**III** complex and its dissociation were found to be much slower processes under such conditions (details can be found in *Appendix 4*), it was possible to determine the half of the *cis*-**I**-[Cu(H$\mathbf{L}^{\mathbf{PP}}$)] complex. The unexpectedly high half-life of approximately 2.7 h makes the complex very kinetically inert. The analogous value for the *cis*-**I**-[Cu($\mathbf{L}^{\mathbf{BPin}}$)] isomer cannot be, however, precisely determined, since it was found that unexpected oxidation of *cis*-**I**-[Cu($\mathbf{L}^{\mathbf{BPin}}$)] to *cis*-**I**-[Cu(H$\mathbf{L}^{\mathbf{PP}}$)] is also occurring. The dissociation kinetics therefore corresponds to the mixture of both species. On the other hand, since the values obtained for experiments starting from either pure *cis*-**I**-[Cu($\mathbf{L}^{\mathbf{BPin}}$)] and *cis*-**I**-[Cu(H$\mathbf{L}^{\mathbf{PP}}$)] yielded almost identical dissociation rates, the *in vitro* kinetic inertness of *cis*-**I**-[Cu($\mathbf{L}^{\mathbf{BPin}}$)]

is probably very similar to that of *cis*-**I**-[Cu(H$\mathbf{L}^{PP}$)]. This indicates that there is no significant influence of the terminal substituent (*i.e.* —H for $H_2\mathbf{L}^{BPin}$ and —OH for $H_3\mathbf{L}^{PP}$) on the overall *in vitro* kinetic inertness.

The half-life obtained for *cis*-**I**-[Cu(H$\mathbf{L}^{PP}$)] is significantly higher than that of complexes of related ligands with two methylphosphonate pendant arms. This can be explained by the geometry of the complexes. One uncoordinated methylphosphonate arm of *cis*-**I**-[Cu($H_2\mathbf{TE_2P^{1,8}}$)] and *cis*-**I**-[Cu($H_2\mathbf{ME_2TE_2P^{1,8}}$)] is protonated at the used pH range[60],[61] and, thus, can assist in the transfer of H^+ ion to one of the ring nitrogen atoms which results in dissociation of the complex. Contrary, the uncoordinated methylphosphonate moiety in the *cis*-**I**-[Cu(H$\mathbf{L}^{PP}$)] complex (also protonated at the used pH range) cannot easily participate in intramolecular protonation of the ring nitrogen atoms due to the steric reasons (this phenomenon can be easily observed on the crystal structure of related *trans*-**III**-[Cu(H$\mathbf{L}^{PP}$)] isomer presented on **Figure 23**). More details about the dissociation kinetics can be found in *Appendix 4*.

5.8. Adsorption properties

The adsorption of ligands $H_2\mathbf{L}^{BPin}$ and $H_3\mathbf{L}^{PP}$ and of their Cu^{2+} complexes (both *cis*-**I** and *trans*-**III** isomers) onto hydroxyapatite (**HA**, commonly used model of bone tissue) was investigated. The experimental conditions were similar to those used for ligand $H_2\mathbf{L^3}$ as mentioned above. It was shown that the ligands as well as their Cu^{2+} complexes possesses low affinity to **HA**. This indicates that adsorption ability of the geminal phosphino-phosphonate group (present in the pendant arm of ligand $H_3\mathbf{L}^{PP}$ and its complexes) resembles much more behaviour of the geminal bis(phosphinate) group than that of geminal bis(phosphonates). As a consequence, the desired low affnity to bone tissue allows attachment of various targeting groups to both ligands $H_2\mathbf{L}^{BPin}$ and $H_3\mathbf{L}^{PP}$ to alter their *in vivo* tissue uptake at will. More details about the adsorption experiments can be found in *Appendix 4*.

6. Conclusions

The fundamental knowledge about geminal bis(phosphinates) was gathered on eleven compounds $H_2\mathbf{L^1}$ – $H_4\mathbf{L^{11}}$ and summarized in three related papers (*Appendix 1 – Appendix 3*). Several synthetic pathways were successfully employed while some unsuccessful attempts led to the discovery of limited stability of the geminal phosphinate moiety with P—H bond in aqueous solutions. The products of hydrolysis were identified and isolated, and decomposition conditions (both structure- and pH-dependent) were determined. This allowed reasonable prediction of chemical stability of geminal bis(phosphinates) in general and was further utilized in the design of macrocyclic derivatives. The acid-base and coordination properties were determined and it was found that position of primary amine group is crucial for thermodynamic stability of complexes with Cu^{2+} and other selected divalent ions. It was also found that presence

of hydroxy group directly attached to the central carbon atom has dominant influence on the coordination modes of the whole bis(phosphinate) molecules. Coordination modes in the solid state were in good agreement with the results obtained in solution. Additionally, it was proven that synthesized geminal bis(phosphinates) possesses the desired low affinity to hydroxyapatite and, thus, low adsorbtion onto bone tissue is expected.

This knowledge about geminal bis(phosphinates) was utilized in the design and synthesis of two novel derivatives of macrocyclic ligand **Cyclam**, bearing either one geminal bis(phospinate) or phosphino-phosphonate pendant arm ($H_2\mathbf{L}^{\mathbf{BPin}}$ and $H_3\mathbf{L}^{\mathbf{PP}}$). Both ligands were synthesized by efficient procedures with high yields, possesses high stability of complexes with divalent transition metal ions and high selectivity for Cu^{2+} ion. Further, neither ligands nor their Cu^{2+} complexes were found to show measurable hydroxyapatite sorption and, so, desired negligible bone uptake *in vivo* could be expected. The ligands show significantly increased rate of Cu^{2+} complexation when compared with non-substituted or acetate-substituted macrocycles. The extremely fast complex formation is result of the ligand structure – presence of weakly coordinating bis(phosphinate) or phosphinato-phosphonate pendant arm forming an *out-of-cage*‡ intermediate complex. Since only phosphinate moiety close to the macrocyclic cavity is coordinated (due to the steric reasons), the second phosphinate or phosphonate group cannot effectively assist in intramolecular protonation of the ring nitrogen atoms; it is probably the reason for the unexpectedly high *in vitro* kinetic inertness of the complexes.

Rare combination of simple ligand synthesis, extremely fast Cu^{2+} complex formation and very high *in vitro* kinetic inertness together with presumed low *in vivo* bone adsorption predestines the ligands for complexation of Cu^{2+} radionuclides and applications in nuclear medicine.

7. Experimental

Commercially available chemicals were obtained with sufficient purity and used as received except ammonium hypophosphite (recrystallized from water and dried over P_2O_5) and H_2**MBPin** (prepared from commercially available methylene-bis(dichlorophosphine) **MBDCP**, **Figure 26**).

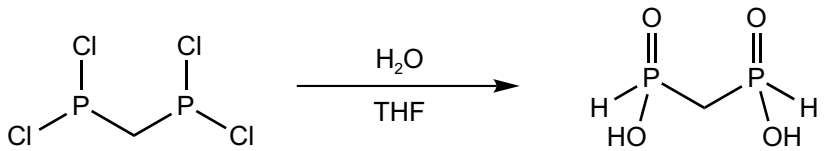

MBDCP H_2**MBPin**

Figure 26. Synthesis of H_2**MBPin** from **MBDCP**.

The synthesized ligands were purrified by commonly used techniques (*e.g.* extraction, crystallization) without need of any HPLC purification. Due to the presence of various polar functional groups in studied ligands, column chromatography with various ion-exchange resins as stationary phases was conveniently used. Compounds were isolated in a form of solid

material (using crystallization, lyophilization, solidification of oils under vacuum or formation of suitable salts) as either in *zwitterionic* form or as a salt (accompanied by elemental analysis for each separate batch). The ligands were also characterized by commonly used techniques (*e.g.* by NMR, MS, HRMS, TLC, RTG difraction). Detailed synthetic procedures of all studied ligands can be found in *Appendix 1 – Appendix 4*.

The complexes with ligands $H_2\mathbf{L^5}$ – $H_4\mathbf{L^{11}}$ were prepared by mixing of ligand with various metal ion salts and adjusting pH to desired values. The complexes were characterized in solution by UV-Vis spectroscopy (both CT and d–d regions) and were not further purified or isolated. Several complexes yielded single crystals suitable for X-ray analysis. More details can be found in *Appendix 2* and *Appendix 3*.

The *cis*-**I**-[Cu($\mathbf{L^{BPin}}$)] and *cis*-**I**-[Cu(H$\mathbf{L^{PP}}$)] isomers were prepared by reaction of the corresponding ligand with $Cu(OAc)_2$ followed by ion-exchange resin purification and isolation as deep blue solids. The *trans*-**III**-[Cu($\mathbf{L^{BPin}}$)] and *trans*-**III**-[Cu(H$\mathbf{L^{PP}}$)] isomers were prepared by incubation of *cis*-**I** isomers in alkaline solutions. The resulting mixtures were purified on column chromatography (on SiO_2 and then on ion-exchange resin) followed by isolations as violet solids. All four isomers were characterized by elemental analysis (for each batch), MS, 2D TLC, UV-Vis (both CT and d–d regions, precise concentration required for molar extinction coeficients were determined by AAS) and, in the case of *trans*-**III**-[Cu(H$\mathbf{L^{PP}}$)], by single-crystal X-ray analysis. More details can be found in *Appendix 4*.

The acidbase and coordination properties of ligands were studied by potentiometric or NMR titrations. Methodology of the potentiometric titrations and processing of the experimental data were analogous to those previously reported.[68]

Formation kinetics of *cis*-**I** species was followed using *stopped-flow* technique (with diode-array detection) at pH range 2.2–6.4. The *cis*-**I** $\rightleftharpoons$ *trans*-**III** interconversion process was studied on UV-Vis spectrophotometer at [OH^-] range 20–100 mM. The acid-assisted decomplexation kinetics were done under standard conditions (*i.e.* in (H, Na)ClO_4 system). Decrease in intensity of both CT and d–d bands were measured by UV-Vis spectroscopy. The kinetic experiments were accompanied by TLC analysis (SiO_2) where all four species are easily distinguishable (**Table 6**). More details can be found in *Appendix 4*.

Table 6. TLC retention factors (R_F) of studied *cis*-**I** and *trans*-**III** species on SiO_2 (Merck 1.0554 F254, iPrOH–*conc. aq.* NH_3–H_2O 7:3:3).

	cis-**I**-[Cu($\mathbf{L^{BPin}}$)]	*trans*-**III**-[Cu($\mathbf{L^{BPin}}$)]	*cis*-**I**-[Cu(H$\mathbf{L^{PP}}$)]	*trans*-**III**-[Cu(H$\mathbf{L^{PP}}$)]
R_F	0.6[a]	0.5[b]	0.3[a]	0.2[b]

[a] Deep blue spot. [b] Violet spot.

Adsorption experiments were performed on hydroxyapatite (**HA**) purchased from Fluka (catalogue number 55496; specific surface area 73 $m^2\ g^{-1}$). Ligands or its complexes were incubated 72 h with **HA** at pH 7.4. Amount of the ligand or complex remaining in the supernatant was determined by UV-Vis spectroscopy (more details in *Appendix 1* and *Appendix 4*).

8. References

[1] Saha, G. B.: *Fundamentals of Nuclear Pharmacy – 5th ed.*, Springer-Verlag: New York, **2004**.

[2] Christian, P. E.; Waterstram-Rich, K. M.: *Nuclear Medicine and PET/CT – 6th ed.*, Mosby Elsevier: St. Louis, **2007**.

[3] Pauwels, E. K. K.; Sturm, E. J. C.; Bombardieri, E.; Cleton, F. J.; Stokkel, M. P. M.: *J. Cancer. Res. Clin. Oncol.*, **126**(10), 549–559 (2000).

[4] Basu, S.; Kwee, T. C.; Surti, S.; Akin, E. A.; Yoo, D.; Alavi, A.: *Ann. N.Y. Acad. Sci.*, **1228**, 1–18 (2011).

[5] McBride, W. J.; Sharkey, R. M.; Karacay, H.; D'Souza, C. A.; Rossi, E. A., Laverman, P.; Chang, C.-H.; Boerman, O. C.; Goldenberg, D. M.: *J. Nucl. Med.*, **50**(6), 991–998 (2009).

[6] Anderson, C. J.; Welch, M. J.: *Chem. Rev.*, **99**(9), 2219–2234 (1999).

[7] Wadas T. J.; Wong E. H.; Weisman, G. R., Anderson, C. J.: *Curr. Pharm. Des.*, **13**(1), 3–16 (2007).

[8] Guo, Y.; Ferdani, R.; Anderson, C. J.: *Bioconjugate Chem.*, 23(7), **1470**–1477 (2012).

[9] Zinn, K. R.; Chaudhuri, T. R.; Cheng, T. P.; Morris, J. S.; Meyer, W. A.: *Cancer*, **73**(3), 774–778 (1994).

[10] Szelecsenyi, F.; Blessing, G.; Qaim, S. M.: *Appl. Radiat. Isot.*, **44**(3), 575–580 (1993).

[11] McCarthy, D. W.; Shefer, R. E.; Klinkowstein, R. E.; Bass, L. A.; Margenau, W. H.; Cutler, C. S.: *Nucl. Med. Biol.*, **24**(1), 35–43 (1997).

[12] Wadas, T. J.; Wong, E. H.; Weisman, G. R.; Anderson, C. J.: *Chem. Rev.*, **110**(5), 2858–2902 (2010).

[13] Perazella, M. A: *Clin. J. Am. Soc. Nephrol.*, **4**(2), 461–469 (2009).

[14] Mewis, R. E; Archibald, S. J.: *Coord. Chem. Rev.*, **245**(15–16), 1686–1712 (2010).

[15] Smith, S. V.: *J. Inorg. Biochem.*, **98**(11), 1874–1901 (2004).

[16] Fleisch, H.: *Bisphosphonates in Bone Disease – 4th ed.*, Academic Press: London, **2000**.

[17] Fleisch, H.: *Endocrinol. Rev.*, **19**(1), 80–100 (1998).

[18] Rogers, M. J.; Crockett, J. C.; Coxon, F. P.; Mönkkönen, J.: *Bone*, **49**(1), 34–41 (2011).

[19] Clezardin, P.: *Bone*, **48**(1), 71–79 (2011).

[20] Coleman, R. E.; McCloskey, E. V.: *Bone*, **49**(1), 71– 76 (2011).

[21] Kubíček, V.; Rudovský, J.; Kotek, J.; Hermann, P.; Vander Elst, L.; Muller, R. N.; Kolar, Z. I.; Wolterbeek, H. T.; Peters, J. A.; Lukeš, I.: *J. Am. Chem. Soc.*, **127**(47), 16477–16485 (2005).

[22] Vitha, T.; Kubíček, V.; Hermann, P.; Vander Elst, L.; Muller, R. N.; Kolar, Z. I.; Wolterbeek, H. T.; Breeman, W. A. P.; Lukeš, I.; Peters J. A.: *J. Med. Chem.*, **51**(3), 677–683 (2008).

[23] Vitha, T.; Kubicek, V.; Kotek, J.; Hermann, P.; Vander Elst, L.; Muller, N. M.; Lukes, I.; Peters, J. A.: *Dalton Trans.*, (17), 3204–3214 (2009).

[24] Luckman, S. P.; Coxon, F. P.; Ebetino, F. H.; Russell, R. G. G.; Rogers, M. J.: *J. Bone Miner. Res.*, **13**(11), 1668–1678 (1998).

[25] Ebetino, F. H.; Jamieson, L. A.: *Phosphorus Sulfur Silicon Rel. Elem.*, **51–52**(1–4), 23–26 (1990).

[26] Gobel, R.; Richter, F.; Weichman, H,: *Phosphorus Sulfur Silicon Rel. Elem.*, **73**(1–4), 67–80 (1992).

[27] Gouault-Bironneau, S.; Deprele, S.; Sutor, A.; Montchamp, J.-L.: *Org. Lett.*, **7**(26), 5909–5912 (2005).

[28] Antczak M. I.; Montchamp, J.-L.: *Tetrahedron Lett.*, **49**(41), 5909–5913 (2008).

[29] Kaboudin, B.; Saadati, F.; Yokomatsu, T.: *Synlett*, (12), 1837–1840 (2010).

[30] Loginova, L. P.; Levin, I. V.; Matveeva, A. G.; Pisareva, S. A.; Nifantev, E. E.: *Russ. Chem. Bull.*, **53**(9), 2000–2007 (2004).

[31] Gaizer, F.; Haegele, G.; Goudetsidis, S.; Papadopoulos, H.: *Z. Naturforsch., B: Chem. Sci.*, **45**(3), 323–328 (1990).

[32] King, C.; Roundhill, D. M.; Fronczek, F. R.: *Inorg. Chem.*, **25**(8), 1290–1292 (1986).

[33] King, C.; Auerbach, R. A.; Fronczek, F. R.; Roundhill, D. M.: *J. Am. Chem. Soc.*, **108**(18), 5626–5627 (1986).

[34] King, C.; Roundhill, D. M.; Fronczek, F. R.: *Inorg. Chem.*, **26**(25), 4288–4290 (1987).

[35] King, C.; Roundhill, D. M.; Dickson, M. K.; Fronczek, F. R.: *J. Chem. Soc., Dalton Trans.*, (11), 2769–2780 (1987).

[36] Roundhill, D. M.; Shen, Z.-P.; King, C.; Atherton, S. J.: *J. Phys. Chem.*, **92**(14), 4088–4094 (1988).

[37] King, C.; Yin, Y.; McPherson, G. L.; Roundhill, D. M.: *J. Phys. Chem.*, **93**(9), 3451–3455 (1989).

[38] Pan, Q.-J.; Fu, H.-G.; Yu, H.-T.; Zhang, H.-X.: *Inorg. Chem.*, **45**(21), 8729–8735 (2006).

[39] Berti, E.; Cecconi, F.; Ghilardi, C. A.; Midollini, S.; Orlandini, A.; Pitzalis, E.: *Inorg. Chem. Commun.*, **5**(12), 1041–1043 (2002).

[40] Cecconi, F.; Dominguez, S.; Masciocchi, N.; Midollini, S.; Sironi, A.; Vacca, A.: *Inorg. Chem.*, **42**(7), 2350–2356 (2003).

[41] Cecconi, F.; Ghilardi, C. A.; Midollini, S.; Orlandini, A.: *Inorg. Chem. Commun.*, **6**(5), 546–548 (2003).

[42] Cecconi, F.; Dakternieks, D.; Duthie, A.; Ghilardi, C. A.; Gili, P.; Lorenzo-Luis, P. A.; Midollini, S.; Orlandini, A.: *J. Solid State Chem.*, **177**(3), 786–792 (2004).

[43] Ciattini, S.; Costantino, F.; Lorenzo-Luis, P.; Midollini, S.; Orlandini, A.; Vacca, A.: *Inorg. Chem.*, **44**(11), 4008–4016 (2005).

[44] Beckmann, J.; Costantino, F.; Dakternieks, D.; Duthie, A.; Ienco, A.; Midollini, S.; Mitchell, C.; Orlandini, A.; Sorace, L.: *Inorg. Chem.*, **44**(25), 9416–9423 (2005).

[45] Costantino, F.; Midollini, S.; Orlandini, A.; Sorace, L.: *Inorg. Chem. Commun.*, **9**(6), 591–594 (2006).

[46] Midollini, S.; Lorenzo-Luis, P.; Orlandini, A.: *Inorg. Chim. Acta*, **359**(10), 3275–3282 (2006)

[47] Midollini, S.; Orlandini, A.: *J. Coord. Chem.*, **59**(13), 1433–1442 (2006).

[48] Costantino, F.; Midollini, S.; Orlandini, A.: *Inorg. Chim. Acta*, **361**(1), 327–334 (2008).

[49] Issleib, K.; Moegelin, W.; Balszuweit, A.: *Z. Chem.*, **25**(10), 370–371 (1985).

[50] Kašpárek, F.: *Monatsh. Chem.*, **100**(6), 2013–2018 (1969).

[51] Prishchenko, A. A.; Livantsov, M. V.; Novikova, O. P.; Livantsova, L. I.: *Russ. J. Gen. Chem.*, **80**(9), 1889–1890 (2010).

[52] Kubíček, V.; Kotek, J.; Hermann, P.; Lukeš, I.: *Eur. J. Inorg. Chem.*, (2), 333–344 (2007).

[53] Rohovec, J.; Lukeš, I.; Vojtíšek, P.; Císařová, I.; Hermann, P.: *J. Chem. Soc., Dalton Trans.*, (13), 2685–2691 (1996).

[54] Kubíček, V.; Vojtíšek, P.; Rudovský, J.; Hermann, P.; Lukeš, I.: *Dalton Trans.*, (20), 3927–3938 (2003).

[55] Martell, A. E.; Smith, R. M.: *Critical Stability Constants*, vol. 1–6; Plenum Press: New York, **1974–1989**.

[56] Vitha, T.; Kubíček, V.; Hermann, P.; Kolar, Z. I.; Wolterbeek, H. T.; Peters, J. A.; Lukeš, I.: *Langmuir*, **24**(5), 1952–1958 (2008).

[57] Bosnich, B.; Poon, C. K.; Tobe, M.: *Inorg. Chem.*, **4**(8), 1102–1108 (1965).

[58] Meyer, M.; Dahaoui-Gindrey, V.; Lecomte C.; Guilard R.: *Coord. Chem. Rev.*, **178–180**(2), 1313–1405 (1998).

[59] Füzerová, S.; Kotek, J.; Císařová, I.; Hermann, P.; Binnemans, K.; Lukeš, I.: *Dalton Trans.*, (17), 2908–2915 (2005).

[60] Kotek, J.; Lubal, P.; Hermann, P.; Císařová, I.; Lukeš, I.; Godula, T.; Svobodová, I.; Táborský, P.; Havel, J.: *Chem. Eur. J.*, **9**(1), 233–248 (2003).

[61] Svobodová, I.; Havlíčková, J.; Plutnar, J.; Lubal, P.; Kotek, J.; Hermann, P.: *Eur. J. Inorg. Chem.*, (24), 3577–3592 (2009).

[62] Lubal, P.; Maleček, J.; Hermann, P.; Kotek, J.; Havel, J.: *Polyhedron*, **25**(9), 1884–1892 (2006).

[63] Ozay, H.; Baran, Y.; Miyamae, H.: *J. Coord. Chem.*, **64**(8), 1469–1480 (2011).

[64] Motekaitis, R. J.; Rogers, B. E.; Reichert, D. E.; Martell, A. E.; Welch, M. J.: *Inorg. Chem.*, **35**(13), 3821–3827 (1996).

[65] Irving, H. M. N. H.; Willams, R. J. P.: *J. Chem. Soc.*, 3192–3210 (1953).

[66] Wu, S.-L.; Horrocks, W. DeW.: *Inorg. Chem.*, **34**(14), 3724–3732 (1995).

[67] Moreau, J.; Guillon, E.; Pierrard, J.-C.; Rimbault, J.; Port, M.; Aplincourt, M.: *Chem. Eur. J.*, **10**(20), 5218–5232 (2004).

[68] Kubíček, V.; Vojtíšek, P.; Rudovský, J.; Hermann P.; Lukeš, I.: *Dalton Trans.*, (20), 3927–3938 (2003).

9. Contribution

Contribution of T. David to the publications included in his PhD. thesis:

David, T.; Křečková, P.; Kotek, J.; Kubíček, V.; Lukeš; I.: 1-Hydroxy-1,1-bis(H-phosphinates): Synthesis, Stability, and Sorption Properties; *Heteroatom Chem.,* **23**(2), 195–201 (2012).

David, T.; Procházková, S.; Havlíčková, J.; Kotek, J.; Kubíček, V.; Hermann, P.; Lukeš; I.: Methylene-bis[(aminomethyl)phosphinic acids]: Synthesis, Acid-base and Coordination Properties; *Dalton Trans.,* **42**(7), 2414–2422 (2013).

David, T.; Procházková, S.; Kotek, J.; Kubíček, V.; Hermann, P.; Lukeš, I.: Aminoalkyl-1,1-bis(phosphinic acids): Stability, Acid-base and Coordination properties; *Eur. J. Inorg. Chem.*, (2014) – **accepted for publication**.

David, T.; Kubíček, V.; Kotek, J.; Hermann, P.; Lubal, P.; Lukeš, I.: Cyclam Derivatives with Bis(phosphinate) and Phosphinato-phosphonate Pendant Arms: Fast and Efficient Cu(II) Complexation for Radiomedical Applications – **manucript in preparation**.

Mr. David's contribution in all presented publications was dominant. He synthesized all the studied bis(phosphinates) and macrocyclic ligands as well as their complexes. All NMR measurements, interpretation of the spectra and adsorption experiments were done exclusively by him. He performed himself all kinetic measurements as well as interpretation of the results including dissociation, formation and isomerisation of Cu^{2+} complexes. Potentiometric titrations were arranged in cooperation with other student (S. Procházková) and technician (J. Havlíčková), one third of these measurements were done by Mr. David. Nevertheless, he participated on the evaluation of all results. X-ray structures were solved by doc. J. Kotek on single crystals prepared by Mr. David.

Mr. David actively participated in evaluation and discussion of the results as well as in preparation of the publications.

In Prague, 25th of June 2014

.....
prof. RNDr. IVAN LUKEŠ, CSc.
(*supervisor*)

.....
doc. RNDr. VOJTĚCH KUBÍČEK, PhD.
(*consultant*)

10. Acknowledgement

I would like to thank my wife Anička, my parents and family for their love, patience and encouragement. This work would certainly not be possible to estabilish without their all-embracing support.

Many thanks belong to Ivan Lukeš, Vojtěch Kubíček and Petr Hermann for kind leadership and opportunity to work in their laboratory with a bunch of fantastic people. I will never forget the time pleasantly spent there.

I would like to thank Přemysl Lubal for opportunity to measure crucial kinetic experiments in his laboratory during my short missions there.

Thanks for the payoff in this work to all contributors, namely Soňa Procházková, Ondrej Gutten, Pavlína Křečková, Jana Havlíčková, Jan Kotek and Ivana Císařová, through which the whole piece become more consistent.

My thanks also belong to Bohumír Grüner and Aleš Růžička for their willingness to oppose my work.

11. Appendixes

Heteroatom Chemistry
Volume 23, Number 2, 2012

1-Hydroxy-1,1-bis(H-phosphinates): Synthesis, Stability, and Sorption Properties

Tomáš David, Pavlína Křečková, Jan Kotek, Vojtěch Kubíček, and Ivan Lukeš

Department of Inorganic Chemistry, Faculty of Science, Charles University in Prague, 128 40 Prague 2, Czech Republic

Received 19 August 2011; revised 24 November 2011

ABSTRACT: *A synthesis of 1-hydroxy-1,1-bis(H-phosphinates) from acylchlorides is described. Solid-state structures of two bis(phosphinates) determined by X-ray diffraction showed variations in the P—C distances. The compounds show negligible sorption on hydroxyapatite and an intermediate chemical stability in aqueous solution. The hydrolysis occurs in acidic as well as alkaline media. Hydrolysis rates of four derivatives show the lowest stability for aromatic derivatives as a result of the electron-withdrawing effect. Main products of hydrolysis are 1-hydroxy-(H-phosphinates) and phosphorous acid.* © 2011 Wiley Periodicals, Inc. Heteroatom Chem 23:195–201, 2012; View this article online at wileyonlinelibrary.com. DOI 10.1002/hc.21003

INTRODUCTION

One of the most studied group of organophosphorus compounds is 1,1-bis(phosphonates) (Fig. 1). The compounds are broadly used in medicine for the treatment of bone diseases and in industry for the protection of various materials against corrosion, and for prevention of salt deposition in technological liquids [1,2]. The applications arise from strong sorption and good coordinating properties of the bis(phosphonate) group. Recently, we have used the bis(phosphonate) group in designing of polydentate ligands that we studied as metal carriers for applications in molecular imaging [3–5]. The compounds show high affinity to calcified tissues as a result of strong sorption on hydroxyapatite (HA). The introduction of the bis(phosphonate) group also brings other advantages, such as fast complexation of metal ions and good solubility of the complexes. Unfortunately, these advantages could not be applied for in vivo applications, as the high uptake of bis(phosphonates) by bone represents their limitation. The limitation could be overcome by using bis(phosphinates) instead of bis(phosphonates). This aim led us to start our research with the investigation of synthesis and characterization of "simple" bis(phosphinates).

Unfortunately, compared with bis(phosphonates), bis(phosphinates) attracted much less attention. Especially for those bearing hydrogen on phosphorus atom bis(H-phosphinates) (Fig. 1), synthetic information is rather scarce [6–15], and data on their properties and behavior are completely missing.

Here, we report on synthesis, sorption, and stability studies of 1-hydroxy-1,1-bis(H-phosphinates). The compounds show negligible sorption on HA and

Correspondence to: V. Kubíček; e-mail: kubicek@natur.cuni.cz.
Contract grant sponsor: Grant Agency of the Czech Republic.
Contract grant number: P207/10/P153.
Contract grant sponsor: Grant Agency of Charles University.
Contract grant number: 310011.
Contract grant sponsor: Long-Term Research Plan of the Ministry of Education of the Czech Republic.
Contract grant number: MSM0021620857.
This work was carried out in the framework of COST CM802 (PhoSciNet) Action.

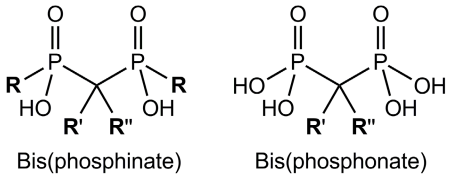

FIGURE 1 Structure of bis(phosphonates) and bis(phosphinates).

limited stability in aqueous solutions. The decomposition yields 1-hydroxy-(H-phosphinates) quantitatively, and so the reaction sequence could be considered as an alternative route for the preparation of 1-hydroxy-(H-phosphinates) starting from acylchlorides.

EXPERIMENTAL

Materials and Methods

Commercially available chemicals were obtained with sufficient purity and used as received. Ammonium hypophosphite was recrystallized from water and dried over P_2O_5. NMR spectra were recorded on a Varian Unity*Plus* 300 (^{1}H) spectrometer. For the measurements in D_2O, *t*-BuOH was used as an internal standard with the methyl signal referenced to 1.2 ppm (^{1}H) or 31.2 ppm (^{13}C). One percent of H_3PO_4 in D_2O was used as an external reference for ^{31}P NMR. NMR spectra were recorded at 25°C. ESI-MS spectra were recorded on a Bruker Esquire 3000 spectrometer equipped with an electrospray ion source and ion trap detection. TLC was performed with silica gel on aluminum sheets (Merck 1,0554 F_{254}); the compounds were detected with UV fluorescence (λ = 254 nm) or visualized by iodine vapors.

1-Hydroxy-1,1-bis(H-phosphinates)—General Method

Under an argon atmosphere, dry $NH_4H_2PO_2$ (20.0 g, 238 mmol) was suspended in $(Me_3Si)_2NH$ (100 mL) and the mixture was heated overnight at 110°C (bath temperature) under a flow of argon. The mixture containing $(Me_3SiO)_2PH$ was cooled to room temperature (RT), and dry dichloromethane (200 mL) was added. The solution of acylchloride (30 mmol) in dry dichloromethane (200 mL) was added dropwise, and the mixture was stirred overnight at RT. Afterward, the resuting solution was dropped into EtOH (400 mL) for hydrolysis of the silyl groups. After removal of volatiles under reduced pressure, the crude product was dissolved in water and purified on a cation exchange resin (Dowex 50, elution H_2O/EtOH 1:1) for the removal of ammonium cations. The fractions containing product were combined and evaporated under reduced pressure. The product was twice dissolved in ethanol and evaporated to remove traces of water. The resulting oil was dissolved in tetrahydrofurane (20 mL), and the solution was slowly dropped into stirred dichloromethane (300 mL).

For 1-hydroxy-1-phenyl-methyl-1,1-bis(H-phosphinic acid) (PhPin2) and 1-hydroxy-2-phenyl-ethyl-1,1-bis(H-phosphinic acid) (BnPin2), the product was slowly crystallized as a white solid and that was filtered, washed with dichloromethane, and dried under reduced pressure.

For 1-hydroxy-ethyl-1,1-bis(H-phosphinic acid) (MePin2) and 1-hydroxy-ethyl-1,1-bis(H-phosphinic acid) (EtPin2), the product was precipitated as colorless oil. The dissolution in tetrahydrofurane and precipitation in dichloromethane were repeated twice to remove remaining hypophosphorous acid. The resulting oil was dissolved in 5% aqueous ammonia and evaporated. Finally, the product obtained as colorless oil was dried under reduced pressure.

1-Hydroxy-1-phenyl-methyl-1,1-bis(H-phosphinic Acid) (PhPin2). Yield: 57% as H_2PhPin2·H_2O. Anal. Calcd. for $C_7H_{10}O_5P_2\cdot H_2O$: C, 33.1; H, 4.7. Found: C, 33.0; H, 4.5. NMR (D_2O): ^{1}H δ7.12 (P*H*, 2H, d, $^1J_{PH}$ = 574 Hz); 7.43–7.61 (arom., 5H); ^{13}C{1H} δ76.8 (P*C*P, t, $^1J_{PC}$ = 97 Hz); 127.7 (arom., t, J_{PC} = 4.35 Hz); 130.6 (arom., s); 131.2 (arom., s); 135.6 (arom., s); ^{31}P δ32.0 (dd, $^1J_{PH}$ = 574 Hz, $^3J_{PH}$ = 31 Hz). ESI-MS: *m/z* 530.7 [2M + Na^++ K – $3H^+$]$^-$; 546.6 [2M + $2K^+$– $3H^+$]$^-$. TLC (MeCN:MeOH:NH_4OH 3:1:2): R_f = 0.4.

1-Hydroxy-2-phenyl-ethyl-1,1-bis(H-phosphinic Acid) (BnPin2). Yield: 57% as H_2BnPin2·1/4H_2O. Anal. Calcd. for $C_8H_{12}O_5P_2\cdot{}^1/_4H_2O$: C, 37.7; H, 5.0. Found: C, 37.9; H, 4.8. NMR (D_2O): ^{1}H δ3.27 (CH_2, t, $^3J_{HP}$ = 13 Hz); 6.87 (P*H*, d, 2H, $^1J_{PH}$ = 542 Hz); 7.30–7.51 (arom., 5H); ^{13}C{1H} δ35.8 (*C*H_2, s); 73.5 (P*C*P, t, $^1J_{PC}$ = 99 Hz); 129.7 (arom., s); 130.8 (arom., s); 133.5 (arom., s); 136.0 (arom., t, J_{CP} = 8.3 Hz); ^{31}P δ29.5 (dt, $^1J_{PH}$ = 566 Hz, $^3J_{PH}$ = 31 Hz). ESI-MS: *m/z* 248.5 [M – H^+]$^-$; 522.7 [2M + K^+– $2H^+$]$^-$; 558.7 [2M + K^++ Na^+– $3H^+$]$^-$. TLC (MeCN:MeOH:NH_4OH 3:1:2): R_f = 0.4.

1-Hydroxy-ethyl-1,1-bis(H-phosphinic Acid) (MePin2). Yield: 55% as $(NH_4)_2$MePin2·H_2O. Anal. Calcd. for $C_2H_9O_5P_2\cdot(NH_3)_2\cdot H_2O$: C, 10.6; H, 7.1; N, 12.4. Found: C, 10.8; H, 7.2; N, 12.5. NMR (D_2O): ^{1}H

δ1.34 (CH_3, t, 3H, $^3J_{HP}$ = 8 Hz); 6.87 (PH, d, 2H, $^1J_{HP}$ = 525 Hz); ^{13}C{^{1}H} δ16.8 (CH_3, s); 73.7 (PCP, t, $^1J_{PC}$ = 89 Hz); ^{31}Pδ25.7 (m). ESI-MS: *m/z* 172.5 [M – H$^+$]$^-$; 384.4 [2M + K$^+$– 2H$^+$]$^-$; 558.6 [3M + K$^+$– 2H$^+$]$^-$; 732.7 [4M + K$^+$– 2H$^+$]$^-$. TLC (MeCN:MeOH:NH_4OH 3:1:2): R_f = 0.3.

1-Hydroxy-ethyl-1,1-bis(H-phosphinic Acid) (EtPin2). Yield: 45% as $(NH_4)_2$EtPin2·1/2H_2O. Anal. Calcd. for $C_2H_9O_5P_2\cdot(NH_3)_2\cdot{}^1/_2H_2O$: C, 15.6; H, 7.4; N, 12.1; P, 26.7. Found: C, 15.4; H, 7.3; N, 11.9; P, 26.7. NMR (D_2O): ^{1}H δ1.07 (CH_3, td, 3H, $^3J_{HH}$ = 8 Hz, $^4J_{HP}$ = 1 Hz); (CH_2, m, 2H); 7.02 (PH, dt, 2H, $^1J_{HP}$ = 549 Hz, $^4J_{HH}$ = 15 Hz); ^{13}C{^{1}H} δ8,1 (CH_3, t, $^3J_{CP}$ = 7 Hz); 24.0 (CH_2, s); 74.2 (PCP, t, $^1J_{PC}$ = 95 Hz); ^{31}P δ26.6 (d, $^1J_{PH}$ = 550 Hz). ESI-MS: *m/z* 186.5 [M – H$^+$]$^-$; 386.5 [2M + Na$^+$– 2H$^+$]$^-$. TLC (MeCN:MeOH:NH_4OH 3:1:2): R_f = 0.3.

1-Hydroxy-(H-Phosphinates)—General Method

1-Hydroxy-1,1-bis(H-phosphinate) (2.5 mmol) was dissolved in 6 M hydrochloric acid (15 mL) and heated at 80°C for 4–50 days (for more details, see below). Then, the solution was evaporated under reduced pressure and the product was purified by column chromatography (SiO_2, for the mobile phase and R_f, see below). Resulting ammonium salts were purified on a strong cation exchange resin (Dowex 50, elution with water). The resulting product was isolated in the form of free acid by freeze–drying (aromatic derivatives) or rotary evaporation (aliphatic derivatives).

1-Hydroxy-1-phenyl-methyl-(H-phosphinic Acid). Reaction time: 4 days. Purification: mobile phase MeCN:MeOH:NH_4OH 3:1:2; R_f = 0.8. Yield: 59% of white powder. Anal. Calcd. for $C_7H_9P_1O_3$: C, 48.8; H, 5.3. Found: C, 48.5; H, 5.1. NMR (DMSO-d_6): ^{1}H δ4.75 (CHP, d, 1H, $^2J_{HP}$ = 9 Hz); 6.85 (PH, d, 1H, $^1J_{HP}$ = 518 Hz); 7.43 (arom., m, 5H); ^{13}C{^{1}H} δ71.7 (CHP, d, $^1J_{CP}$ = 105 Hz); 127.0, (arom., d, J_{CP} = 5 Hz), 130.1 (arom., d, J_{CP} = 3 Hz), 130.7 (arom., d, J_{CP} = 2 Hz), 137.6 (arom., s); ^{31}P δ28.8 (dd, $^1J_{PH}$ = 518 Hz, $^2J_{PH}$ = 9 Hz). ESI-MS: *m/z* 170.5 [M – H$^+$]$^-$. TLC (MeCN:MeOH:NH_4OH 10:5:1): R_f = 0.6.

1-Hydroxy-2-phenyl-ethyl-(H-phosphinic Acid). Reaction time: 15 days. Purification: mobile phase MeCN:MeOH:NH_4OH 3:1:2; R_f = 0.4. Yield: 72% of white powder. Anal. Calcd. for $C_8H_{11}P_1O_3$: C, 51.6; H, 6.0. Found: C, 51.7; H, 5.8. NMR (DMSO-d_6): ^{1}H δ2.94 (CH_2, m, 2H); 3.82 (CHP, m, 1H); 6.85 (PH, d, 1H, $^1J_{HP}$ = 510 Hz); 7.36 (arom., m, 5H); ^{13}C{^{1}H} δ38.2 (CH_2, d, $^2J_{CP}$ = 5 Hz) 74.4 (CHP, d, $^1J_{CP}$ = 108 Hz); 126.5 (arom., s), 128.6 (arom., s), 129.3 (arom., s), 138.4 (arom., d, J_{CP} = 14 Hz); ^{31}P δ31.1 (d, $^1J_{PH}$ = 510 Hz). ESI-MS: *m/z* 184.5 [M – H$^+$]$^-$. TLC (MeCN:MeOH:NH_4OH 10:5:1): R_f = 0.6.

1-Hydroxy-ethyl-(H-phosphinic Acid). Reaction time: 50 days. Purification: mobile phase MeCN:MeOH:NH_4OH 3:1:2; R_f = 0.8. Yield: 65% of colorless oil. NMR (DMSO-d_6): ^{1}H δ1.18 (CH_3, m, 3H); 3.67 (CH, m, 1H); 6.67 (PH, d, 1H, $^1J_{HP}$ = 520 Hz); ^{13}C{^{1}H} δ15.8 (CH_3, d, $^2J_{CP}$ = 3 Hz); 64.4 (CH, d, $^1J_{CP}$ = 113 Hz); ^{31}P δ34.3 (dq, $^1J_{PH}$ = 520 Hz; $^3J_{PH}$ = 17 Hz). ESI-MS: *m/z* 108.7 [M – H$^+$]$^-$. TLC (MeCN:MeOH:NH_4OH 10:5:1): R_f = 0.4.

1-Hydroxy-propyl-(H-phosphinic Acid). Reaction time: 25 days. Purification: mobile phase MeCN:MeOH:NH_4OH 3:1:2; R_f = 0.8. Yield: 57% of yellowish oil. NMR (DMSO-d_6): ^{1}H δ0.84 (CH_3, t, 3H, $^3J_{HH}$ = 7 Hz); 1.51 (CH_2, m, 2H); 3.53 (CH, m, 1H); ^{13}C{^{1}H} δ10.1 (CH_3, d, $^3J_{CP}$ = 13 Hz); 22.9 (CH_2, d, $^2J_{CP}$ = 4 Hz); 70.8 (CH, d, $^1J_{CP}$ = 111 Hz); ^{31}P δ34.3 (d, $^1J_{PH}$ = 541 Hz). ESI-MS: *m/z* 122.7 [M – H$^+$]$^-$. TLC (MeCN:MeOH:NH_4OH 10:5:1): R_f = 0.5.

Kinetics of Hydrolysis

The hydrolysis of the bis(phosphinates) was followed by ^{31}P NMR at the compound concentration of 10 mM. The experiments were performed at constant temperature (80°C) maintained by a thermostated bath. The experiments were carried in buffered solutions (concentration 1 mol dm^{-3}; HCl, pH 0; $ClCH_2COOH$/NaOH, pH 2.7; Tris/HCl, pH 8.5; ethanolamine/HCl, pH 9.8; NaOH, pH 14).

X-Ray Diffraction

Single crystals of H_2PhPin2·2H_2O and H_2BnPin2 were obtained by diffusion of dichloromethane vapor into the tetrahydrofurane solution. The diffraction data were collected at 150 K (Cryostream Cooler, Oxford Cryosystem) using a Nonius Kappa CCD diffractometer and Mo K_α radiation (λ = 0.71073 Å) and analyzed using the HKL DENZO program package [16]. The structures were solved by using direct methods (SIR92) [17] and refined by using a full-matrix least-squares technique (SHELXL97) [18]. All non-hydrogen atoms were refined anisotropically. All hydrogen atoms were located in the difference map of electron density; however, they were placed in theoretical (C—H) or original (O—H) positions with thermal parameters U_{eq}(H) = 1.2 U_{eq}(X) as their free refinement led to some

TABLE 1 Experimental Data of Reported Crystal Structures

	$H_2PhPin2{\cdot}2H_2O$	$H_2BnPin2$
Formula	$C_7H_{14}O_7P_2$	$C_8H_{12}O_5P_2$
Mol wt	272.12	250.12
Color	Colorless	Colorless
Shape	Rod	Rod
Dimensions (mm)	0.33 × 0.25 × 0.14	0.50 × 0.20 × 0.20
Crystal system	Orthorhombic	Monoclinic
Space group	*Pccn* (no. 56)	$P2_1/n$ (no. 14)
a (Å)	14.1991(3)	5.4945 (2)
b (Å)	23.6462 (5)	30.4340 (8)
c (Å)	6.9316 (2)	6.9601(2)
β(°)	90	111.1556 (13)
V (Å^3)	2327.32 (10)	1085.42 (6)
Z	8	4
D_c (g cm^{-3})	1.553	1.531
μ(mm^{-1})	0.391	0.399
F(000)	1136	520
diffractions; observed ($I_o > 2\sigma(I_o)$)	2665; 2447	2473; 2051
parameters	150	136
G-o-f on F^2	1.088	1.050
R; *R*′ (all data)	0.0268; 0.0296	0.0332; 0.0423
wR; *wR*′ (all data)	0.0728; 0.0746	0.0849; 0.0899
difference max; min (e Å^{-3})	0.370; −0.320	0.291; −0.435

unrealistic bond lengths. The compound $H_2PhPin2{\cdot}2H_2O$ can be viewed as $(H_3O)^+$ $(HPhPin2)^-{\cdot}H_2O$ because of a closer location of the corresponding proton to one of solvate water molecules, thus forming an oxonium ion. Both crystal structures are stabilized by a strong hydrogen bond network. Table 1 lists selected crystallographic parameters for the structures reported in this paper. Complete data for the structures have been deposited at the Cambridge Crystallographic Data Centre as CCDC-840182 ($H_2PhPin2{\cdot}2H_2O$) and –840181 ($H_2BnPin2$). A copy of the data can be obtained free of charge on application to CCDC, e-mail: deposit@ccdc.cam.ac.uk.

RESULTS AND DISCUSSION

Synthesis of Bis(phosphinates)

Four derivatives of 1-hydroxy-1,1-bis(H-phosphinic acid) have been synthesized by modification of a described procedure [11]. In comparison with the original work, our reaction sequence proceeds at milder conditions and is performed without isolation of intermediates (Fig. 2). In the first reaction step bis(trimethylsilyl)hypophosphite was generated from ammonium hypophosphite and hexamethyldisilazane [19]. In the second step, the ester was treated at RT with an acid halide to yield the trimethylsilyl derivative of 1-hydroxy-1,1-bis(H-phosphinate). Bis(trimethylsilyl)hypophosphite was used in an excess to reach full conversion of acid chloride. In the final step, the silyl ester groups were removed by a reaction with ethanol. After removing ammonium cations on the ion exchange resin (Dowex 50), the product was isolated by precipitation. The excess of hypophosphorous acid was efficiently removed, as it is soluble in all common solvents. Finally, the aromatic derivatives were isolated in the form of white stable solid and aliphatic derivatives in the form of colorless oil. The compounds are soluble in water, alcohols, and ethers. To assure stability upon storage, the oily

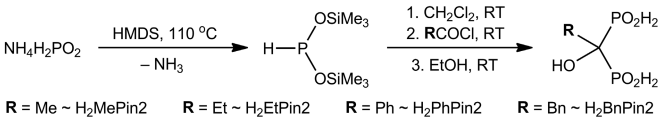

FIGURE 2 Synthesis of 1-hydroxy-1,1-bis(H-phosphinates).

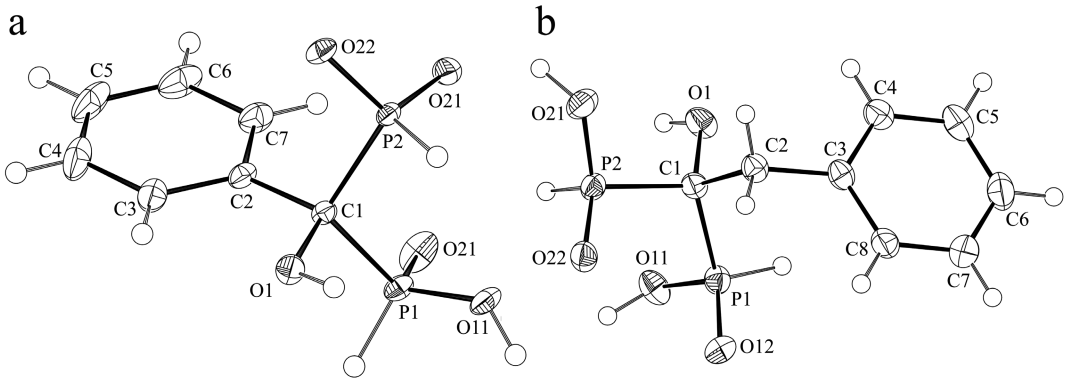

FIGURE 3 Molecular structures of (a) $(HPhPin2)^-$ and (b) $H_2BnPin2$ found in the solid-state structures.

products were converted to ammonium salts by evaporation with aqueous ammonia. The reaction sequence results in high yields (~90%) according to ^{31}P NMR spectra. Although the purification procedure is simple, it resulted in loss of some material, and, therefore, the isolated yields are low (~50%–60%).

X-Ray Structure of Bis(phosphinates)

Single-crystals of both aromatic derives were prepared, and their solid-state structure was determined by X-ray diffraction analysis (Fig. 3). In these structures, the phosphinic acid groups are protonated. The comparison with the previously reported structures of methylenebis(H-phosphinic acid) (H_2mpin) [12], methylenebis(phenylphosphinic acid) (H_2pcp) [20], and benzylidenebis(phosphonic acid) (H_4PhPon2) [21] shows that the geometry of the bis(phosphinic acid) group is mainly governed by steric factors (Table 2). In the case of bis(phosphinates), the presence of the bulky group on the bridging carbon atom results in lengthening of P—C bond distances and increasing of P—C—P angles. The P···P distance is comparable for all compounds except bis(phosphonates). The longest P···P distance found in bis(phosphonate) is most likely due to the steric hindrance of phosphonate groups and a phenyl ring.

Sorption onto Hydroxyapatite

Bone affinity of various compounds is mostly tested in vitro using HA suspension as a model for bone tissue. The compound $H_2BnPin2$ was chosen for sorption experiments as it contains an aromatic group that allows quantification by UV-Vis spectroscopy. A solution of the compound in a Tris buffer (pH 7.5) was treated with various amounts of HA. The results are compared with the sorption curve of 1-hydroxyethyl-1,1-bis(phosphonic acid) (H_4hedp; Fig. 4) that was simulated on the basis of previously published data [22]. Both molecules are of a similar size and, consequently, similar sorption capacity could be expected. Under experimental conditions, H_4hedp is fully adsorbed when using 0.12 g of HA. At the same time, more than 85% of $H_2BnPin2$ remains in the solution. This amount is not significantly decreased even after using a twice higher amount of HA. The results clearly indicate very weak

TABLE 2 Geometry of Bis(phosphinate) Group in Solid State

	H_2PhPin2	*H_2BnPin2*	*H_4PhPon2 [21]*	*H_2mpin [12]*	*H_2pcp [20]*
Distances (Å)					
C1–P1	1.836 (1)	1.833 (2)	1.824/1.835	1.783	1.806
C1–P2	1.847 (1)	1.835 (2)	1.840/1.867	1.792	1.804
P···P	3.060 (1)	3.033 (2)	3.109/3.114	3.045	3.087
Angles (°)					
P1–C1–P1	112.3 (1)	111.5 (1)	116.1/114.5	116.8	117.5

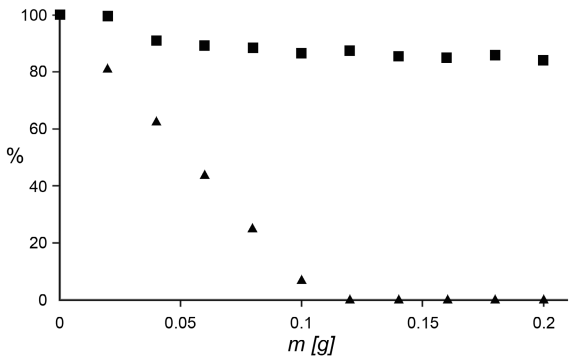

FIGURE 4 Sorption of H_2BnPin2 on HA. The sorbate concentration in solution (expressed as a percentage of the initial concentration) as a function of the added amount of HA. Experimental results obtained for H_2BnPin2 (squares) are compared with the simulation of H_4hedp (triangles) based on previously published data [22].

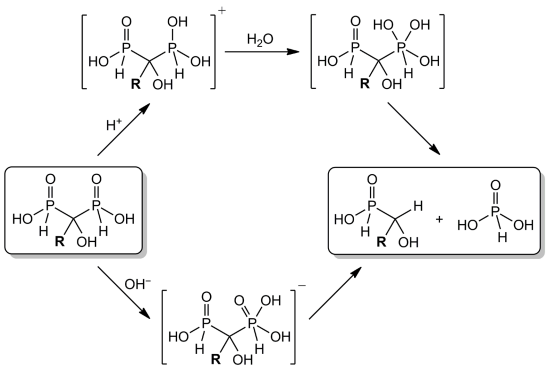

FIGURE 5 Degradation of 1-hydroxy-1,1-bis(H-phosphinates).

adsorption of bis(phosphinate) in comparison with bis(phosphonate).

Stability of Bis(phosphinates) and Synthesis of Mono(phosphinates)

In organic chemistry, malonates are used for the synthesis of monocarboxylates as they undergo a cleavage of one carboxylate group under acidic conditions. On the contrary, 1,1-bis(phosphonates) show an unlimited stability of the P—C—P fragment in aqueous solutions. Our experiments have shown that the stability of 1-hydroxy-1,1-bis(H-phosphinates) is limited in aqueous solutions. The compounds undergo hydrolysis of one P—C bond, yielding 1-hydroxy-(H-phosphinates) and phosphorous acid. As the compound stability is crucial for its chemistry and applications, we studied hydrolysis of the prepared derivatives under various conditions. The hydrolysis was investigated in sealed NMR tubes at 80°C in a thermostated bath and monitored with ^{31}P NMR.

The reactions proceeded under acidic as well as alkaline conditions. The reaction rates differ significantly as a function of the substituent on the bridging carbon atom as well as a function of pH (Table 3). At RT, all studied compounds show negligible or very slow decomposition. Thus, the hydrolysis was followed at 80°C. Maximum conversion found at neutral or weakly alkaline solutions after 30 days for H_2PhPin2 was 7% and 15% at pH 8.5 and 9.8, respectively. In the acidic or in the strongly alkaline environment, the hydrolysis rate is faster. Thus, one could expect two different mechanisms of hydrolysis (Fig. 5). Under acidic conditions, a possibility is the protonation of the P=O group followed by attack of water onto the phosphorus to form a pentacovalent intermediate. The intermediate is unstable, and it immediately collapses and dissociates. Under alkaline conditions, the reaction is probably initiated with an attack of the hydroxide anion on a phosphorus atom followed by dissociation of the P—C bond. In the case of H_2BnPin2, H_2MePin2, and H_2EtPin2, the hydrolysis rate is significantly higher in the acidic solution compared with the alkaline conditions. The most labile compound is H_2PhPin2 with the similar reaction half times of 5–6 h at pH 0 and 14. The low stability of H_2PhPin2 can be ascribed to the electron-withdrawing effect of the aromatic ring.

According to ^{31}P NMR spectra, prolonged heating (4–50 days, 80°C) under the strongly acidic conditions results in almost a quantitative conversion of

TABLE 3 Conversions after 720 h or Half Times for Hydrolysis of Studied Bis(phosphinates) (80°C, I = 1.0 M)

pH	*0.0*	*2.7*	*8.5*	*9.8*	*14.0*
H_2PhPin2	5.6 h	43 h	7%	15%	5.4 h
H_2BnPin2	51 h	122 h	8%	2%	21%
H_2MePin2	286 h	22%	0%	0%	20%
H_2EtPin2	330 h	643 h	0%	3%	6%

bis(phosphinates) to mono(phosphinates) and phosphorous acid. In the case of very long reaction times, traces of hypophosphorous acid could be observed in the solution. The reaction mixtures were purified using column chromatography, and monophosphinates were obtained with moderate yields (57%–72%). Commonly, 1-hydroxyphosphinates are prepared from aldehydes [23,24]. The described preparation of 1-hydroxy-1,1-bis(H-phosphinates) and their consequent hydrolysis could be considered as an alternative route for the preparation of 1-hydroxy-(H-phosphinates) starting from acylchlorides.

CONCLUSION

The synthesis of 1-hydroxy-1,1-bis(H-phosphinates) from acylchlorides results in high yields under mild conditions. The compounds show negligible sorption on HA that indicates low affinity to the bone tissue. The compounds undergo hydrolysis in aqueous solutions. Hydrolysis proceeds under acidic as well as alkaline conditions. The reaction rates are strongly dependent on pH and the nature of the substituent on the bridging carbon atom. The hydrolysis yields 1-hydroxy-(H-phosphinates) and phosphorous acid. The described reaction sequence represents a new way to produce 1-hydroxy-(H-phosphinates) from acylchlorides.

ACKNOWLEDGMENTS

We thank Dr. Ivana Císařová (Charles University in Prague) for performing the X-ray measurements.

REFERENCES

[1] Fleisch, H. Bisphosphonates in Bone Disease; Academic Press: London, 2000.
[2] Quin, L. D. A Guide to Organophosphorus Chemistry; Wiley: New York, 2000.
[3] Kubíček, V.; Rudovský, J.; Kotek, J.; Hermann, P.; Vander Elst, L.; Muller, R. N.; Kolar, Z. I.; Wolterbeek, H. T.; Peters, J. A.; Lukeš I. J Am Chem Soc 2005, 127, 16477–16485.
[4] Vitha, T.; Kubíček, V.; Hermann, P.; Vander Elst, L.; Muller, R. N.; Kolar, Z. I.; Wolterbeek, H. T.; Breeman, W. A. P.; Lukeš, I.; Peters J. A. J Med Chem 2008, 51, 677–683.
[5] Vitha, T.; Kubíček, V.; Kotek, J.; Hermann, P.; Vander Elst, L.; Muller, R. N.; Lukeš, I.; Peters J. A. Dalton Trans 2009, 3201–3214.
[6] Prishchenko, A. A.; Livantsov, M. V.; Novikova, O. P.; Livantsova, L. I.; Petrosyan, V. S. Heteroatom Chem 2009, 20, 319–324.
[7] Prishchenko, A. A.; Livantsov, M. V.; Novikova, O. P.; Livantsova, L. I. Russ J Gen Chem 2009, 79, 1936–1938.
[8] Antczak, M. I.; Montchamp, J.-L. Tetrahedron Lett 2008, 49, 5909–5913.
[9] Gouault-Bironneau, S.; Deprele, S.; Sutor, A.; Montchamp, J.-L. Org Lett 2005, 7, 5909–5912.
[10] Novikova, Z. S.; Odinets, I. L.; Lutsenko, I. F. Zh Obsh Khim 1987, 57, 525–533.
[11] Issleib, K.; Moegelin, W.; Balszuweit, A. Z Chem 1985, 25, 370–371.
[12] King, Ch.; Roundhill, D. M.; Fronczek, F. R. Inorg Chem 1986, 25, 1290–1292.
[13] Prishchenko, A. A.; Novikova, Z. S.; Lutsenko, I. F. Zh Obsh Khim 1977, 47, 2689–2698.
[14] Kašpárek, F. Monatsh Chem 1969, 100 2013–2018.
[15] Prishchenko, A. A.; Livantsov, M. V.; Novikova, O. P.; Livantsova, L. I. Russ J Gen Chem 2010, 80, 1889–1890.
[16] (a) Otwinovski, Z.; Minor, W. HKL DENZO and Scalepack Program Package; Nonius BV: Delft, the Netherlands; 1997; (b) Otwinovski, Z.; Minor, W. Methods Enzymol 1997, 276, 307–326.
[17] Altomare, A.; Cascarano, G.; Giacovazzo, C.; Guagliardi, A.; Burla, M. C.; Polidori G.; Camalli, M. J Appl Crystallogr 1994, 27, 435.
[18] Sheldrick, G. M. SHELXL97, Program for Crystal Structure Refinement from Diffraction Data, University of Göttingen: Göttingen, Germany; 1997.
[19] Voronkov, M. G.; Marmur, L. Z. Zh Obshch Khim 1970, 40, 2135–2136.
[20] Costantino, F.; Ienco, A.; Midollini, S.; Orlandini, A.; Sorace, L.; Vacca A. Eur J Inorg Chem 2008, 3046–3055.
[21] Lecouvey, M.; Barbey, C.; Navaza, A.; Neuman, A.; Prané, T. Acta Cryst C 2002, 58, o521–o524.
[22] Vitha, T.; Kubíček, V.; Hermann, P.; Kolar, Z. I.; Wolterbeek, H. T.; Peters, J. A.; Lukeš, I. Langmuir 2008, 24, 1952–1958.
[23] Hata, T.; Mori, H.; Sekine, M. Chem Lett 1977, 1431–1434.
[24] Albouy, D.; Brun, A.; Munoz A.; Etemad-Moghadam, G. J Org Chem 1998, 63, 7223–7230.

Dalton Transactions

RSC Publishing

PAPER

Methylene-bis[(aminomethyl)phosphinic acids]: synthesis, acid–base and coordination properties†

Cite this: *Dalton Trans.*, 2013, **42**, 2414

Tomáš David, Soňa Procházková, Jana Havlíčková, Jan Kotek, Vojtěch Kubíček,* Petr Hermann and Ivan Lukeš

Three symmetrical methylene-bis[(aminomethyl)phosphinic acids] bearing different substituents on the central carbon atom, $(NH_2CH_2)PO_2H–C(R^1)(R^2)–PO_2H(CH_2NH_2)$ where R^1 = OH, R^2 = Me ($H_2\mathbf{L^1}$), R^1 = OH, R^2 = Ph ($H_2\mathbf{L^2}$) and R^1,R^2 = H ($H_2\mathbf{L^3}$), were synthesized. Acid–base and complexing properties of the ligands were studied in solution as well as in the solid state. The ligands show unusually high basicity of the nitrogen atoms (log K_1 = 9.5–10, log K_2 = 8.5–9) if compared with simple (aminomethyl)phosphinic acids and, consequently, high stability constants of the complexes with studied divalent metal ions. The study showed the important role of the hydroxo group attached to the central carbon atom of the geminal bis(phosphinate) moiety. Deprotonation of the hydroxo group yields the alcoholate anion which tends to play the role of a bridging ligand and induces formation of polynuclear complexes. Solid-state structures of complexes $[H_2N{=}C(NH_2)_2][Cu_2(H_{-1}\mathbf{L^2})_2]CO_3{\cdot}10H_2O$ and $Li_2[Co_4(H_{-1}\mathbf{L^1})_3(OH)]{\cdot}17.5H_2O$ were determined by X-ray diffraction. The complexes show unexpected geometries forming dinuclear and cubane-like structures, respectively. The dinuclear copper(II) complex contains a bridging μ_2-alcoholate group with the $^-O–P(=O)–CH_2–NH_2$ fragments of each ligand molecule chelated to the different central ion. In the cubane cobalt(II) complex, one μ_3-hydroxide and three μ_3-alcoholate anions are located in the cube vertices and both phosphinate groups of one ligand molecule are chelating the same cobalt(II) ion while each of its amino groups are bound to different neighbouring metal ions. All such three metal ions are bridged by the alcoholate group of a given ligand.

Received 4th September 2012,
Accepted 14th November 2012

DOI: 10.1039/c2dt32045b

www.rsc.org/dalton

Introduction

Aminoalkylphosphonic and -phosphinic acids represent a group of organophosphorus compounds with a wide range of applications.[1–3] A specific group of compounds among aminoalkylphosphonates are those containing the geminal bis(phosphonic acid) group. The geminal bis(phosphonic acids) (BPs) exhibit high affinity to hydroxyapatite, the main inorganic component of bone tissue, and they are regularly applied as drugs for treatment of osteoporosis, Paget's disease and other disorders of calcified tissues metabolism. They are engaged not only in protection of the bone surface, but also in growth regulation of cells which are responsible for bone formation and resorption. The geminal BPs containing a nitrogen atom in the side chain attached to the bridging carbon atom inhibit farnesyl diphosphate synthase.[3] The BPs without the nitrogen atom are metabolized into non-hydrolysable methylene-containing ATP analogues, which are accumulated inside the cell and exhibit cytotoxicity.[4] Unfortunately, the BP's cytotoxicity and inhibition activity cannot be used for other than bone-associated applications due to the extremely strong affinity of BPs to calcified tissues.[5] An alternative could be found in geminal bis(phosphinates), BPis. The geminal bis(phosphinates) maintain the P–C–P fragment and show low affinity to hydroxyapatite.[6,7] Whereas geminal BPs have been widely studied, geminal BPis have attracted much less attention. Some of them have been synthesized[6–11] but there have been published only a few papers dealing with their coordination behaviour[12,13] except for two simple ligands, methylene-bis(phosphinic acid), where phosphorus is directly bound to Pt(II) or Pd(II),[14] and methylene-bis[(phenyl)phosphinic acid] H_2pcp^{Ph} (Scheme 1).[15]

However, amine-containing geminal BPis offer various coordination modes and, thus, we turned our attention to the synthesis and characterization of methylene-bis[(aminomethyl)phosphinic acids]. Here, we report on results of the study of the symmetrical ligands bearing different substituents

Department of Inorganic Chemistry, Faculty of Science, Charles University in Prague, Hlavova 2030128 40 Prague 2, Czech Republic. E-mail: kubicek@natur.cuni.cz; Fax: +420 221921253; Tel: +420 221921264

†Electronic supplementary information (ESI) available: Overall protonation constants and stability constants; distribution diagrams of $H_2\mathbf{L^2}$ and $H_2\mathbf{L^3}$; HR-MS spectra of Cu-$\mathbf{L^1}$ and Cu-$\mathbf{L^2}$ systems; geometrical parameters of the bis(phosphinate) moiety and coordination spheres in the solid state. CCDC 898276, 898277, 898278 and 898279. For ESI and crystallographic data in CIF or other electronic format see DOI: 10.1039/c2dt32045b

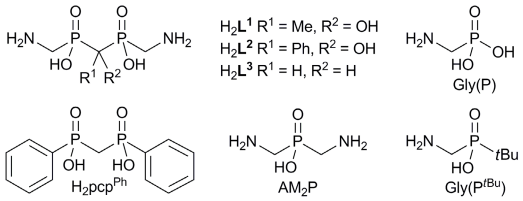

Scheme 1 Structures of studied methylene-bis[(aminomethyl) phosphinic acids] and other compounds discussed in the text.

on the central carbon atom (Scheme 1). The ligands can be convenient in applications where rather strong acidity and weak complexation ability of the phosphinic acid group is desired.

Experimental

Materials and methods

Commercially available chemicals had synthetic purity and were used as received. NMR spectra were recorded at 25 °C on a Varian NMR system operating at 300 MHz proton frequency with an ASW probe. Chemical shifts were referenced to TMS ($\delta_H = \delta_C = 0$ ppm) or *t*BuOH ($\delta_H = 1.25$, $\delta_C = 31.2$ ppm) and H_3PO_4 (external standard, $\delta_P = 0$ ppm) and are given in the ppm scale and the coupling constants are given in Hz. ESI-MS spectra were recorded on a Bruker Esquire 3000 spectrometer with ESI ionization and ion-trap detection. High resolution MS spectra were measured on a Bruker APEX-Q FTMS. UV-Vis spectra were measured on a Schimadzu UV-2401PC spectrometer at 25 °C in the wavelength range 200–800 nm. TLC was performed with silica gel on aluminium sheets (Merck 10554 F_{254}); the spots were detected with UV fluorescence (λ = 254 nm) or visualized by iodine vapours.

Phthalimido-methylphosphinic acid (2). Under an argon atmosphere, dry $(NH_4)H_2PO_2$ (20.0 g, 241 mmol) was suspended in hexamethyldisilazane (HMDS, 100 mL) and the mixture was heated at 110 °C under a gentle flow of argon overnight. The mixture containing $HP(OTMS)_2$ (**1**) was cooled to room temperature (RT) and dry CH_2Cl_2 (100 mL) was added. The solution of (*N*-bromomethyl)phthalimide (15.0 g, 62.5 mmol) in dry CH_2Cl_2 (300 mL) was added dropwise and the mixture was stirred at RT overnight. Then, the resulting solution was dropped into EtOH (800 mL) and the solution was evaporated to dryness under reduced pressure. Crude product was dissolved in boiling 1% aq. HCl (100 mL) and the resulting suspension was filtered on a fine glass frit while hot. The filtrate was cooled down and left standing overnight. The precipitate formed was collected on a glass frit and dissolved in boiling water until a clear solution was formed. The solution was cooled down and left overnight. The precipitate formed (containing mainly the disubstituted product) was filtered off on a glass frit and the filtrate was evaporated to dryness. The solid residue was dissolved in a minimum amount of water and left standing overnight. A white crystalline solid was collected by filtration on a glass frit, washed with cold water and dried in a desiccator over P_2O_5 to give the product (17.2 g, 31%).

NMR (dmso-d_6): ^{1}H δ 3.86 (2H, dd, $^2J_{HP}$ = 10, $^3J_{HH}$ = 2, N–CH_2–P); 7.18 (1H, dt, $^1J_{HP}$ = 558, $^3J_{HH}$ = 2, P–*H*); 7.80–7.90 (4H, m, aryl H); ^{13}C{^{1}H} δ 38.0 (d, $^1J_{CP}$ = 98, N–*C*H_2–P); 123.4, 131.5, 134.8 (aryl C); 167.3 (s, *C*=O); ^{31}P δ 17.6 (dt, $^1J_{PH}$ = 558, $^2J_{PH}$ = 10). ESI-MS(−): *m*/*z* 223.5 [(M − H)$^-$, calcd 224.1]. TLC (EtOH : aq. NH_4OH 1 : 1): R_f = 0.8. Elem. anal. (calcd for $C_9H_8NO_4P$, M_r = 225.1): C 48.0 (48.0); H 3.5 (3.2); N 6.2 (6.3). mp 202 °C (with decomposition).

1-Hydroxy-ethane-1,1-bis[(aminomethyl)phosphinic acid] (H_2L^1). Under an argon atmosphere, compound **2** (6.15 g, 27.3 mmol) was suspended in HMDS (100 mL) and the mixture was heated at 110 °C under a gentle flow of argon overnight. The mixture was cooled to RT and dry CH_2Cl_2 (200 mL) was added. A solution of acetyl chloride (1.13 g; 14.4 mmol) in dry CH_2Cl_2 (20 mL) was added dropwise and the mixture was stirred at RT overnight. Then, the resulting solution was dropped into EtOH (500 mL) and the resulting suspension was evaporated to dryness under reduced pressure. The solid was dissolved in boiling water (50 mL) and treated with charcoal while hot. The filtrate was cooled to RT and conc. aq. HCl (10 mL) was slowly added. The mixture was left to stand for 2 h and the solid was collected on a medium-coarse glass frit, washed with water and dried over P_2O_5 in vacuum. This crude intermediate **3** (5.5 g, obtained as a yellowish powder) was dissolved in 6 M aq. HCl (100 mL) and the solution refluxed for 24 h. After cooling to RT, precipitated phthalic acid was filtered off. The filtrate was evaporated to dryness under reduced pressure and further co-evaporated three times with water (50 mL). The crude product was purified on cation-exchange resin (Dowex 50, H^+-form). Impurities were eluted off with water and water : EtOH 1 : 1 mixtures. The pure product was eluted with 5% aq. ammonia. Fractions containing product were treated with charcoal and the filtrate was evaporated to dryness. The residue was suspended in water (100 mL). The solid was collected on a glass frit, washed with EtOH and dried over P_2O_5 in vacuum to give the product as a white powder (1.74 g, 47%).

3: NMR (5% Et_3N in dmso-d_6): ^{1}H δ 1.35 (3H, t, $^3J_{HP}$ = 14, CH_3); 4.09 (4H, m, N–CH_2–P); 7.75–7.90 (8H, m, aryl H); ^{13}C{^{1}H} δ 18.3 (s, *C*H_3); 37.0 (dd, $^1J_{CP}$ = 106; $^3J_{CP}$ = 9, N–*C*H_2–P); 70.8 (t, $^1J_{CP}$ = 97 Hz, $P_2C(CH_3)$–OH); 122.7, 132.0, 134.1 (aryl C); 167.6 (s, *C*=O); ^{31}P{^{1}H} δ 28.8 (s). ESI-MS(−): *m*/*z* 490.8 [(M − H)$^-$, calcd 491.0]. TLC (MeCN : MeOH : aq. NH_4OH 3 : 1 : 2): R_f = 0.4.

H_2L^1: NMR (NaOD/D_2O, pD = 12): ^{1}H δ 1.47 (3H, t, $^3J_{HP}$ = 14, CH_3); 2.89 (4H, m, N–CH_2–P); ^{13}C{^{1}H} δ 20.9 (s, *C*H_3); 41.4 (dd, $^1J_{CP}$ = 98; $^3J_{CP}$ = 9, N–*C*H_2–P); 77.0 (t, $^1J_{CP}$ = 86, $P_2C(CH_3)$–OH); ^{31}P{^{1}H} δ 36.8 (s). ESI-MS(−) *m*/*z*: 230.5 [(M − H)$^-$, calcd 231.0]; ESI-MS(+) *m*/*z*: 203.7 [(M + H − CH_2NH_2)$^+$, calcd 204.1]; 232.7 [(M + H$^+$)$^+$, calcd 233.05]; 254.7 [(M + Na)$^+$, calcd 255.0]; 276.7 [(M + 2Na − H)$^+$, calcd 277.0]. TLC (EtOH : aq. NH_4OH 1 : 1): R_f = 0.4. Elem. anal. (calcd for $C_4H_{14}N_2O_5P_2{\cdot}1.5H_2O$, M_r =

259.1): C 18.5 (18.4); H 6.6 (6.8); N 10.8 (10.5). mp 276 °C (with decomposition).

(Hydroxy)(phenyl)methylene-bis[(aminomethyl)phosphinic acid] (H_2L^2). Under an argon atmosphere, the compound **2** (5.00 g, 22.2 mmol) was suspended in HMDS (30 mL) and the mixture was heated at 110 °C under a gentle flow of argon overnight. The mixture was cooled to RT and dry CHt_2Cl_2 (20 mL) was added. The solution of benzoyl chloride (1.64 g, 11.7 mmol) in dry CH_2Cl_2 (20 mL) was added dropwise and the mixture was stirred at RT overnight. Then, the reaction mixture was dropped into EtOH (200 mL) and the resulting suspension was evaporated to dryness under reduced pressure. The solid was dissolved in boiling H_2O (50 mL) and treated with charcoal while hot. The filtrate was then cooled to RT and conc. aq. HCl was slowly added (5 mL). After 2 h, the suspension was decanted off, the solid was dissolved in a mixture of MeCN : $CHCl_3$: MeOH 1 : 1 : 1 (50 mL) and the resulting solution was left standing overnight. The precipitate was collected on a medium-coarse glass frit, washed several times with water and dried over P_2O_5 in vacuum. This crude intermediate **4** (3.93 g, obtained as a white powder) was dissolved in a mixture of 75% aq. N_2H_4 (80 mL) and EtOH (80 mL) and stirred at RT overnight. The mixture was evaporated to dryness and three times co-evaporated with EtOH. The residue was dissolved in a minimum amount of water and excess of EtOH was added. After standing overnight, the precipitate was collected on a medium-coarse glass frit. The solid was dissolved in water and purified on anion-exchange resin (Dowex 1, OH^--form). Impurities were eluted off with water, and the product was eluted with 6 M aq. HCl. The fractions containing the product were combined and evaporated to dryness. The solid was suspended in water (100 mL) and excess of EtOH was added. After standing overnight, the precipitate was collected on a medium-coarse glass frit, washed with EtOH and dried over P_2O_5 in vacuum to give the product as a white powder (1.63 g, 40%).

4: NMR (5% Et_3N in dmso-d_6): ^{1}H δ 3.74 (4H, m, N–CH_2–P); 7.10–7.20 (1H, m, aryl H); 7.20–7.30 (2H, m, aryl H); 7.82 (10H, bs, aryl H); ^{13}C{^{1}H} δ 36.0 (d, $^1J_{CP}$ = 100 Hz, N–CH_2–P); 77.2 (t, $^1J_{CP}$ = 80 Hz, P_2C(Ph)–OH); 122.8, 126.0, 126.2, 127.3, 131.7, 134.3, 137.3 (aryl C); 167.6 (s, *C*=O); ^{31}P{^{1}H} δ 30.4 (s). TLC (MeCN : MeOH : aq. NH_4OH 3 : 1 : 2): R_f = 0.5. ESI-MS(−) *m*/*z*: 552.8 [(M − H^+)$^-$, calcd 553.1]; ESI-MS(+) *m*/*z*: 577.0 [(M + Na^+)$^+$, calcd 577.1]; 656.1 [(M + $NHEt_3^+$)$^+$, calcd 656.2].

H_2L^2: NMR (NaOD/D_2O, pD = 6): ^{1}H δ 3.11 (4H, m, N–CH_2–P); 7.35–7.50 (3H, m, aryl H); 7.70–7.80 (2H, m, aryl H); ^{13}C{^{1}H} δ 35.6 (d, $^1J_{CP}$ = 99, N–CH_2–P); 81.7 (t, $^1J_{CP}$ = 96, P_2C(Ph)–OH); 126.5 (t, $^3J_{CP}$ = 4, ^{ar}C–^{ar}C–C–P_2); 128.4 (s, aryl C); 129.1 (s, aryl C); 137.4 (s, aryl C); ^{31}P{^{1}H} δ 28.3 (s). ESI-MS(−) *m*/*z*: 292.5 [(M − H)$^-$, calcd 293.1]; ESI-MS(+) *m*/*z*: 294.7 [(M + H)$^+$, calcd 295.1]; 316.8 [(M + Na)$^+$, calcd 317.0]; 332.7 [(M + K)$^+$, calcd 333.0]. TLC (EtOH : aq. NH_4OH 1 : 1): R_f = 0.4. Elem. anal. (calcd for $C_9H_{16}N_2O_5P_2$·HCl·H_2O, M_r = 348.7): C 31.0 (31.0); H 5.5 (5.1); N 8.0 (7.8); Cl 11.2 (11.4). mp 225 °C (with decomposition).

Methylene-bis(phosphinic acid) (6). Under an argon atmosphere, a solution of $CH_2(PCl_2)_2$ (**5**) (20.0 g; 91.8 mmol) in dry THF (50 mL) was slowly added to a cooled mixture (5 °C) of water (150 mL) and THF (50 mL). After stirring for 1 h, volatiles were evaporated under reduced pressure. The resulting oil was dissolved in a minimum amount of MeOH and an excess of Me_2CO was added until two phases were formed. The upper phase was discarded and the resulting oil was dried in vacuum for several days. The oil solidified to a colourless mass after standing at 5 °C overnight (10.8 g, 82%).

NMR (dmso-d_6): ^{1}H δ 2.40 (2H, t, $^2J_{HP}$ = 17, CH_2); 7.10 (2H, d, $^1J_{HP}$ = 561, P–*H*); ^{13}C{^{1}H} δ 33.4 (t, $^1J_{CP}$ = 80, CH_2); ^{31}P δ 19.3 (dt, $^1J_{PH}$ = 561, $^2J_{PH}$ = 17). ESI-MS(−) *m*/*z*: 330.6 [(2M − 3H^+ + 2Na^+)$^-$, calcd 330.9]; ESI-MS(+) *m*/*z*: 332.8 [(2M − H^+ + 2Na^+)$^+$, calcd 332.9]. TLC (EtOH : NH_4OH 1 : 1): R_f = 0.8. Elem. anal. (calcd for $CH_6O_4P_2$·H_2O, M_r = 162.0): C 7.6 (7.4); H 4.8 (5.0).

Methylene-bis[(aminomethyl)phosphinic acid] (H_2L^3). In a 250 mL round-bottom flask, methylene-bis(phosphinic acid) **6** (3.45 g; 21.3 mmol), dibenzylamine (5.00 mL; 95.5 mmol) and paraformaldehyde (2.90 g; 96.6 mmol) were suspended in a mixture of 6 M aq. HCl (40 mL) and THF (40 mL) and stirred overnight at 50 °C. The reaction mixture was evaporated to dryness and then co-evaporated three times with CH_2Cl_2, until the residue solidified. The crude intermediate **7** (containing a large amount of dibenzylamine hydrochloride) was used for subsequent reaction without further purification. It was dissolved in MeOH (250 mL) under an argon atmosphere and ammonium formate (47.9 g; 760 mmol) and catalyst (10% w/t Pd/C; 4.00 g) were added. The reaction mixture was refluxed for 2 h. Another portion of ammonium formate (28.7 g; 455 mmol) and catalyst (2.40 g) was added and the reaction mixture was refluxed for a further 3 h. After removal of volatiles under reduced pressure, the residue was co-evaporated several times with MeOH. The black residue was treated with water and the suspension was filtered off on a fine glass frit. The filtrate was evaporated to dryness, the residue was dissolved in water and the amino acid was adsorbed on anion exchange resin (Amberlite IRA 402, OH^--form). Impurities were eluted off with water and the product was eluted with 6 M aq. HCl. Fractions containing product were treated with charcoal, the filtrate was evaporated to dryness and the residue was co-evaporated three times with water. The solid was dried in vacuum over P_2O_5 to give the product as a white powder (3.84 g, 63%).

7: NMR ($CDCl_3$): ^{1}H δ 1.99 (2H, t, $^2J_{HP}$ = 16, P–CH_2–P); 3.03 (4H, d, $^2J_{HP}$ = 10, P–CH_2–N); 4.35 (8H, m, CH_2Ph); 7.35–7.45 (12H, m, aryl H); 7.50–7.60 (8H, m, aryl H); ^{13}C{^{1}H} δ 38.5 (t, $^1J_{CP}$ = 81, P–*C*H_2–P); 51.4 (d, $^1J_{CP}$ = 90, P–*C*H_2–N); 58.1 (s, *C*H_2Ph); 129.0, 129.5, 129.9, 131.0 (s, aryl C); ^{31}P{^{1}H} δ 17.4 (s). ESI-MS(−) *m*/*z*: 560.9 [(M − H^+)$^-$, calcd 561.2]; ESI-MS(+) *m*/*z*: 563.2 [(M + H^+)$^+$, calcd 563.2]; 585.2 [(M + Na^+)$^+$, calcd 585.2]; 601.2 [(M + K^+)$^+$, calcd 601.2]. TLC (MeCN : $CHCl_3$: MeOH 1 : 1 : 1): R_f = 0.5.

H_2L^3: NMR (NaOD/D_2O, pH = 7): ^{1}H δ 2.47 (2H, t, $^2J_{HP}$ = 17, P–CH_2–P); 3.18 (4H, d, $^2J_{HP}$ = 11, P–CH_2–N); ^{13}C{^{1}H} δ 36.3 (t, $^1J_{CP}$ = 83, P–*C*H_2–P); 39.5 (d, $^1J_{CP}$ = 99, P–*C*H_2–N); ^{31}P{^{1}H} δ 18.5 (s). ESI-MS(−) *m*/*z*: 201.1 [(M − H^+)$^-$, calcd 201.0]; ESI-MS (+) *m*/*z*: 203.3 [(M + H^+)$^+$, calcd 203.0]; 225.4 [(M + Na^+)$^+$, calcd 225.0]; 241.4 [(M + K^+)$^+$, calcd 241.0]. TLC (EtOH : aq. NH_4OH

1 : 1): R_f = 0.7. Elem. anal. ($C_3H_{12}N_2O_4P_2$·0.5HCl·H_2O, M_r = 238.3): C 15.1 (14.8); H 6.1 (5.8); N 11.8 (11.5), Cl 7.4 (7.8). mp 310 °C (with decomposition).

Potentiometric titrations. Methodology of the potentiometric titrations and processing of the experimental data were analogous to those previously reported.[16] Titrations were carried out in a vessel thermostatted at 25 ± 0.1 °C at ionic strength I = 0.1 M KNO_3. The ligand-to-metal ratio was 1 : 1 (and 2 : 1 in some cases) with c_M = 0.004 M, the pH range was 1.7–12 (or till precipitation of metal hydroxide). Titrations were carried out at least three times, each consisting of about 40 points. The water ion product, pK_w = 13.78, and stability constants of M^{2+} − OH^- systems were taken from ref. 17. The protonation constants β_n calculated are concentration constants and are defined by $\beta_n = [H_nL]/([H]^n \times [L])$ ($\log K_1 = \log \beta_1$; $\log K_n = \log \beta_n - \log \beta_{n-1}$). The stability constants are defined by $\beta_{hlm} = [M_mH_hL_l]/[M]^m \times [H]^h \times [L]^l$. The constants (with standard deviations) were calculated with the program OPIUM.[18] Throughout the paper, pH means −log [H^+].

Preparation of single crystals

H_2L^1·0.5H_2O. Powdered H_2L^1·1.5H_2O (26 mg) was dissolved in a mixture of 0.1 M aq. $CuCl_2$ (1 mL) and 6 M aq. HCl (1 mL). Volatiles were removed under reduced pressure and the oily residue was dissolved in water (1 mL). Single crystals of H_2L^1·0.5H_2O were formed on standing at RT for one week.

H_2L^3·H_2O. Powdered H_2L^3·0.5HCl·H_2O (29 mg) was suspended in 0.1 M aq. $CoCl_2$ (1 mL). The 1 M aq. LiOH was added dropwise until all material dissolved and the solution reached pH 8. Diffusion of ethanol vapour at RT yielded oil which slowly crystallized. Single crystals of H_2L^3·H_2O were obtained on standing for three weeks.

$Li_2[Co_4(H_{-1}L^1)_3(OH)]$·17.5$H_2O$. Powdered H_2L^1·1.5H_2O (26 mg, 0.1 mmol) was suspended in 0.1 M aq. $CoCl_2$ (1 mL, 0.1 mmol). The 1 M aq. LiOH was added dropwise until all material dissolved and the solution reached pH 8. Diffusion of ethanol vapour at RT yielded oil which slowly crystallized. Single crystals of $Li_2[Co_4(H_{-1}L^1)_3(OH)]$·17.5$H_2O$ were obtained on standing for six weeks.

$(Hgua)_4[Cu_2(H_{-1}L^2)_2]CO_3$·10$H_2O$. Powdered H_2L^2·HCl·H_2O (35 mg, 0.1 mmol) was dissolved in 0.1 M aq. $CuCl_2$ (1 mL, 0.1 mmol). The 1 M aq. $(Hgua)_2CO_3$ was added dropwise to reach pH 10. Diffusion of ethanol vapour at RT yielded single crystals of $[H_2N{=}C(NH_2)_2]_4[Cu_2(H_{-1}L^2)_2]CO_3$·10$H_2O$ on standing for five days.

X-ray diffraction study

The diffraction data were collected at 150 K (Cryostream Cooler, Oxford Cryosystem) using a Nonius Kappa CCD diffractometer and Mo-K_α radiation (λ = 0.71073 Å) and analyzed using the HKL DENZO program package.[19] The structures were solved by direct methods (SIR92),[20] and refined by full-matrix least-squares techniques (SHELXL97).[21] All non-hydrogen atoms were refined anisotropically. All hydrogen atoms were located in the difference map of electron density; however, they were placed in theoretical (C–H) or original (O–H) positions with thermal parameters $U_{eq}(H) = 1.2\ U_{eq}(X)$ as their free refinement led to some unrealistic bond lengths. Table 1 contains selected crystallographic parameters for the structures reported in this paper. Data for the structures have been deposited with the Cambridge Crystallographic Data Centre with CCDC-898276 (H_2L^1·0.5H_2O), 898277 (H_2L^3·H_2O), 898278 ($Li_2[Co_4(H_{-1}L^1)_3(OH)]$·17.5$H_2O$), and 898279 {$(Hgua)_4[Cu_2(H_{-1}L^2)_2]CO_3$·10$H_2O$} reference numbers.

Table 1 Experimental data of reported crystal structures

Parameter	H_2L^1·0.5H_2O	H_2L^3·H_2O	$Li_2[Co_4(H_{-1}L^1)_3(OH)]$·17.5$H_2O$	$(Hgua)_4[Cu_2(H_{-1}L^2)_2]CO_3$·10$H_2O$
Formula	$C_4H_{15}N_2O_{5.5}P_2$	$C_3H_4N_2O_5P_2$	$C_{12}H_{69}Co_4Li_2N_6O_{33.5}P_6$	$C_{23}H_{70}Cu_2N_{16}O_{23}P_4$
M_w	241.12	220.10	1269.15	1189.91
Colour	Colourless	Colourless	Red	Brownish green
Shape	Plate	Prism	Plate	Plate
Dimensions (mm)	0.10 × 0.31 × 0.45	0.20 × 0.45 × 0.50	0.14 × 0.25 × 0.56	0.12 × 0.35 × 0.69
Crystal system	Monoclinic	Orthorhombic	Orthorhombic	Triclinic
Space group	*C*2/*c*	*Pbcn*	$P2_12_12_1$	*P*1
a (Å)	16.4183(4)	11.5649(4)	13.0426(3)	14.1333(4)
b (Å)	6.7200(2)	8.9009(3)	13.2471(4)	14.2073(4)
c (Å)	17.8230(4)	8.3936(3)	26.9972(7)	14.4339(4)
α (°)	—	—	—	69.875(1)
β (°)	101.253(1)	—	—	76.646(1)
γ (°)	—	—	—	65.391(1)
V (Å^3)	1928.62(9)	864.02(5)	4664.5(2)	2461.05(12)
Z	8	4	4	2
D_c (g cm^{-3})	1.661	1.692	1.807	1.606
μ (mm^{-1})	0.454	0.493	1.706	1.086
F (000)	1016	464	2620	1244
Diffractions; observed ($I_o > 2\sigma(I_o)$)	2218; 2003	993; 944	10 660; 9956	22 429; 21 349
Parameters	124	56	622	1226
G-o-f on F^2	1.077	1.127	1.038	1.027
R; *R*′ (all data)	0.0261; 0.0302	0.0232; 0.0246	0.0293; 0.0331	0.0237; 0.0262
w*R*; w*R*′ (all data)	0.0713; 0.0739	0.0690; 0.0702	0.0721; 0.0737	0.0604; 0.0618
Difference max; min (e Å^{-3})	0.489; −0.262	0.325; −0.368	0.839; −0.517	0.428; −0.338

Results and discussion

Synthesis

The studied compounds were synthesized using two different strategies (Scheme 2). Those containing a hydroxy group attached to the bridging carbon atom were prepared from Pht-protected (aminomethyl)phosphinate fragments. The reaction of bis(trimethylsilyloxy)phosphine **1** with (*N*-bromomethyl)-phthalimide followed by hydrolysis of the silylester groups gives a mixture of hypophosphorous acid, and monosubstituted and disubstituted products as previously reported.[22] To improve the procedure, we developed a simple and efficient method for separation of the mixture based on different solubility of the components in water. In the next step, the obtained phthalimido-methylphosphinic acid **2** is converted to the corresponding trimethylsilylphosphinate by reaction with hexamethyldisilazane and treated with acetyl- or benzoylchloride. The reaction is analogous to that previously reported for geminal bis(H-phosphinates)[7,23] and for cyclic amino-bis-(phosphinates)[11] and proceeds in high yield. The target ligands $H_2\mathbf{L}^1$ and $H_2\mathbf{L}^2$ were obtained after removal of the phthalimide protecting groups by hydrochloric acid or by hydrazine, respectively. Compound $H_2\mathbf{L}^3$ was prepared using a "build up" strategy starting from commercially available bis (dichlorophosphino)methane **5**. The compound was hydrolyzed yielding methylene-bis(phosphinic acid) **6** (ref. 24) that was consequently treated with paraformaldehyde and dibenzylamine. The three component Mannich-type reaction yields protected bis(phosphinate) **7** in high yield. The target ligand $H_2\mathbf{L}^3$ was obtained by hydrogenolysis of benzyl groups using Pd/C as the catalyst. This synthesis is more straightforward than the amine alkylation approach used in synthesis of similar (aminomethyl)phosphinic-phosphonic acid, $NH_2CH_2–PO_2H–CH_2–PO_3H_2$.[25] Unlike geminal bis(H-phosphinates) slowly decomposing in aqueous solution,[7] all the ligands are fully stable in aqueous solution at any pH.

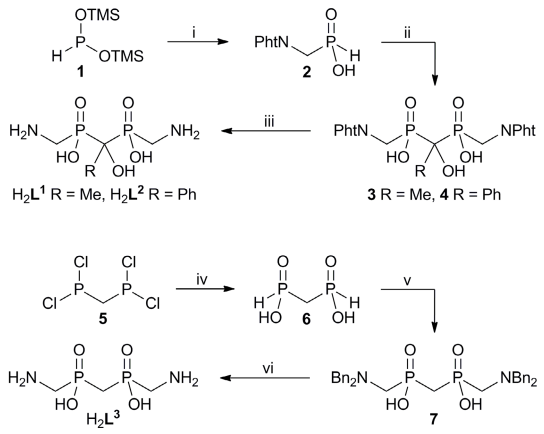

Scheme 2 Synthesis of studied geminal bis(phosphinates). (i) (*N*-Bromomethyl)phthalimide in CH_2Cl_2, RT; (ii) 1. HMDS, 110 °C; 2. RCOCl in CH_2Cl_2, RT; 3. EtOH; (iii) conc. aq. HCl, reflux or N_2H_4 in EtOH, RT; (iv) H_2O in THF, RT; (v) dibenzylamine, paraformaldehyde, aq. HCl in THF, 50 °C; (vi) $NH_4(HCOO)$, Pd/C in MeOH, reflux.

Acid–base and coordination properties in solution

Solution behaviour of the title geminal bis(phosphinic acids) and their complexes was studied by potentiometry. The studied bis[(aminomethyl)phosphinates] show similar protonation constants (Table 2 and S1†). Phosphinic acid groups are strongly acidic and their protonation takes place at pH < 3 (Fig. 1A). At weakly acidic and neutral regions, the only species present in the solution is the neutral zwitterionic form, H_2L, where both protons are bound on amine nitrogen atoms. The pK_a values assigned to the amino groups are surprisingly high if compared to those of simple (aminoalkyl)phosphinic acids (Table 2). For the studied ligands, the values of the highest constants are comparable to those of carboxylic and phosphonic amino acids. Also values of the second protonation constants are noticeably high. The small differences between the first and the second constants indicate independent protonation of both distant amino groups. The high basicity of the nitrogen atoms could be ascribed to the presence of intramolecular hydrogen bonds similar to those found in the solid state (see below).

Stability constants of complexes of the title geminal bis[(aminomethyl)phosphinates] with Cu^{2+}, Zn^{2+}, Ni^{2+} and Co^{2+} ions were determined from potentiometric titrations at 1 : 1 and 2 : 1 ligand-to-metal ratios. Despite excess of the ligand used in the latter cases, no species of ML_2 stoichiometry could be identified. Experimentally determined stability constants of the complexes are summarized in Table S2† and the derived stability constants are given in Table 3. The distribution diagrams are shown in Fig. 2, S1, S2 and S3.† Similarly to protonation constants of the ligands, stability constants of their complexes, log K_{ML}, do not follow typical trends among amino acids. The presence of two highly basic nitrogen atoms and

Table 2 Protonation constants, log K_a, of the studied methylene-bis[(aminomethyl)phosphinic acids] (25 °C, I = 0.1 M) and related ligands

Constant	$H_2\mathbf{L}^1$	$H_2\mathbf{L}^2$	$H_2\mathbf{L}^3$	AM_2P[16]	Gly(P)[26]	Gly(P^{tBu})[27]	Gly[26]	H_2pcp^{Ph} [15e]
log K_a(L)	10.00	9.84	9.49	8.51	10.05	8.42	9.56	3.33[a]
log K_a(HL)	8.89	8.55	8.80	7.07	5.39	1.20	2.36	1.35[a]
log K_a(H_2L)	1.35	<1	2.09	0.77	0.40	—	—	—

[a] I = 0.5 M NMe_4Cl.

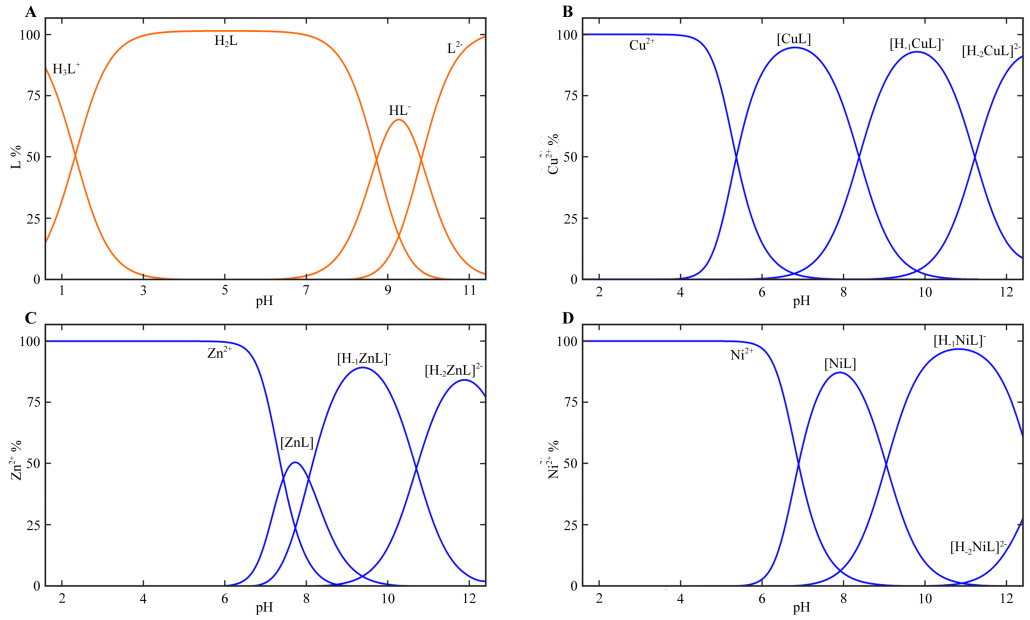

Fig. 1 Distribution diagrams of $H_2\mathbf{L}^1$ in the absence of metal ions (A) and in the presence of Cu^{2+} (B), Zn^{2+} (C) and Ni^{2+} (D) ions ($c_L = c_M = 4$ mM, $I = 0.1$ M, 25 °C).

Table 3 Equilibrium constants (log K_{ML} or pK_a) in systems containing the title ligands and some divalent metal ions

		Ligand		
Metal ion	Equilibrium[a]	$H_2\mathbf{L}^1$	$H_2\mathbf{L}^2$	$H_2\mathbf{L}^3$
Cu^{2+}	$Cu^{2+} + (L)^{2-} \rightleftharpoons [Cu(L)]$	10.76	11.13	9.87
	$[Cu(L)] \rightleftharpoons [CuH_{-1}(L)]^{-} + H^+$	8.41	8.07	8.82
	$[CuH_{-1}(L)] \rightleftharpoons [CuH_{-2}(L)]^{2-} + H^+$	11.26	12.29	10.53
Zn^{2+}	$Zn^{2+} + (L)^{2-} \rightleftharpoons [Zn(L)]$	6.78	6.51	6.29
	$[Zn(L)] \rightleftharpoons [ZnH_{-1}(L)]^{-} + H^+$	8.04	8.77	8.58
	$[ZnH_{-1}(L)] \rightleftharpoons [ZnH_{-2}(L)]^{2-} + H^+$	10.72	11.02	—
Ni^{2+}	$Ni^{2+} + (L)^{2-} \rightleftharpoons [Ni(L)]$	7.87	7.13	7.51
	$[Ni(L)] \rightleftharpoons [NiH_{-1}(L)]^{-} + H^+$	9.04	8.57	8.41
	$[NiH_{-1}(L)] \rightleftharpoons [NiH_{-2}(L)]^{2-} + H^+$	12.77	12.50	—
Co^{2+}	$Co^{2+} + (L)^{2-} \rightleftharpoons [Co(L)]$	[b]	7.28	5.79
	$[Co(L)] \rightleftharpoons [CoH_{-1}(L)]^{-} + H^+$	[b]	7.84	[b]
	$[CoH_{-1}(L)] \rightleftharpoons [CoH_{-2}(L)]^{2-} + H^+$	8.18	8.01	[b]
	$[CoH_{-2}(L)] \rightleftharpoons [CoH_{-3}(L)]^{3-} + H^+$	11.69	10.03	[b]

[a] Proton dissociation sites are not distinguished (see text). [b] Not determined due to the formation of precipitate.

two phosphinate groups result in higher stability constants of the complexes when compared to those found for other aminoalkylphosphonic/phosphinic acids (Table 4). Despite that, determination of several stability constants was disabled by formation of hydroxide precipitates in the alkaline region (pronounced mainly in the case of the Co^{2+} ion). The complexes with stoichiometry $H_{-1}ML$, $H_{-2}ML$ and $H_{-3}ML$ are formed at pH > 7; here, the negative stoichiometric coefficients represent (i) dissociation of a coordinated water molecule (*i.e.* formation of hydroxido complexes) and/or (ii) dissociation of a proton from the hydroxo group attached to the central carbon atom and the alcoholate coordination, as suggested in the case of the $H_2\mathbf{L}^1$ and $H_2\mathbf{L}^2$ ligands. The sites of the deprotonations cannot be distinguished by potentiometry; however, both coordination modes might be present in the solutions (see below).

Coordination modes in solution were studied more in detail for the Cu^{2+} complexes. Presence of the hydroxyl group in the molecule results in significantly different behaviour among the Cu^{2+} complexes. Ligands $H_2\mathbf{L}^1$ and $H_2\mathbf{L}^2$ form dark green water-soluble complexes at pH above 5. The electronic spectra of the complexes (Fig. 2) were measured at pH corresponding to the maximum abundance of [CuL] and [CuH_{-1}L] species in the distribution diagrams. The colour of the complexes is mostly given by strong CT-bands, which are shifted to the visible region with maxima around 310 and 360 nm for $Cu\mathbf{L}^1$ and $Cu\mathbf{L}^2$, respectively. The shift of the CT-bands indicates coordination of the alcoholate groups in the solution in a similar manner as was found in the solid state (see below). Analogous behaviour of dinuclear Cu^{2+} complexes was previously reported for various ligands.[28] Similar spectra were observed for both [CuL] and [CuH_{-1}L] species. In the case of the [CuL] complex, coordination of the alcoholate group indicates protonation of one nitrogen atom. Thus, the ligand is more likely coordinated in the tridentate manner by amine nitrogen, phosphinate and alcoholate oxygen atoms. For the case of coordination through the alcoholate oxygen atom, any form of tetradentate binding is not possible for geometrical

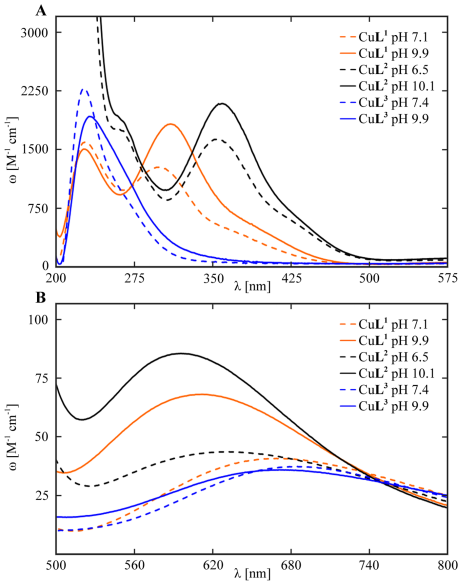

Fig. 2 UV-Vis spectra of Cu^{2+} complexes with the title bis[(aminomethyl)phosphinic acids] (25 °C, water).

Table 4 Comparison of stability constants, log K_{ML}, of complexes with the title ligands and with the related amino acids

Metal ion	H_2L^1	H_2L^2	H_2L^3	AM_2P[16]	Gly(P)[26]	Gly(P^{tBu})[27]	Gly[26]
Cu^{2+}	10.76	11.13	9.87	7.64	8.12	5.37	8.12
Zn^{2+}	6.78	6.51	6.29	4.12	5.00	—	4.96
Ni^{2+}	7.87	7.13	7.51	5.58	5.25	3.62	5.78
Co^{2+}	—	7.28	5.79	4.07	4.52	3.17	4.67

reasons. In the case of the $[MH_{-1}L]$ complex, one could expect similar dimeric species as was found in the solid state of the CuL^2 complex (see below). For both ligands L^1 and L^2 the dinuclear complexes were also identified as major signals in the high resolution MS spectra (Fig. S4†). Unfortunately, potentiometry could not easily distinguish between monomeric and oligomeric species.

In contrast, ligand H_2L^3 forms a light blue poorly soluble Cu^{2+} complex and this system could be studied in solution only due to slow kinetics of crystallization. The electronic spectra (Fig. 2) show a weak d–d transition at around 680 nm and a strong CT-band in the UV region (<300 nm) that could be expected for amine and phosphinate coordination. Colour and electronic spectra of the complex resemble those of the bis(glycinato)copper complex.[29] Thus, tetradentate coordination through both phosphinate oxygen atoms and both amine groups could be expected.

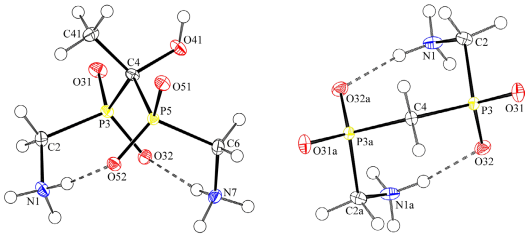

Fig. 3 Molecular structures of H_2L^1 (left) and H_2L^3 (right) found in the solid-state structures of $H_2L^1 \cdot 0.5H_2O$ and $H_2L^3 \cdot H_2O$, showing medium–strong intramolecular hydrogen bonds.

Solid-state structure of the bis[(aminomethyl)phosphinic acids] and their complexes

The structures of two ligands and two complexes in the solid state were determined by X-ray diffraction. The ligands, H_2L^1 and H_2L^3, are practically insoluble in water and, therefore, the single-crystals suitable for the analysis were isolated only from mixtures containing metal ions. The presence of metal ions increases solubility due to metal–ligand interaction and slows down crystallization of the ligands. In both structures, the molecules are in the zwitterionic forms with protons localized on nitrogen atoms. Presence of the substituents attached to the central carbon atom of ligand H_2L^1 results in longer distances from phosphorus to the central carbon and a smaller P–C–P angle (Table S3†). Both structures are stabilized by hydrogen bonds between the amine group and the oxygen atom of the opposite phosphinate group (Fig. 3). The hydrogen bond lengths are 2.67/2.80 Å and 2.76 Å for ligands H_2L^1 and H_2L^3, respectively. These medium–strong hydrogen bonds are probably also present in solution and they could explain the high values of amine protonation constants.

Single-crystals of $[H_2N{=}C(NH_2)]_4[Cu_2(H_{-1}L^2)_2]CO_3 \cdot 10H_2O$ were obtained by slow diffusion of ethanol into the solution containing ligand H_2L^2 and Cu^{2+} ions neutralized at pH 10 with guanidinium carbonate. An independent unit contains two dinuclear complexes. Both independent complex units possess the same coordination motif and their angles and distances differ only slightly (Fig. 4 and Table S4†). All Cu^{2+} ions are coordinated in distorted octahedral geometry with two amine nitrogen atoms and two alcoholate oxygen atoms originating from two different ligand molecules coordinated in the equatorial plane. These two μ^2-alcoholate oxygen atoms form the bridge to the other Cu^{2+} ion which is also coordinated by the remaining two amine groups. The Cu···Cu separations are 3.032 and 3.047 Å in the two independent units. Axial positions of the copper coordination polyhedrons are occupied by phosphinate oxygen atoms. Due to Jahn–Teller distortion, the coordination bonds to phosphinate oxygen atoms are significantly longer (~2.4–3.1 Å) compared to the distances between the metal centre and the equatorial donor atoms (~1.9–2.0 Å), see Table S4.† The structure contains hydrate water molecules, guanidinium and carbonate ions forming a rich system of medium–strong hydrogen bonds.

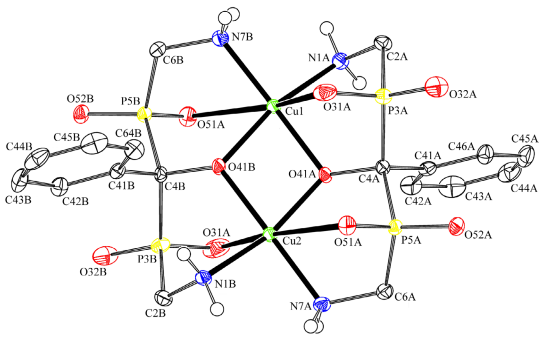

Fig. 4 One of the $[Cu_2(H_{-1}\mathbf{L}^2)_2]^{2-}$ units found in the solid-state structure of $(Hgua)_4[Cu_2(H_{-1}\mathbf{L}^2)_2]CO_3{\cdot}10H_2O$. Hydrogen atoms attached to carbon atoms are omitted for clarity reasons.

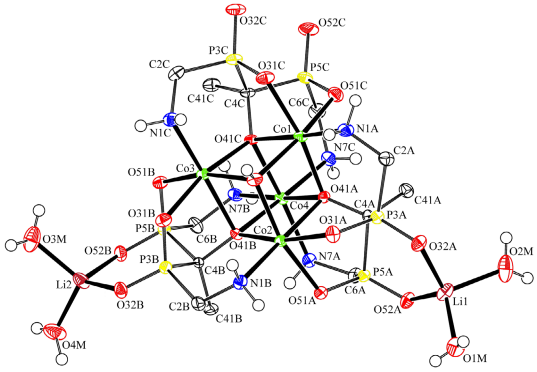

Fig. 5 Solid-state structure of the $[Co_4(OH)(H_{-1}\mathbf{L}^1)_3\{Li(H_2O)_2\}_2]$ unit found in the crystal structure of $Li_2[Co_4(H_{-1}\mathbf{L}^1)_3(OH)]{\cdot}17.5H_2O$. Hydrogen atoms attached to carbon atoms are omitted for clarity reasons.

Slow diffusion of ethanol into the solution containing ligand $H_2\mathbf{L}^1$ and Co^{2+} ions (at pH 8) yielded single-crystals of $Li_2[Co_4(H_{-1}\mathbf{L}^1)_3(OH)]{\cdot}17.5H_2O$. The core of the complex consists of a cubane-like structure composed of four Co^{2+} ions and four oxygen atoms forming μ_3-bridges (Fig. 5). Three oxygen atoms originate from the deprotonated hydroxo group attached to the central carbon atoms of three ligand molecules. The last oxygen atom belongs to a hydroxide anion. Each of the bis(phosphinate) ligands is coordinated through two phosphinate groups and one bridging alcoholate oxygen atom to one Co^{2+} ion forming two five-membered chelate rings. Such tridentate coordination disables coordination of nitrogen atoms to the same metal ion and, thus, the amine groups of each ligand are coordinated to two different neighbouring Co^{2+} ions (those coordinated by the alcoholate in μ_3-bridging fashion). The coordination bonds, Co–O and Co–N, are in the range expected for the Co^{2+} ion (~2.1–2.2 Å). The separation of Co···Co is in the range 3.13–3.22 Å, with slightly closer separations of cobalt(II) ions bound through a μ_3-hydroxido bridge (3.13–3.16 Å) rather than those separated by an alcoholate donor (3.18–3.22 Å). The cubane-like core is slightly distorted, with Co–O–Co and O–Co–O angles in the ranges 94–99° and 81–85°, respectively. However, the geometry of the cubane-like core is very similar to those found in analogous structures bridged by polydentate ligands, like in citrato or tris(carboxylato)methoxo complexes.[30,31] The negative charge of the whole cubane is compensated by two Li^+ ions chelated by uncoordinated phosphinate oxygen atoms of the same ligand molecule. The coordination sphere of each Li^+ ion is completed by two water molecules. Selected relevant distances and angles are compiled in Tables S5 and S6.†

Conclusions

Three symmetrical methylene-bis[(aminomethyl)phosphinic acids] bearing different substituents on the central carbon atom, $(NH_2CH_2)PO_2H{-}C(R^1)(R^2){-}PO_2H(CH_2NH_2)$ where R^1 = OH, R^2 = Me ($H_2\mathbf{L}^1$), R^1 = OH, R^2 = Ph ($H_2\mathbf{L}^2$) and R^1,R^2 = H ($H_2\mathbf{L}^3$), were synthesized. The compounds exhibit high basicities of nitrogen atoms and high stabilities of the complexes with divalent metal ions that are unusual for α-aminoalkylphosphinic acids. The solution and solid state studies of the complexes have shown an important role of the hydroxo group attached to the central carbon atom of the bis(phosphinate) moiety that induces formation of dinuclear or polynuclear complexes.

Acknowledgements

Support from the Grant Agency of the Czech Republic (No. P207/10/P153), the Grant Agency of Charles University (No. 310011) and from the Long-Term Research Plan of the Ministry of Education of the Czech Republic (No. MSM0021620857) is acknowledged. This work was carried out in the framework of COST CM802 (PhoSciNet) Action. We thank Dr Ivana Císařová (Charles University in Prague) for performing X-ray measurements.

Notes and references

1 N. J. Wardle, S. W. A. Bligh and H. R. Hudson, *Curr. Org. Chem.*, 2007, **11**, 1635–1651.
2 F. Orsini, G. Sello and M. Sisti, *Curr. Med. Chem.*, 2010, **17**, 264–289.
3 A. Mucha, P. Kafarski and L. Berlicki, *J. Med. Chem.*, 2011, **54**, 5955–5980.
4 D. G. G. Russel and M. J. Rogers, *Bone*, 1999, **29**, 97–106.
5 H. Fleisch, *Bisphosphonates in Bone Disease*, Academic Press, London, 2000.
6 S. P. Luckman, F. P. Coxon, F. H. Ebetino, R. G. G. Russell and M. J. Rogers, *J. Bone Miner. Res.*, 1998, **13**, 1668–1678.
7 T. David, P. Křečková, J. Kotek, V. Kubíček and I. Lukeš, *Heteroatom Chem.*, 2012, **23**, 195–201.

8 F. H. Ebetino and L. A. Jamieson, *Phosphorus, Sulfur Silicon Relat. Elem.*, 1990, **51**, 23–26.

9 R. Gobel, F. Richter and H. Weichman, *Phosphorus, Sulfur Silicon Relat. Elem.*, 1992, **73**, 67–80.

10 (*a*) S. Gouault-Bironneau, S. Deprele, A. Sutor and J.-L. Montchamp, *Org. Lett.*, 2005, **7**, 5909–5912; (*b*) M. I. Antczak and J.-L. Montchamp, *Tetrahedron Lett.*, 2008, **49**, 5909–5913.

11 B. Kaboudin, F. Saadati and T. Yokomatsu, *Synlett*, 2010, 1837–1840.

12 L. P. Loginova, I. V. Levin, A. G. Matveeva, S. A. Pisareva and E. E. Nifanťev, *Russ. Chem. Bull.*, 2004, **53**, 2000–2007.

13 F. Gaizer, G. Haegele, S. Goudetsidis and H. Papadopoulos, *Z. Naturforsch., B: Chem. Sci.*, 1990, **45**, 323–328.

14 (*a*) C. King, R. A. Auerbach, F. R. Fronczek and D. M. Roundhill, *J. Am. Chem. Soc.*, 1986, **108**, 5626–5627; (*b*) C. King, D. M. Roundhill and F. R. Fronczek, *Inorg. Chem.*, 1987, **26**, 4288–4290; (*c*) C. King, D. M. Roundhill, M. K. Dickson and F. R. Fronczek, *J. Chem. Soc., Dalton Trans.*, 1987, 2769–2780; (*d*) D. M. Roundhill, Z.-P. Shen, C. King and S. J. Atherton, *J. Phys. Chem.*, 1988, **92**, 4088–4094; (*e*) C. King, Y. Yin, G. L. McPherson and D. M. Roundhill, *J. Phys. Chem.*, 1989, **93**, 3451–3455; (*f*) Q.-J. Pan, H.-G. Fu, H.-T. Yu and H.-X. Zhang, *Inorg. Chem.*, 2006, **45**, 8729–8735.

15 (*a*) E. Berti, F. Cecconi, C. A. Ghilardi, S. Midollini, A. Orlandini and E. Pitzalis, *Inorg. Chem. Commun.*, 2002, **5**, 1041–1043; (*b*) F. Cecconi, S. Dominguez, N. Masciocchi, S. Midollini, A. Sironi and A. Vacca, *Inorg. Chem.*, 2003, **42**, 2350–2356; (*c*) F. Cecconi, C. A. Ghilardi, S. Midollini and A. Orlandini, *Inorg. Chem. Commun.*, 2003, **6**, 546–548; (*d*) F. Cecconi, D. Dakternieks, A. Duthie, C. A. Ghilardi, P. Gili, P. A. Lorenzo-Luis, S. Midollini and A. Orlandini, *J. Solid State Chem.*, 2004, **177**, 786–792; (*e*) S. Ciattini, F. Costantino, P. Lorenzo-Luis, S. Midollini, A. Orlandini and A. Vacca, *Inorg. Chem.*, 2005, **44**, 4008–4016; (*f*) J. Beckmann, F. Costantino, D. Dakternieks, A. Duthie, A. Ienco, S. Midollini, C. Mitchell, A. Orlandini and L. Sorace, *Inorg. Chem.*, 2005, **44**, 9416–9423; (*g*) F. Costantino, S. Midollini, A. Orlandini and L. Sorace, *Inorg. Chem. Commun.*, 2006, **9**, 591–594; (*h*) S. Midollini, P. Lorenzo-Luis and A. Orlandini, *Inorg. Chim. Acta*, 2006, **359**, 3275–3282; (*i*) S. Midollini and A. Orlandini, *J. Coord. Chem.*, 2006, **59**, 1433–1442; (*j*) F. Costantino, S. Midollini and A. Orlandini, *Inorg. Chim. Acta*, 2008, **361**, 327–334.

16 V. Kubíček, P. Vojtíšek, J. Rudovský, P. Hermann and I. Lukeš, *Dalton Trans.*, 2003, 3927–3938.

17 C. F. Baes Jr. and R. E. Mesmer, *The Hydrolysis of Cations*, Wiley, New York, 1976.

18 M. Kývala and I. Lukeš, *International Conference, Chemomotrics '95*, Pardubice, Czech Republic, 1995, p. 63; Full version of "*OPIUM*" is available (free of charge) on http://www.natur.cuni.cz/~kyvala/opium.html

19 (*a*) Z. Otwinovski and W. Minor, *HKL DENZO and Scalepack Program Package*, Nonius BV, Delft, 1997; (*b*) Z. Otwinovski and W. Minor, *Methods Enzymol.*, 1997, **276**, 307–326.

20 A. Altomare, G. Cascarano, C. Giacovazzo, A. Guagliardi, M. C. Burla, G. Polidori and M. Camalli, *J. Appl. Crystallogr.*, 1994, **27**, 435.

21 G. M. Sheldrick, *SHELXL97. Program for Crystal Structure Refinement from Diffraction Data*, University of Göttingen, Göttingen, 1997.

22 S. Chen and J. K. Coward, *J. Org. Chem.*, 1998, **63**, 502–509.

23 K. Issleib, W. Moegelin and A. Balszuweit, *Z. Chem.*, 1985, **25**, 370–371.

24 C. King, D. M. Roundhill and F. R. Fronczek, *Inorg. Chem.*, 1986, **25**, 1290–1292.

25 A. Flohr, A. Aemissegger and D. Hilvert, *J. Med. Chem.*, 1999, **42**, 2633–2640.

26 A. E. Martell and R. M. Smith, *Critical Stability Constants*, Plenum Press, New York, 1974–1989, vol. 1–6; *NIST Standard Reference Database 46 (Critically Selected Stability Constants of Metal Complexes), version 5.0*, 1994.

27 J. Rohovec, I. Lukeš, P. Vojtíšek, I. Císařová and P. Hermann, *J. Chem. Soc., Dalton Trans.*, 1996, 2685–2691.

28 (*a*) T. C. Higgs, K. Spartalian, C. J. O'Connor, B. F. Matzanke and C. J. Carrano, *Inorg. Chem.*, 1998, **37**, 2263–2272; (*b*) N. A. Rey, A. Neves, A. J. Bortoluzzi, W. Haase and Z. Tomkowicz, *Dalton Trans.*, 2012, **41**, 7196–7200; (*c*) R. Prabu, A. Vijayaraj, R. Suresh, L. Jagadish, V. Kaviyarasan and V. Narayanan, *Bull. Korean Chem. Soc.*, 2011, **32**, 1669–1678.

29 H. Borsook and K. V. Thimann, *J. Biol. Chem.*, 1932, **98**, 671–705.

30 T. A. Hudson, K. J. Berry, B. Moubaraki, K. S. Murray and R. Robson, *Inorg. Chem.*, 2006, **45**, 3549–3556.

31 B. F. Abrahams, T. A. Hudson and R. Robson, *J. Am. Chem. Soc.*, 2004, **126**, 8624–8625.

EurJIC European Journal of Inorganic Chemistry

ChemPubSoc Europe

DOI: 10.1002/ejic.201((will be filled in by the editorial staff))

Aminoalkyl-1,1-bis(phosphinic acids): stability, acid-base and coordination properties

Tomáš David,[a] Soňa Procházková,[a] Jan Kotek,[a] Vojtěch Kubíček,*[a] Petr Hermann,[a] Ivan Lukeš[a]

Keywords: phosphinic acids / geminal bis(phosphinates) / phosphinate complexes / hydrolytic stability / stability constants

Four geminal bis(phosphinic acids), aminomethyl-bis(H-phosphinic acid) ($H_2\mathbf{L}^1$) and 4-aminobutyl-1-hydroxy-1,1-bis(R-phosphinic acids) with R = H ($H_2\mathbf{L}^2$), Me ($H_2\mathbf{L}^3$) and CH_2CH_2COOH ($H_4\mathbf{L}^4$), were studied. The acid-base properties and coordination ability towards Cu^{2+}, Ni^{2+} and Zn^{2+} ions were studied by potentiometry, UV-Vis and NMR spectroscopy. Amino group in $H_2\mathbf{L}^1$ shows decreased protonation constant ($\log K_a$ = 6.79) compared to those found for other studied bis(phosphinates) ($\log K_a$'s = 10.75–11.05) with distant amino group. The structure of $[Ca(H_2\mathbf{L}^2\text{-}O,O')(H\mathbf{L}^2\text{-}O,O')]Cl$ revealed octahedral arrangement of the metal coordination sphere and linear polymeric structure through eight-membered $Ca(–O–P–O–)_2Ca$ rings. The structure of the $[Cu(H\mathbf{L}^3\text{-}O,O')_2(H_2O)]\cdot 5H_2O$ complex shows two chelating bis(phosphinate) groups in equatorial O_4. The structure of the $[Cu(H_{0.5}\mathbf{L}^3\text{-}O,O')(NO_3)_{0.5}]\cdot 2.25H_2O$ complex shows two different coordination environments – elongated tetragonal pyramid and trigonal bipyramid with bidentately bound nitrate ion.

Introduction

Geminal bis(phosphonates), BP's, are an important group of organophosphorus compounds. The proximity of two phosphonate groups leads to strong chelating ability[1] and strong interactions with surface of various inorganic materials.[2,3] Their high affinity to hydroxyapatite, that is the main inorganic component of bone tissue, brings extensive medical applications in treatment of osteoporosis and other diseases of calcified tissues.[4] Anchoring of BP's on the surface of titanium dioxide,[5–7] iron oxides[8–11] and many other inorganic materials has been employed in broad range of academic and industrial applications.[2,3,12,13] An important class of BP's are those bearing an amino group in the side chain. They show specific pharmaceutical properties and, in addition, the amino group could be utilized as a reactive moiety for attachment of various functionalities such as different drugs, fluorescent labels, complexes of metal radioisotopes, peptides etc. to deliver their cargo to bone or calcified tissues.[12–15] Bis(phosphonates) may also act as inhibitors in biochemical pathway as they interact with metal ions that are typically present in active centers of enzymes such as ATPases, farnesyl transferase, squalene synthase or tyrosine phosphatase,[16] however, the high hydroxyapatite affinity excludes any biomedical application that is not related to bone tissue.

Coordination properties of geminal bis(phosphonate) group have been found to be very advantageous. Thus, polydentate ligands bearing this group have been designed and synthesized, and coordination to metal ions in aqueous solutions as well as in the solid state has been investigated.[1] The geminal bis(phosphonate) group interacts strongly with hard metal ions and often bridges two or more metal ions, which leads to polymeric structures. Due to excellent coordination ability, bis(phosphonate) group might be considered as an excellent building block in the design of polydentate ligands. These ligands are mainly investigated as metal carriers for biomedical applications such as magnetic resonance imaging (MRI), radiodiagnosis (PET, SPECT) or radiotherapy. However, the strong adsorption to bone mineral and the strong affinity to inorganic materials disable some applications of the bis(phosphonates) conjugates in biomedical fields.

The disadvantage of bis(phosphonates) could be overcome using geminal bis(phosphinates) (Scheme 1) having similar metal ion binding motif as BP's but showing negligible adsorption on inorganic surfaces.[17,18] Unlike BP's, much less attention has been devoted to geminal bis(phosphinates)[19–21] and only few complexation studies have been published.[22] Whereas research on BP's is mostly focused on bone or calcium-related issues, bis(phosphinates) might be studied as inhibitors of various enzymes or as chelating groups in biomedical applications where strong bone affinity is undesirable. Furthermore, bis(phosphinates) bring new structural motifs (Scheme 1) as each phosphinate group can be attached to two carbon atoms. This allows for synthesis of polydentate ligands bearing bis(phosphinate) groups in the middle of e.g. polyamine chain, and fine tuning of coordination properties of such ligands. Due to the chain-forming ability, the bis(phosphinate) ligands might be interesting building blocks for MOF (metal-organic-framework) materials.

Recently, we have reported on 1-hydroxyalkyl-bis(H-phosphinic acids)[18] and symmetrical methylene-bis[(aminomethyl)phosphinic acids] (Scheme 2, $H_2\mathbf{L}^{5–7}$) with amino groups at the opposite ends of the molecules.[23] As continuation of this study, we present here four geminal bis(phosphinates): $H_2\mathbf{L}^1$, $H_2\mathbf{L}^2$, $H_2\mathbf{L}^3$ and $H_4\mathbf{L}^4$ with

[a] Department of Inorganic Chemistry, Faculty of Science, Charles University in Prague, Hlavova 2030, 128 40 Prague 2, Czech Republic
Fax: +420 221951253
E-mail: kubicek@natur.cuni.cz
www: http://web.natur.cuni.cz/anorchem/19/
Supporting information for this article is available on the WWW under http://www.eurjic.org/ or from the author.

EurJIC European Journal of Inorganic Chemistry
www.eurjic.org

an aminoalkyl group attached to the central carbon atom (Scheme 2). They are analogues of aminomethyl-bis(phosphonic acid) (H_4**meth**) and 4-aminobutyl-1,1-bis(phosphonic acid) (alendronate; H_4**ale**). Acid-base properties and coordination ability of these new bis(phosphinates) were studied to get more information on this class of chelating agents, and to define structural motifs suitable for molecules/conjugates where low bone affinity and a rather weak complexing power are necessary requirements. The data will be used in design of polydentate ligands for biomedical applications.

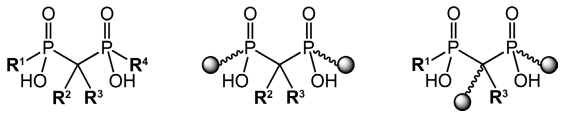

Scheme 1. General structure of bis(phosphinates) and possibilities of their utilization as chain forming groups.

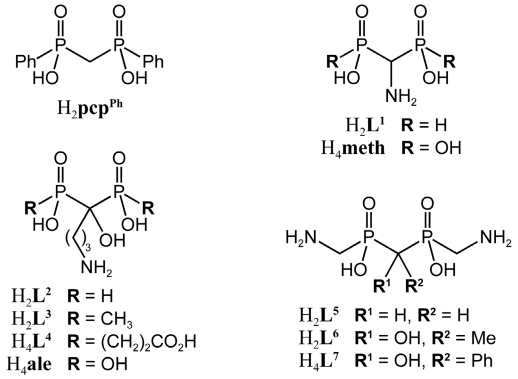

Scheme 2. Structures of studied aminoalkyl-1,1-bis(phosphinates) and related compounds.

Results and Discussion

Synthesis and stability of the ligands

The synthetic pathways used for preparation of compounds H_2**L**^{1}, H_2**L**^{2}, H_2**L**^{3} and H_4**L**^{4} are depicted in Schemes 3 and 4. Compound H_2**L**^{1} was synthesized by modification of the previously reported method utilizing reaction of ethyl formimidate **I** with bis(trimethylsilyl)hypophosphite **IIa**.[24] Our approach employs *in situ* formation of pyrophoric phosphine **IIa** and an easy purification without need of distillation of the silylated intermediate. Compounds H_2**L**^{2}, H_2**L**^{3} and H_4**L**^{4} were synthesized by reaction of *N*-protected 4-aminobutanoyl chloride **IV** with two equivalents of phosphine **IIa** or appropriate bis(trimethylsilyl)phosphonites **IIb** or **IIc**. The reaction is analogous to those previously reported for geminal bis(H-phosphinates)[18,25] and for cyclic amino-bis(phosphinates).[20] The protected intermediates **Va-c** were treated with aq. HCl or with hydrazine to remove the phthalimide protecting group; the *t*-butyl ester groups of compound **Vc** were removed during the reaction with hydrazine as well. The reaction mixture obtained after deprotection of compound **Vc** contained a side-product (~ 30 %) that was identified as monohydrazide of the ligand H_4**L**^{4} (Figure S1).

Bis(phosphinic acids) H_2**L**^{1} and H_2**L**^{2} show limited stability in aqueous solutions due to presence of geminal H-phosphinic acid groups. The decomposition is very slow in alkaline solutions (1 M aq. NaOH) and only traces (<10 %) of decomposition products were found after 20 days at 80 °C. In contrary, both compounds show complete decomposition in acidic media (1 M aq. HCl). Half-lives for compounds H_2**L**^{1} and H_2**L**^{2} were 3.2 h and 194 h at 80 °C, respectively (Figure S2). In the latter case, the value is in the same range as half-lives previously reported for other geminal bis(H-phosphinic acids)[18] and the decomposition (formally, hydrolysis) yields the appropriate α-hydroxoalkyl(H-phosphinic acid) **VI** and phosphorous acid. Contrary, decomposition of compound H_2**L**^{1} in acidic solution is significantly faster indicating a low stability of the aminomethyl-bis(H-phosphinic acid) fragment. The decomposition yields quantitatively aminomethyl-(H-phosphinic acid) **III**[26] (Scheme 3) and 4-amino-1-hydroxobutylphosphinic acid **VI**[27] (Scheme 4); it could be considered as a new synthetic route for the preparation of H-phosphinic acids. On the other hand, compounds H_2**L**^{3} and H_4**L**^{4} are fully stable in aqueous solution at any pH.

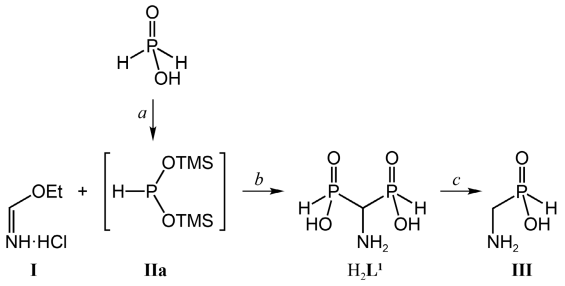

Scheme 3. Synthesis of the compound H_2**L**^{1}. Reagents and conditions: (*a*) HMDS, 100 °C; (*b*) 1. CH_2Cl_2, RT; 2. EtOH, RT; (*c*) 1 M aq. HCl, 80 °C.

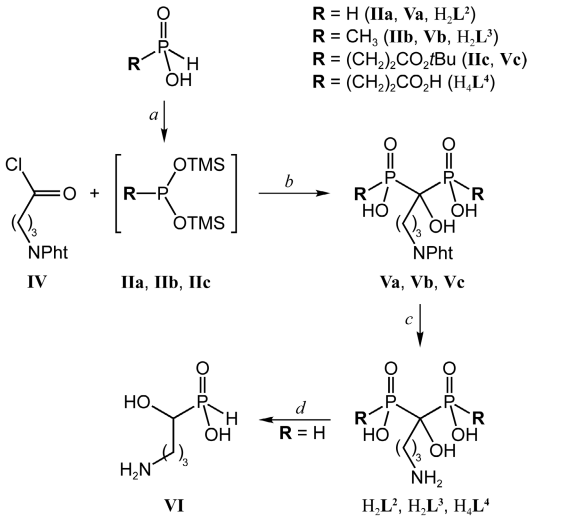

Scheme 4. Synthesis of the studied bis(phosphinates). Reagents and conditions: (*a*) TMSCl/NEt_3, CH_2Cl_2, RT; (*b*) 1. CH_2Cl_2, RT; 2. EtOH, RT; (*c*) $N_2H_4{\cdot}H_2O$ in EtOH, RT; or conc. aq. HCl, reflux; (*d*) 1 M aq. HCl, 80 °C. Pht = phthaloyl.

EurJIC European Journal of Inorganic Chemistry
ChemPubSoc Europe

Acid-base and coordination properties

Solution behaviour of the hydrolytically stable geminal bis(phosphinates) $H_2\mathbf{L}^3$ and $H_4\mathbf{L}^4$ and their complexes was studied by potentiometry. In parallel, amino group protonation constant, which is the crucial factor for coordination properties of the ligands, was determined by NMR titration of $H_2\mathbf{L}^1$ and $H_2\mathbf{L}^2$ (Figures S3 and S4). Values of the protonation constants are summarised in Table 1. The highest constant was assigned to protonation of the amino group (for the protonation schemes see Schemes S1 and S2). The basicity of amino group in $H_2\mathbf{L}^1$ was found to be significantly lower than those found for $H_2\mathbf{L}^2$, $H_2\mathbf{L}^3$ and $H_2\mathbf{L}^4$ due to presence of two proximate strongly electron-withdrawing H-phosphinate groups. In addition, basicities of the studied compounds are significantly lower than those published for the analogous BP's, H_4**meth** and H_4**ale** (Scheme 2, Table 1).[28] This could be explained by lower charge of the deprotonized phosphinate groups in comparison with that of fully ionized phosphonates; fully deprotonized phosphonate group is strongly electron donating and increases basicity of adjacent amino groups.[29] The other protonation constants of $H_2\mathbf{L}^3$ are ascribed to protonation of bis(phosphinate) groups and they are similar to those previously published for $H_2\mathbf{pcp}^{\mathbf{Ph}}$ (Scheme 2, Table 1).[30] For $H_4\mathbf{L}^4$, next two protonations proceed on carboxylate groups and the last determined protonation constant belongs to phosphinate group. The values are in the expected range for the $-PO_2^-$–$CH_2CH_2CO_2^-$ fragment.[31,32] Protonation constant of the second phosphinate group was not accesible as it is too low to be determined by potentiometry. The hydroxyl group cannot undergo deprotonation in aqueous solution unless metal ions are present (see below).

Coordination properties of bis(phosphinates) were studied in the systems with Cu^{2+}, Zn^{2+} and Ni^{2+} ions for 1:1 and 1:2 and 2:1 (2:1 only for ligand $H_4\mathbf{L}^4$) metal:ligand ratios. Results are summarized in Tables 2 and S1 and the distribution diagrams are shown in Figures 1 and S5–S10. Dominant complexes formed are those having 1:1 M:L ratio. Complexation starts at pH < 2 with formation of protonated complexes. The protons are very probably localized on amino and/or carboxylate groups (for $H_4\mathbf{L}^4$). Values of the stability constants, $\log K_{ML}$, are higher for $H_4\mathbf{L}^4$ and it is in agreement with a higher basicity of its amine group and with presence of additional carboxylate group resulting in a higher denticity of the ligand. Lower overall basicities of $H_2\mathbf{L}^3$ and $H_4\mathbf{L}^4$ lead to lower values of stability constants of their complexes when compared with $\log K_{ML}$ for complexes of their bis(phosphonate) analogues, H_4**meth** and H_4**ale** (Table 2).[28] Surprisingly, Zn^{2+} complexes show higher stability than Ni^{2+} complexes, which points to rather hard character of the studied bis(phosphinate) ligands.

Values of the protonation constants of [LM] or [HLM] species indicate that the protons are bound to distant amine and/or carboxylate groups and the ligands are probably coordinated only through phosphinates, similarly as it was found for complexes in the solid-state (see below). In most of the studied systems, stabilities of the complexes are not high enough to prevent precipitation of the metal hydroxides and, thus, the titrations had to be terminated in neutral region. That was not the case of the Cu^{2+}:$H_2\mathbf{L}^3$, Cu^{2+}:$H_4\mathbf{L}^4$ and Ni^{2+}:$H_2\mathbf{L}^3$ systems, where [H_{-1}LM] and [H_{-2}LM] species were identified; here, the negative index values represent formation of hydroxido complexes or metal-induced deprotonation of hydroxo group attached to the bridging carbon atom. For both $H_2\mathbf{L}^3$ and $H_4\mathbf{L}^4$, a high abundance and broad dominance range of the [H_{-1}ML] species as well as their electronic spectra (see below) point to deprotonation of the central hydroxo group. Close proximity of two strongly electron-withdrawing phosphinate groups results in increased acidity of the hydroxo group and, thus, the metal ions induce its deprotonation and simultaneous coordination even at neutral pH. In addition, the metal-induced deprotonation can be driven by formation of two five-membered chelate rings. Analogous behaviour of *P*-methylhydroxo group has been recently reported for hydroxomethylene-bis[(aminomethyl)phosphinates] $H_2\mathbf{L}^5$ and $H_2\mathbf{L}^6$ (Scheme 2)[22] and macrocyclic complexes bearing *N*-methylene(hydroxomethyl)phosphinate pendant arms.[32,33]

For both $H_2\mathbf{L}^3$ and $H_4\mathbf{L}^4$, species with different stoichiometries were also identified. High denticity of ligand $H_4\mathbf{L}^4$ allows formation of [LM_2] dinuclear complexes. Contrary, due to its lower denticity, ligand $H_2\mathbf{L}^3$ forms [H_2L_2M] species where coordination of two ligand molecules protonated on the distant amino group is supposed (see below). Coordination of the second ligand molecule or the second metal ion is not thermodynamically favoured and, thus, both types of complexes are present in solution as minor species (Figure 1).

To get more information about coordination modes in the species suggested by the potentiometric models, UV-Vis spectra of the Cu^{2+}–$H_2\mathbf{L}^3$ and Cu^{2+}–$H_4\mathbf{L}^4$ systems were recorded under conditions under which one species is dominant in solution according to the distribution diagrams (Figures 1, S5 and S8). At slightly acidic pH, light blue protonated species are present in solution. Their electronic spectra (Figure 2) show *d-d* transitions with maxima at 792 nm (ε = 30 M^{-1} cm^{-1}) and 776 nm (ε = 35 M^{-1} cm^{-1}), and ligand-to-metal CT bands with maxima at 212 nm (ε = 2500 M^{-1} cm^{-1}) and 218 nm (ε = 3030 M^{-1} cm^{-1}) for the complexes of $H_2\mathbf{L}^3$ and $H_4\mathbf{L}^4$, respectively. The spectra are similar to those of the $[Cu(H_2O)_6]^{2+}$ complex, suggesting a coordination sphere formed by oxygen atoms of phosphinate groups and water molecules as observed in the solid state (see below). At slightly alkaline pH, where the [H_{-1}LCu] species are exclusively present, colour is changed to more intensive green in accordance with the shift of the *d-d* transition maxima (673 nm, ε = 57 M^{-1} cm^{-1}, and 694 nm, ε = 55 M^{-1} cm^{-1}, for $[Cu(H_{-1}\mathbf{L}^3)]^-$ and $[Cu(H_{-1}\mathbf{L}^4)]^{3-}$ species, respectively). In addition to the high-energy CT band, another UV band with maxima at 272 nm (ε = 2280 M^{-1} cm^{-1}) and 268 nm (ε = 2300 M^{-1} cm^{-1}) for complexes of $H_2\mathbf{L}^3$ and $H_4\mathbf{L}^4$, respectively, appeared, probably corresponding to ligand-to-metal CT transition originating from alcoholate oxygen atom on the central carbon atom. Thus, these data point to presence of a different chromophore in the [H_{-1}LM] species probably containing two phosphinate and the alcoholate oxygen atoms. The data are similar to those observed for the analogous Cu^{2+} complexes of hydroxomethylene-bis(phosphinates) $H_2\mathbf{L}^5$ and $H_2\mathbf{L}^6$, where coordination of the central alcoholate group was confirmed by solid-state X-ray diffraction.[23]

EurJIC European Journal of Inorganic Chemistry
www.eurjic.org

Table 1. Overall ($\log\beta$) and stepwise (pK_a) protonation constants of the studied geminal bis(phosphinates) and related ligands.

	$H_2\mathbf{L}^{1}$ [a]	$H_2\mathbf{L}^{2}$ [a]	$H_2\mathbf{L}^{3}$ [b]		$H_4\mathbf{L}^{4}$ [b]		H_4**meth** [c]	H_4**ale** [c]	H_2**pcp**^{Ph} [d]
Specie	pK_a	pK_a	$\log\beta$	pK_a	$\log\beta$	pK_a	pK_a	pK_a	pK_a
HL	6.79(2)	10.78(3)	10.75(1)	10.75	11.05(1)	11.05	11.43	12.68	3.33
H_2L	[e]	[e]	14.38(2)	3.63	16.43(1)	5.38	8.29	11.07	1.35
H_3L	[e]	[e]	16.33(2)	1.95	20.74(1)	4.31	5.35	6.36	–
H_4L	–	–	–	–	23.35(1)	2.61	1.18	2.19	–

[a]This work, determined by ^{1}H and ^{31}P NMR (25 °C, without ionic strength control). [b]This work, determined by potentiometry (25 °C, I = 0.1 M KNO_3). [c]Ref. [28], determined by potentiometry (25 °C, I = 0.1 M $(NMe_4)Cl$). [d]Ref. [30], determined by potentiometry (25 °C, I = 0.5 M $(NMe_4)Cl$). [e]Were not determined due to low stability of the compounds under acidic conditions.

Table 2. Equilibrium constants (25 °C, I = 0.1 M KNO_3) of the complexes in the systems containing the title ligands and selected divalent metal ions. The negative hydrogen stoichiometry represents formation/coordination of alcoholate anion or formation of hydroxido complexes.

Metal ion	Equilibrium	$H_2\mathbf{L}^3$	$H_2\mathbf{L}^4$
Cu^{2+}	$Cu^{2+} + (L)^{2-} \leftrightarrow [Cu(L)]$	8.12	9.25
	$Cu^{2+} + (HL)^{-} \leftrightarrow [Cu(HL)]^{+}$	4.58	5.67
	$[Cu(L)] + H^{+} \leftrightarrow [Cu(HL)]^{+}$	7.21	7.47
	$[Cu(HL)]^{+} + H^{+} \leftrightarrow [Cu(H_2L)]^{2+}$	–	4.68
	$[CuH_{-1}(L)]^{-} + H^{+} \leftrightarrow [Cu(L)]$	6.69	7.67
	$[CuH_{-2}(L)]^{2-} + H^{+} \leftrightarrow [CuH_{-1}(L)]$	11.97	11.50
	$[Cu(HL)]^{+} + (HL)^{-} \leftrightarrow [Cu(HL)_2]$	2.66	–
	$[Cu(L)]^{2-} + Cu^{2+} \leftrightarrow [Cu_2(L)]$	–	4.67
Zn^{2+}	$Zn^{2+} + (HL)^{-} \leftrightarrow [Zn(HL)]^{+}$	4.00	4.01
	$[Zn(HL)]^{+} + H^{+} \leftrightarrow [Zn(H_2L)]^{2+}$	2.77	4.65
	$[Zn(HL)]^{+} + (HL)^{-} \leftrightarrow [Zn(HL)_2]$	2.74	–
Ni^{2+}	$Ni^{2+} + (HL)^{-} \leftrightarrow [Ni(HL)]^{+}$	3.05	3.36
	$[Ni(HL)]^{+} + H^{+} \leftrightarrow [Ni(H_2L)]^{2+}$	–	4.66
	$[NiH_{-1}(L)]^{-} + 2H^{+} \leftrightarrow [Ni(HL)]^{+}$	2 × 8.53	–
	$[NiH_{-2}(L)]^{2-} + H^{+} \leftrightarrow [NiH_{-1}(L)]^{-}$	10.65	–

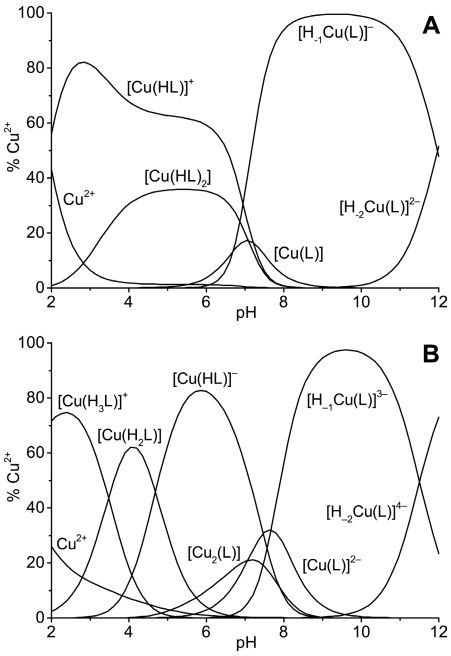

Figure 1. Distribution diagrams of (**A**): Cu^{2+}–$H_2\mathbf{L}^3$ (c_L = 4 mM, c_{Cu} = 2 mM) and (**B**): Cu^{2+}–$H_4\mathbf{L}^4$ ($c_L = c_{Cu}$ = 4 mM) systems.

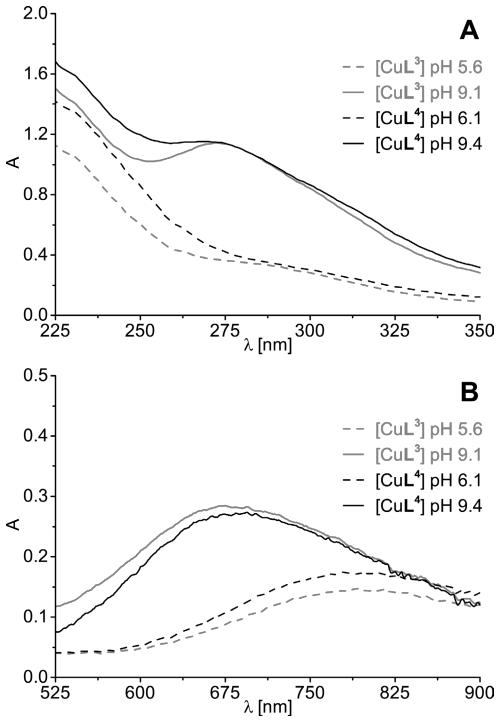

Figure 2. UV-Vis spectra of Cu^{2+} complexes with the ligands $H_2\mathbf{L}^3$ and $H_2\mathbf{L}^4$ (25 °C, water) – c_M = 5 mM, c_L = 10 mM (A); c_M = 0.5 mM, c_L = 1.0 mM (B).

The X-ray diffraction study

During the attemps to crystallize $H_2\mathbf{L}^2$, single crystals were obtained. Surprisingly, X-ray structure analysis revealed presence of polymeric Ca^{2+} complex. Presence of Ca^{2+} ions was confirmed by AAS and was explained by a long-time crystallization resulting in slow Ca^{2+} leaching from the glass vial used. The slow complex formation is essential for growth of single-crystals. Any attempts to synthesize the complex directly from Ca^{2+} salts and the ligand led to precipitation of colloidal solids.

The metal ion was octahedrally coordinated only by phosphinate oxygen atoms, leaving amino group of the ligand distant and protonated. One of phosphinate groups was disordered with P–O distances ~1.50 Å in the first arrangement and 1.51 and 1.55 Å in the second one (Table S2), pointing to probable protonation of one

EurJIC European Journal of Inorganic Chemistry
ChemPubSoc Europe

of oxygen atom in the latter case. Indeed, an electronic maximum was present close to the oxygen atom bound to phosphorus with the longest P–O bond, which was attributable to hydrogen atom. Therefore, the phosphinate was modelled as disordered in two positions with equal occupancy – one deprotonated, and the other protonated, leading to equal abundance of $H_2\mathbf{L}^2$ and $(H\mathbf{L}^2)^-$ species. Such a half protonation of the ligand leads to equal abundance of $[(Ca^{2+})_{0.5}(Cl^-)_{0.5}\{(H_2\mathbf{L}^2)\}]^{0.5+}$ and $[(Ca^{2+})_{0.5}(Cl^-)_{0.5}\{(H\mathbf{L}^2)^-\}]^{0.5-}$ species, and thus, to overall formula $[Ca(H_2\mathbf{L}^2\text{-}O,O')(H\mathbf{L}^2\text{-}O,O')]Cl$. Coordination geometry of the Ca^{2+} centre is given in Table S3 and the structure is depicted in Figures 3, S11 and S12. The bis(bisphosphinate) groups exhibit two different coordination motifs. Equatorial plane of the octahedron is defined by two ligands in *O*,*O*′-bidentate mode forming six-membered chelates – i.e. one oxygen atom originate from each phosphinate. This motif is typical for germinal bis(phosphonate)/bis(phosphinate) complexes.[1,33] The other motif is formed by one phosphinate group of each ligand that is simultaneously coordinated in axial position of neighbouring metal centre forming M–O–P–O–M bridge. Two neighbouring metal centres are connected through two of these bridges forming an eight-membered ring that is typical for solid-state structures of phosphinate complexes.[35] Both coordination motifs are similar to those found for amino-bis(phosphonate) Ca^{2+} complexes. 4-amino-1-hydroxo-butyl-1,1-bis(phosphonic acid) (alendronate, H_4**ale**) as well as 3-amino-1-hydroxo-propyl-1,1-bis(phosphonic acid) (pamidronate) form polymeric complexes containing both motifs – *O*,*O*′-bidentate mode (one oxygen from each phosphonate) and M–O–P–O–M bridges.[36] However, presence of three oxygen atoms on each phosphonate leads to different overall arrangement of metal centres and ligand molecules. In addition, 1-hydroxo-1,1-bis(phosphonates) exhibit also tridentate coordination to Ca^{2+} ions through two phosphonates and hydroxyl oxygen atom as it has been recently reported for other Ca^{2+}-alendronate complex.[37] Similarly to our structure, all the mentioned bis(phosphonate) complexes also contain protonated amine group which is not involved in metal ion coordination.

Attempts for crystallisation of the transition metal complexes studied by potentiometry were mostly unsuccessful due to formation of oily or microcrystalline products. We were successful in growing single crystals from Cu^{2+}–$H_2\mathbf{L}^3$ system, where (based on experimental conditions) two different solid phases were obtained. In the first case (diffusion of dibenzylamine/*i*PrOH solution into aqueous $Cu(NO_3)_2$–$H_2\mathbf{L}^3$ solution resulting in pale blue crystals), the X-ray diffraction analysis revealed the formula $[Cu(H\mathbf{L}^3\text{-}O,O')_2(H_2O)]\cdot 5H_2O$. The Cu^{2+} ion is coordinated in almost regular square-pyramidal coordination sphere ($\tau = 0.05$)[38] formed by four in-plane oxygen atoms of two different chelating bis(phosphinate) groups (each oxygen atom originates from a different phosphinate group) and apically coordinated water molecule (Figures 4 and S13, Table 3). Nitrogen atoms of the ligand molecules are protonated and lay apart from the coordination sphere. The tetragonal base is slightly distorted with coordination bond lengths d_{Cu-O} = 1.93–1.98 Å (Table 3) and mean difference of the atoms from the average O_4 plane is ±0.022(1) Å. The distance Cu–O_{1c} of the axial water molecule is ~2.25 Å. The in-plane O–Cu–O angles defined by oxygen atoms originating from one ligand molecule are slightly larger (90 and 92°, respectively) comparing to the angles defined by oxygen atoms originating from different ligand molecules (~88°). The Cu^{2+} ion is located very close to the tetragonal base – it is placed only slightly above the O_4 plane by 0.160(1) Å. The in-plane location of Cu^{2+} ion mostly predestines coordination of the sixth donor atom below the basal plane completing octahedral sphere. But surprisingly, there is no such interaction. It results from the geometry of the crystal packing shown in Figures 5 and S14. The neighbouring complex units are closely packed in direction of the Cu–O_{1c} coordination bond, allowing not enough space for coordination in the octahedral mode, as there is short distance (3.40 Å) between Cu^{2+} ion and coordinated water molecule from the (x; ½–y; ½+z) neighbouring unit, which blocks the sixth position. Water solvate molecules fill the space between the complex units, and are located close to the coordinated water molecule. Whole structure is stabilised by rich network of strong to medium-strong hydrogen bonds between phosphinates, protonated amines, ligand hydroxo groups and water molecules.

Similar to Ca^{2+} complexes, the bis(phosphinate) coordination mode and geometry in Cu^{2+} complexes resemble those that have been reported for complexes of aminoalkyl-bis(phosphonates), however, a lower number of oxygen atoms results in monomeric nature of the bis(phosphinate) complex, contrary to the bis(phosphonates) forming mostly dinuclear complexes or coordination polymers.[1] The monomeric structure is rather unusual among structures of complexes of simple aminoalkylphosphinates where, if amino group is protonated, the phosphinate group often bridges metal ions leading to dimeric or polymeric structure motifs.[35] On the other hand, bis(phosphinate) H_2**pcp**^{Ph} forms often square pyramidal Cu^{2+}-complexes,[30,34] which possess both, monomeric as well polymeric structure, and the Cu–O coordination bonds (1.9–2.0 Å) are of the same length as those found in the structure of $[Cu(H\mathbf{L}^3\text{-}O,O')_2(H_2O)]\cdot 5H_2O$. Despite significantly lower basicity, bis(phosphinates) show Cu–O bond lengths similar to those found in Cu^{2+} complexes of bis(phosphonates). It points to the ionic nature of the coordination bonds in complexes of both kinds of ligands.

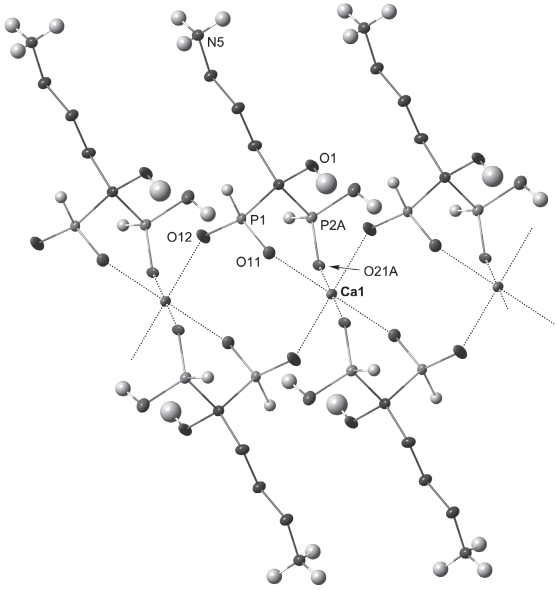

Figure 3. Part of coordination polymer found in the crystal structure of $[Ca(H_2\mathbf{L}^2\text{-}O,O')(H\mathbf{L}^2\text{-}O,O')]Cl$. From variants caused by disorder of phosphinate function, the one representing protonated phosphinate $[(Ca^{2+})_{0.5}(Cl^-)_{0.5}\{(H_2\mathbf{L}^2)\}]^{0.5+}$ is shown. Carbon-bound hydrogen atoms are omitted for the sake of clarity.

EurJIC European Journal of Inorganic Chemistry
www.eurjic.org

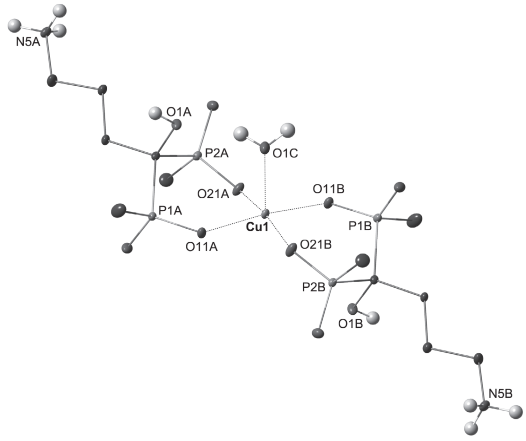

Figure 4. Structure of the [Cu(H**L**^{3}-*O*,*O*′)$_2$(H$_2$O)] complex unit as found in the crystal structure of [Cu(H**L**^{3}-*O*,*O*′)$_2$(H$_2$O)]·5H$_2$O. Carbon-bound hydrogen atoms are omitted for the sake of clarity.

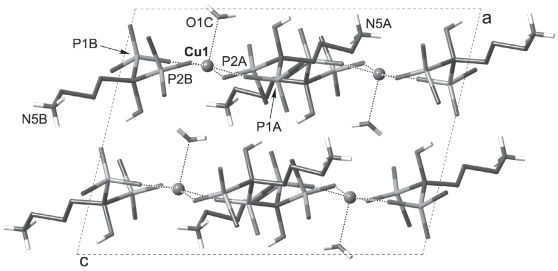

Figure 5. Crystal packing found in the solid-state structure of [Cu(H**L**^{3}-*O*,*O*′)$_2$(H$_2$O)]·5H$_2$O; view along *y* axis. Solvate water molecules and carbon-bound hydrogen atoms are omitted for the sake of clarity.

Table 3. Geometry of the Cu^{2+} coordination sphere of the [Cu(H**L**^{3}-*O*,*O*′)$_2$(H$_2$O)]·complex.

Bond lengths (Å)		Bond angles (°)	
Cu1–O1C	2.2457(13)	O1C-Cu1-O11A	92.62(5)
Cu1–O11A	1.9789(11)	O1C-Cu1-O21A	99.81(5)
Cu1–O21A	1.9447(11)	O1C-Cu1-O11B	95.39(5)
Cu1–O11B	1.9784(11)	O1C-Cu1-O21B	90.93(5)
Cu1–O21B	1.9343(12)	O11A-Cu1-O21A	90.33(5)
		O11A-Cu1-O11B	171.98(5)
		O11A-Cu1-O21B	87.91(5)
		O21A-Cu-O11B	88.03(5)
		O21A-Cu-O21B	169.18(5)
		O11B-Cu-O21B	92.24(5)

When solution of Cu^{2+}–H$_2$**L**^{3} in water-*i*PrOH mixture was crystallized in presence of nitrate anions at pH ≈ 4.5, light blue-green crystals of coordination polymer with formula [Cu(H$_{0.5}$**L**^{3}-*O*,*O*′)(NO$_3$)$_{0.5}$]·2.25H$_2$O were isolated. The structure is polymeric, and, similarly to the previous case, the ligand molecules are coordinated only through phosphinate oxygen atoms. The part of the coordination polymer is shown in Figures 6 and S15. In this structure, two different coordination environments of copper(II) are present. Copper(II) ion Cu1 is coordinated in centrosymmetric tetragonal bipyramid elongated by Jahn-Teller effect, with Cu–O axial distances (2.42 Å) significantly longer than the equatorial ones (~1.95 Å). Equatorial sites are occupied by phosphinate oxygen atoms from two ligand molecules, while in the axial sites, oxygen atoms of the nitrate anions are bound (Figure 6). The coordination sphere of the copper(II) ion Cu2 is very irregular, although the Cu-centre possess two-fold symmetry. The coordination sphere can be viewed as trigonal bipyramid with one equatorial position occupied by bidentately-bound κ-*O*,*O*′-nitrate ligand with very long coordination interaction ($d_{Cu–O}$ = 2.63 Å). Other equatorial as well as the axial bonds are much shorter (1.98 and 1.95 Å, respectively). Selected relevant structural parameters are listed in Table 4. Similar to previous structures, bis(phosphinate) group is coordinated to each metal centre in *O*,*O*′-bidentate mode – one oxygen from each phosphinate. Each of the bis(phosphinate) groups is coordinated to two metal centres in such chelating mode.

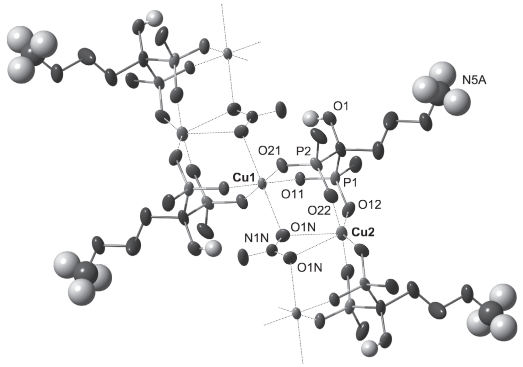

Figure 6. Part of the structure of the complex polymer [Cu(H$_{0.5}$**L**^{3}-*O*,*O*′)(NO$_3$)$_{0.5}$] unit as found in the crystal structure of [Cu(H$_{0.5}$**L**^{3}-*O*,*O*′)(NO$_3$)$_{0.5}$]·2.25H$_2$O. Water solvate molecules and carbon-bound hydrogen atoms are omitted for the sake of clarity. From two disordered positions of the aminopropyl side-chain, the one with tentative protonation to RNH$_3^+$ group is shown.

Conclusions

Four geminal bis(phosphinic acids) were synthesized as a new class of chelating agents. The acids bearing H–P bond show limited stability in acidic solutions. Hydrogen atom, having here a rather hydride character, behaves as electron-withdrawing substituent decreasing stability of C–P bond in formally hydrolytic reaction. On the other hand, presence of the other P–C bonds leads to fully stable compounds. Presence of two electron-withdrawing phosphinate groups leads to a low electron density on the adjacent amine group in H$_2$**L**^{1} and, thus, to the low value of its protonation constant. The same effect leads also to easy metal-assisted deprotonation of the central hydroxo groups in H$_2$**L**^{3} and H$_4$**L**^{4} and the alcoholate coordination stabilizes their complexes at neutral and slightly alkaline pH. In connection with our recent results, this phenomenon seems to be general for coordination properties of ligands with the *P*-hydroxomethyl moiety. The studied bis(phosphinates) show lower basicity of their amino groups and, thus, lower stability of complexes with divalent metal ions in comparison with their bis(phosphonate) analogues. The bis(phosphinate) moiety forms six-membered chelate rings which are preferred over coordination of weakly basic amine groups. Due to presence of very acidic phosphinic acid groups, complexation of the studied metal ions proceeds even at solutions having low pH what is highly desirable property in design of new polydentate ligands for biomedical applications.

EurJIC European Journal of Inorganic Chemistry
ChemPubSoc Europe

Table 4. Geometry of the coordination spheres of both independent Cu^{2+} ions in the structure of $[Cu(H_{0.5}\mathbf{L}^3\text{-}O,O')(NO_3)_{0.5}]\cdot 2.25H_2O$.

Bond lengths (Å)		Bond angles (°)		Bond angles (°)	
Cu1–O11	1.952(2)	O11-Cu1-O21	93.26(7)	O12-Cu2-O22	94.74(8)
Cu1–O21	1.945(2)	O11-Cu1-O1N	86.04(6)	O12-Cu2-O1N	82.91(7)
Cu1–O1N	2.428(2)	O11-Cu1-O11# [a]	180	O12-Cu2-O12# [b]	146.1(1)
		O11-Cu1-O21# [a]	86.74(7)	O12-Cu2-O22# [b]	87.14(8)
Cu2–O12	1.981(2)	O11-Cu1-O1N# [a]	93.96(6)	O12-Cu2-O1N# [b]	130.95(7)
Cu2–O22	1.946(2)	O21-Cu1-O1N	90.06(8)	O22-Cu2-O1N	88.95(7)
Cu2–O1N	2.627(2)	O21-Cu1-O21# [a]	180	O22-Cu2-O22# [b]	173.5(1)
		O21-Cu1-O1N# [a]	89.94(8)	O22-Cu2-O1N# [b]	85.14(7)
		O1N-Cu1-O1N# [a]	180	O1N-Cu2-O12# [b]	130.95(7)
				O1N-Cu2-O1N# [b]	48.04(8)

[a] Symmetry-related atom through centre of symmetry (2–x, –y, 2–z). [b] Symmetry-related atom through two-fold axis (2–x, y, 2½–z).

Experimental Section

Materials and methods: Commercially available chemicals had synthetic purity and were used as received. Organic solvents had synthetic purity and were also used as recieved. Dry CH_2Cl_2 was freshly distilled with P_2O_5. Deionized water was used for synthesis and measurements. [2-(*t*-butyloxycarbonyl)ethyl]phosphinic acid was prepared according to the published procedure.[39] The ^1H, ^{13}C and 2D NMR (H,H-COSY, H,C-HSQC and H,C-HMBC) spectra were recorded at 25 °C on Bruker Avance III 600 MHz spectrometer equipped with the triple-resonance cold probe. The ^{31}P NMR spectra were recorded at 25 °C on Varian NMR system operating at 300 MHz proton frequency with ASW probe. NMR spectra were referenced to *t*BuOH (internal standard, δ_H = 1.25, δ_C = 30.3 ppm) and 85 % H_3PO_4 (external standard, δ_P = 0 ppm). Chemical shifts are given in the ppm scale and the coupling constants are given in Hz. ESI-MS spectra were recorded on a Bruker Esquire 3000 spectrometer with ESI ionization and ion-trap detection. TLC was performed with silica on aluminium sheets (Merck 1.0554 F_{254}); the spots were detected with UV fluorescence (λ = 254 nm) or visualized by iodine vapours. Mobile phases for TLC were freshly prepared prior to use.

Aminomethyl-bis(H-phosphinic acid) ($H_2\mathbf{L}^1$): Under an argon atmosphere, dry $(NH_4)H_2PO_2$ (10.0 g; 120 mmol) was suspended in hexamethyldisilazane (HMDS, 100 mL) and the mixture was heated at 110 °C under a gentle flow of argon overnight. The mixture containing pure $HP(OTMS)_2$ was cooled to room temperature (RT) and dry CH_2Cl_2 (100 mL) was added. The suspension of ethyl formimidate hydrochloride (3.31 g; 30.2 mmol) in dry CH_2Cl_2 (150 mL) was added dropwise and the mixture was stirred at RT overnight. Then, the resulting solution was added dropwise into EtOH (500 mL) to hydrolyse the silylester groups. The precipitate was collected on glass frit and this crude product was purified on strong cation exchange resin (Dowex 50; H^+-form; elution with water followed by 50 % aq. EtOH). The fractions containing product were combined and evaporated under reduced pressure. The resulting oil was further dried under reduced pressure for several days at RT. The product was obtained as colourless oil, which solidified on standing (1.95 g; 37 % yield).

NMR ($NaOD/D_2O$, pD = 7): ^1H δ 2.94 (*CH*, t, 1H, $^2J_{HP}$ = 15); 7.08 (P*H*, d, 2H, $^1J_{HP}$ = 541); $^{13}C\{^1H\}$ δ 54.4 (*C*H, t, $^1J_{CP}$ = 80); ^{31}P δ 17.0 (dm, $^1J_{PH}$ = 541). MS: **(–)** 158.6 $[M–H^+]^-$, **(+)** 160.7 $[M+H^+]^+$. TLC (MeCN:MeOH:conc. aq. NH_3 3:1:2): R_f = 0.2. Elemental analysis (calc. for $CH_7NO_4P_2$, M_r = 159.0): C 7.6 (7.8); H 4.4 (4.5); N 8.8 (8.7).

Aminomethyl-(H-phosphinic acid) (III): In a glass vial, compound $H_2\mathbf{L}^1$ (40.1 mg; 252 μmol) was dissolved in 1 M aq. HCl (0.5 mL) and the mixture was heated at 80 °C for 2 d. After cooling to RT, the mixture was evaporated to dryness. The residue was dissolved in water (0.5 mL) and *i*PrOH (3.0 mL) was then added to produce cloudiness. After standing in a fridge overnight, the upper phase was discarded and the resulting oil was purified on strong cation exchange resin (Dowex 50; H^+-form; elution with water followed by 10 % aq. pyridine). Pyridine fraction was evaporated to dryness and several times co-evaporated with water. The resulting oily product (^{31}P NMR purity > 95 %) was characterized without further purification or isolation.

NMR (D_2O, pD = 4): ^1H δ 3.04 (CH_2, d, 2H, $^2J_{HP}$ = 11); 7.08 (P–*H*, d, 1H, $^1J_{HP}$ = 541); $^{13}C\{^1H\}$ δ 39.3 (*C*H$_2$, d, $^1J_{CP}$ = 89); ^{31}P δ 14.5 (dt, $^1J_{PH}$ = 541, $^2J_{PH}$ = 11). MS: **(–)** 94.2 $[M–H^+]^-$. TLC (MeCN:MeOH:conc. aq. NH_3 3:1:2): R_f = 0.6.

Solution of 4-(phthalimido)butanoylchloride (IV): In 50 mL flask, 4-(phthalimido)butanoic acid (3.79 g; 15.1 mmol) was dissolved in CH_2Cl_2 (25 ml) and $(COCl)_2$ (3.20 mL; 37.5 mmol) was added. Resulting mixture was stirred at RT for 3 h and then evaporated to dryness. Residue was co-evaporated three-times with dry CH_2Cl_2 and then dissolved in dry CH_2Cl_2 (10 mL). The solution was used immediately as obtained in the next reactions.

4-Amino-1-hydroxybutyl-1,1-bis(H-phosphinic acid) ($H_2\mathbf{L}^2$): Under an argon atmosphere, dry $(NH_4)H_2PO_2$ (5.00 g; 60.2 mmol) was suspended in HMDS (50 mL) and the mixture was heated at 110 °C under a gentle flow of argon overnight. The mixture containing pure $HP(OTMS)_2$ was cooled to RT and dry CH_2Cl_2 (25 mL) was added. Then, freshly prepared solution of **IV** obtained from 4-(phthalimido)butanoic acid (3.79 g; 15.1 mmol) was added and the mixture was stirred at RT overnight. Then, the resulting solution was added dropwise into EtOH (200 mL) to hydrolyse the silylester groups. The precipitate was collected on glass frit and washed with EtOH (50 mL). Another fraction of the solid was collected from the filtrate after standing overnight. Both fractions were combined and dried over P_2O_5 in vacuum desiccator. The crude 4-(phthalamido)butyl-1,1-bis(H-phosphinic acid) (**Va**) was obtained as a white powder (5.85 g) and was not further purified. Crude **Va** was dissolved in a mixture of 75 % aq. N_2H_4 (60 mL) and EtOH (60 mL) and stirred at RT overnight. Excess of EtOH (300 mL) was then added and the flask was kept in fridge for 3 days. The upper phase was decanted off and the resulting oil was dissolved in water (40 mL) and EtOH (300 mL) was added. Next day the upper phase was decanted off and the remaining oil was dissolved in conc. aq. ammonia (100 mL), evaporated to dryness and further co-evaporated three times with water. Residue was dissolved in water (100 mL) and pH of the resulting solution was adjusted to 8 using 2 M aq. NaOH. Solution was evaporated to dryness, the residue was dissolved in water (100 mL) and the pH was again adjusted to 8 using 2 M aq. NaOH. This procedure was repeated until the pH of the re-dissolved aq. solution reached 8. Then, the solution was concentrated to 10 mL and slowly added dropwise into a vigorously stirred mixture of anhydrous EtOH:THF (1:1; 400 mL). The precipitate was collected on glass frit and washed with MeOH (200 mL). The resulting solid was dissolved in water (100 mL) and some charcoal was added. The mixture was filtered and the filtrate was evaporated to dryness and further co-evaporated several times with water (100 mL). Resulting solid was dried over P_2O_5 in vacuum desiccator. The product was obtained as white crystalline powder in a form of a mixed ammonium-sodium salt (2.29 g, 54 %).

NMR (D_2O, pD = 7): ^1H δ 1.90 (*CH*$_2$–C–P, m, 2H); 1.99 (*CH*$_2$–CH$_2$–N, m, 2H); 3.05 (*CH*$_2$–N, t, 2H, $^3J_{HH}$ = 7); 6.96 (P*H*, dt, 2H, $^1J_{HP}$ = 527, $^3J_{HP}$ = 17); $^{13}C\{^1H\}$ δ 23.6 (CH$_2$–*C*–P, t, $^2J_{CP}$ = 6); 29.5 (CH$_2$–*C*–N, s); 42.2 (*C*H$_2$–N, s); 75.8 (*C*–P, t, $^1J_{CP}$ = 93); ^{31}P δ 24.5 (dm, $^1J_{PH}$ = 527); $^{31}P\{^1H\}$ δ 24.5 (s). MS: **(–)** 215.4 $[M–H^+]^-$. TLC (EtOH:conc. aq. NH_3 1:1): R_f = 0.3. Elemental analysis (calc. for $Na_{1.6}(NH_4)_{0.4}C_4H_{11}NO_5P_2\cdot 0.5H_2O$, M_r = 282.2): C 17.0 (17.2); H 4.7 (4.8); N 6.9 (6.7).

4-Amino-1-hydroxybutyl-1-(H-phosphinic acid) (VI): In a glass vial, $H_2\mathbf{L}^2$ (300 mg; 1.06 mmol) was dissolved in 1 M aq. HCl (5 mL) and the mixture was heated at 80 °C for 30 d. After cooling to RT, the mixture was evaporated to dryness. The crude product was purified on strong cation exchange resin (Dowex 50; H^+-form; elution with water followed by 10 % aq. pyridine). Pyridine fraction was evaporated to dryness and several times co-evaporated with water. The resulting oily product (94 % purity as determined by ^{31}P NMR) was analysed without further purification.

NMR (D_2O, pD = 4): ^1H δ 1.64 (*CH*$_2$–C–P, m, 1H); 1.79 (*CH*$_2$–C–P, m, 1H); 1.79 (*CH*$_2$–CH$_2$–N, m, 1H); 1.93 (*CH*$_2$–CH$_2$–N, m, 1H); 3.06 (*CH*$_2$–N, m, 2H); 3.58 (*CH*–P, m, 1H); 6.79 (P*H*, dm, 1H, $^1J_{HP}$ = 509); $^{13}C\{^1H\}$ δ 24.1 (*C*H$_2$–CH$_2$–N, d, $^3J_{CP}$ = 12); 26.7 (CH$_2$–*C*–P, s); 39.9 (*C*H$_2$–N, s); 70.3 (*C*–P, d, $^1J_{CP}$ = 109); ^{31}P δ 29.1 (d, $^1J_{PH}$ = 509); $^{31}P\{^1H\}$ δ 29.15 (s). MS: **(–)**

152.0 ($M–H^+$)$^-$; **(+)** 154.2 [$M+H^+$]$^+$. TLC (EtOH:conc. aq. NH_3 1:1): R_f = 0.5.

4-Amino-1-hydroxybutyl-1,1-bis[(methyl)phosphinic acid] (H_2L^3): In a 100 mL flask, *N*,*N*-ethyl-diisopropylamine (DIPEA, 12.0 mL; 68.8 mmol) was added to a solution of methylphosphinic acid (2.21 g; 27.6 mmol) in dry CH_2Cl_2 (25 mL). Subsequently, chlorotrimethylsilane (TMSCl, 8.80 mL; 69.0 mmol) was slowly added and the resulting mixture was stirred at RT for 3 h. Then, freshly prepared solution of **IV** obtained from 4-(phthalimido)butanoic acid (2.78 g; 11.1 mmol) was added and the mixture was stirred at RT overnight. Ethanol (50 mL) was then slowly added to the reaction mixture to hydrolyse the silylester groups. Resulting solution was evaporated to dryness and then co-evaporated with CH_2Cl_2. Residue was dissolved in 2 M aq. NaOH (50 mL) and extracted with CH_2Cl_2 (4×50 mL). Aqueous phase was evaporated to dryness and the residue was purified on strong cation exchange resin (Dowex 50; H^+-form; elution with water) and the eluate was evaporated to dryness. Resulting mixture was dissolved in 6 M aq. HCl (100 mL) and refluxed for 3 d. Then, the reaction mixture was cooled to RT. After 3 h, precipitated phthalic acid was filtered off and the filtrate was evaporated to dryness. The residue was dissolved in a mixture of THF:MeOH:water (2:1:2; 5 mL) and purified by column chromatography (SiO_2; elution with THF:MeOH:conc. aq. NH_3 2:1:2 followed by 1:1:2; R_f (product) = 0.1 → 0.4). The fractions containing pure product were combined and evaporated to dryness. Remains of ammonia from the crude product were removed on strong cation exchange resin (Dowex 50; H^+-form; elution with water followed by 10 % aq. pyridine). The pyridine fraction was evaporated to dryness and co-evaporated several times with water. Residual pyridine was removed on weak cation exchange resin (Amberlite CG50; H^+-form; water elution). The fractions containing the product were combined and evaporated to dryness. Resulting solid was dried over P_2O_5 in vacuum desiccator. Product was obtained as white powder (1.81 g; 60 %).

NMR (D_2O, pD = 6): ^{1}H δ 1.38 (CH_3, m, 6H); 2.01 (CH_2–CH_2–N and CH_2–C–O, m, 4H), 3.04 (CH_2–N, t, 2H, $^3J_{HH}$ = 7); ^{13}C{^{1}H} δ 16.9 (*C*H$_3$, m); 24.4 (*C*H_2–C–O, s); 31.9 (*C*H_2–CH_2–N, s); 42.5 (*C*H_2–N, s); 77.8 (*C*–P, t, $^1J_{CP}$ = 93); ^{31}P{^{1}H} δ 39.9 (s). MS: **(–)** 243.7 [$M–H^+$]$^-$; 488.8 [$2M–H^+$]$^-$. TLC (THF:MeOH:conc. aq. NH_3 1:1:2): R_f = 0.4. Elemental analysis (calc. for $C_6H_{17}NO_5P_2·1.5H_2O$, M_r = 272.2): C 26.5 (26.7); H 7.4 (7.0); N 5.2 (5.5).

4-Amino-1-hydroxybutyl-1,1-bis[(2-carboxyethyl)phosphinic acid] (H_4L^4): In a 50 mL flask, DIPEA (7.21 mL; 41.4 mmol) was added to a solution of [2-(*t*-butyloxycarbonyl)ethyl]phosphinic acid (1.34 g; 6.90 mmol) in dry CH_2Cl_2 (10 mL). Subsequently, TMSCl (5.25 mL; 41.4 mmol) was slowly added and the resulting mixture was stirred at RT for 3 h. Then, freshly prepared solution of **IV** obtained from 4-(phthalimido)butanoic acid (600 mg; 2.57 mmol) was added and the mixture was stirred at RT overnight. Ethanol (20 mL) was then slowly added to the reaction mixture for hydrolysis of the silylester groups. Resulting solution was evaporated to dryness and then co-evaporated with CH_2Cl_2. The residue was dissolved in 3 % aq. HCl (30 mL) and extracted with CH_2Cl_2 (5×15 mL). Organic layers were combined and evaporated to dryness. The crude compound **Vc** was dissolved in a mixture of N_2H_4 (75 % aq. solution; 20 mL) and EtOH (20 mL) and stirred at RT for 3 d. Excess of EtOH (100 mL) was then added and the mixture was kept in fridge overnight. The upper phase was decanted and the resulting oil was purified on strong anion exchange resin (Dowex 1; OH^--form; elution with water followed by 20 % and 50 % aq. AcOH). The product-containing fractions (eluted with 50 % aq. AcOH) were combined, evaporated to dryness and further co-evaporated with water. The resulting solid was dried over P_2O_5 in vacuum desiccator. The product was obtained as white hygroscopic powder (486 mg; 49 %).

NMR (D_2O, pD = 2): ^{1}H δ 2.03 (CH_2–CH_2–N and CH_2–C–OH, m, 4H); 2.16 (CH_2–P, m, 4H); 2.67 (CH_2–CO_2H, m, 4H); 3.05 (CH_2–N, t, 2H, $^3J_{HH}$ = 7); ^{13}C{^{1}H} δ 24.4 (*C*H_2–C–OH, s); 23.3 (*C*H_2–P, m); 27.4 (*C*H_2–C_2H, s); 30.1 (*C*H_2–CH_2–N, s); 40.5 (*C*H_2–N, s); 76.0 (*C*–P, t, $^1J_{CP}$ = 92); 178.2 (*C*O, d, $^3J_{CP}$ = 15); ^{31}P{^{1}H} δ 44.4 (s). MS: **(–)** 359.1 [$M–H^+$]$^-$; **(+)** 361.2 [$M+H^+$]$^+$; 383.4 [$M+Na^+$]$^+$; 399.2 [$M+K^+$]$^+$. TLC (THF:MeOH:conc. aq. NH_3 2:1:2): R_f = 0.2. Elemental analysis (calc. for $C_{10}H_{21}NO_9P_2·1.5H_2O$, M_r = 388.2): C 30.9 (30.7); H 6.2 (5.8); N 3.6 (3.9).

The fractions eluted from the strong anion exchange resin with 20% aq. AcOH contained a side-product (~ 30 % yield) that was identified as hydrazide of the compounds H_4L^4 (for structure see Figure S1): NMR (D_2O, pD = 2): ^{1}H δ 1.90–2.23 (CH_2–CH_2–N, CH_2–C–OH, CH_2–P, m, 8H); 2.56–2.73 (CH_2–COOH, m, 4H); 3.05 (CH_2–N, m, 2H); ^{13}C{^{1}H} δ 22.5 (*C*H_2–C–OH, s); 23.1–24.3 (*C*H_2–P, m); 26.8 (*C*H_2–CO, s); 27.6 (*C*H_2–CO, s); 30.2 (*C*H_2–CH_2–N, m); 40.6 (*C*H_2–N, s); 76.3 (*C*–P, t, $^1J_{CP}$ = 93 Hz); 174.5 (*C*O–NH, d, $^3J_{CP}$ = 13); 178.6 (*C*O–OH, d, $^3J_{CP}$ = 14); ^{31}P{^{1}H} δ 41.2 (*P*, d, 1P, $^2J_{PP}$ = 28); 42.9 (*P*, d, 1P, $^2J_{PP}$ = 28). MS: (–) 374.3 [$M–H^+$]$^-$, (+) 375.9 [$M+H^+$]$^+$.TLC (THF:MeOH:conc. aq NH_3 2:1:2): R_f = 0.3.

Kinetics of hydrolysis: The hydrolysis of H_2L^1 and H_2L^2 was followed by ^{31}P NMR at the compound concentration 10 mM. The experiments were performed at constant temperature (80 °C) maintained by a thermostated bath or by NMR spectrometer. The experiments were carried in 1 M aq. HCl (pH 0) or 1 M aq. NaOH (pH 14).

Potentiometric titrations: Methodology of the potentiometric titrations and processing of the experimental data were analogous to those previously reported.[40] Titrations were carried out in a vessel thermostated at 25 ± 0.1 °C at ionic strength I = 0.1 M KNO_3. Ligand-to-metal ratio was 1:1, 2:1 (and 1:2 for H_4L^4) with c_L = 0.004 M, pH range was 1.7–12 (or till precipitation of metal hydroxide). Titrations were carried out at least three times, each consisting of about 40 points. The water ion product, pK_w = 13.78, and stability constants of the M^{2+}–OH^- systems were taken from ref. [41]. The protonation constants β_n calculated are concentration constants and are defined by β_n = [H_nL] / ([H]^n×[L]) ($\log K_1 = \log\beta_1$; $\log K_n = \log\beta_n - \log\beta_{n-1}$). The overall stability constant are defined by β_{hlm} = [$M_mH_hL_l$] / ([M]^m×[H]^h×[L]^l). The constants (with standard deviations) were calculated with program OPIUM.[42] Throughout the paper, pH means –log[H^+].

NMR Titrations: The ^{31}P{^{1}H} and ^{1}H NMR titration experiments for determination of the nitrogen protonation constants of ligands H_2L^1 and H_2L^2 (pH in range 4–13, about 15 points) were carried without control of ionic strength, at 25.0 °C and ligand concentration c_L = 0.004 M. A coaxial capillary tube with D_2O and H_3PO_4 was used for the lock and referencing. pH of the samples were adjusted with 0.1 M aq. HCl or 0.1 M aq. NaOH. Protonation constants were obtained by software OPIUM[40] by simultaneous treatment of ^{1}H and ^{31}P NMR data. Overlap of both ^{1}H NMR signals in P–C–CH_2–CH_2 fragment of ligand H_2L^2 disabled precise analysis and, thus, only the signal of methylene group attached to amine group was used for evaluation of the data.

UV-Vis measurements: UV-Vis spectra were measured on Schimadzu UV-2401PC spectrometer at 25 °C in the wavelength range 200–900 nm. Solution of ligand and metal ion were mixed and pH was adjusted to the desired values by addition of 0.1 M aq. HCl or 0.1 M aq. NaOH. Then samples were diluted with water to reach final metal concentration c_M = 5 mM for measurements in visible region or c_M = 0.5 mM for measurements in UV region.

X-ray diffraction: Few single crystals of [Ca(H_2L^2-*O*,*O*′)(HL^2-*O*,*O*′)]Cl were obtained by long time (1 month) standing of the closed vial containing mixture of the ligand H_2L^2 (18.5 mg – mixed sodium ammonium salt), 3 % aq. HCl (160 µL), *i*PrOH (400 µL) and water (200 µL). Source of calcium is probably the glass of the vial; its presence in the mother solution was confirmed by AAS analysis.

Single crystals of [Cu(HL^3-*O*,*O*′)$_2$(H_2O)]·5H_2O were obtained by slow diffusion of the 4 % dibenzylamine solution in *i*PrOH (1 mL) into a solution of H_2L^3 (19.5 mg, 71.6 µmol) and $Cu(NO_3)_2·6H_2O$ (9.6 mg, 32.6 µmol) in water (0.5 mL).

Single crystals of [$Cu(H_{0.5}L^3$-*O*,*O*′)$(NO_3)_{0.5}$]·2.25H_2O were prepared by mixing H_2L^3 (19.6 mg, 72.0 µmol), $Cu(NO_3)_2·6H_2O$ (19.3 mg, 65.5 µmol), picric acid (16.5 mg, 72.0 µmol) in water (0.5 mL). Guanidinium carbonate was added till dissolution of all matter (pH ~4.5) and the mixture was shortly heated at 80 °C. A blue powder formed during few weeks was filtered, disoolved in water (0.5 mL) and crystallized by addition *i*PrOH (0.5 mL). The complex was also formed in absence of picric acid and guanidinium carbonate; however, the single-crystals were of low quality.

The diffraction data were collected at 150 K (Cryostream Cooler, Oxford Cryosystem) using a Nonius Kappa CCD diffractometer and Mo-K$_\alpha$ radiation (λ = 0.71073 Å). The frames were integrated with the Bruker SAINT software package using a narrow-frame algorithm.[43] Data were corrected for absorption effects using the multi-scan method (SADABS).[44] The structure was solved by direct methods (SHELXS97),[45] and refined by full-matrix least-squares techniques (SHELXL97).[46] All non-hydrogen atoms were refined anisotropically. All hydrogen atoms were located in the electron density difference map; however, they were placed in theoretical (C–H, N–H) or original (O–H) positions with thermal parameters U_{eq}(H) = 1.2 U_{eq}(X), as their free refinement led to several unrealistic bond lengths. In the case of crystal structure of [Ca(H_2L^2-*O*,*O*′)(HL^2-*O*,*O*′)]Cl, the independent unit is formed by Ca, Cl and one ligand molecule, with Ca and Cl atoms laying in special positions with half-occupancy. The amino group of the ligand is protonated. One of phosphinate functions was found to be disordered and was modelled in two positions with equal occupancy (Figure S11). In one possibility, the phosphinate function is protonated, while in the second possibility it is not, as documented also by P–O bond distances (Table S2). Such half-protonation is a result of need to

EurJIC European Journal of Inorganic Chemistry
ChemPubSoc Europe

compensate the overall charge of Ca^{2+} and Cl^- ions, resulting in formal formula $(Ca^{2+})_{0.5}(Cl^-)_{0.5}\{(H_{1.5}\mathbf{L}^2)^{0.5-}\}$, i.e. $[Ca(H_2\mathbf{L}^2\text{-}O,O')(H\mathbf{L}^2\text{-}O,O')]Cl$. In the case of $[Cu(H\mathbf{L}^3\text{-}O,O')_2(H_2O)]\cdot 5H_2O$, no special treatment was needed. In the case of $[Cu(H_{0.5}\mathbf{L}^3\text{-}O,O')(NO_3)_{0.5}]\cdot 2.25H_2O$, the independent unit is formed by one ligand molecule, two half-occupied copper(II) ions, half-occupied nitrate anion and some solvate water molecules. Ligand oxygen atoms are deprotonated and coordinated to Cu^{2+} ions, and ligand hydroxy group was clearly found as protonated. Therefore, the ligand molecule must be partially protonated by 0.5H on the side amino group to ensure electroneutrality of the overall formula. It is probably a reason for an observed disorder of the aliphatic part of the molecule – therefore, this disorder was modelled by splitting of the side chain in two positions with half occupancy. However, although some maxima in electron difference map could be attributed to hydrogen atoms, not all hydrogen atoms could be located (as the disorder is probably more complicated) and, therefore, hydrogen atoms were placed in theoretical or original positions using the riding model. The amino group in one of two positions was tentatively declared as protonated and AFIX 137 instruction was used, and protons of the second half of amino group placed in other position were located in the electronic map. In the cavities of polymeric complex framework, some maxima of electron density were found in the free space between the polymeric chains, and were attributed to solvate water molecules. However, their mutual geometry and low intensities point to a complicated disorder, which was modelled by their attributing to water molecules with 0.25–0.5 occupancy. It resulted in finding of more than 2 H_2O per formula unit, but a number of small maxima still remained close to these partially occupied water molecules, pointing to a very complicated disorder. Therefore, all solvent-related maxima were squeezed off using PLATON.[47] The squeezed electronic intensity ($2.25H_2O$) well corresponds to previous finding. Table 5 contains selected crystallographic parameters for the reported structures. The structural data were deposited the Cambridge Crystallographic Data Centre as CCDC 983603 ($[Ca(H_2\mathbf{L}^2\text{-}O,O')(H\mathbf{L}^2\text{-}O,O')]Cl$), 983601 ($[Cu(H\mathbf{L}^3\text{-}O,O')_2(H_2O)]\cdot 5H_2O$) and 983602 ($[Cu(H_{0.5}\mathbf{L}^3\text{-}O,O')(NO_3)_{0.5}]\cdot 2.25H_2O$).

Table 5. Experimental data of reported crystal structures.

Compound	$[Ca(H_2\mathbf{L}^2\text{-}O,O')(H\mathbf{L}^2\text{-}O,O')]Cl$	$[Cu(H\mathbf{L}^3\text{-}O,O')_2(H_2O)]\cdot 5H_2O$	$[Cu(H_{0.5}\mathbf{L}^3\text{-}O,O')(NO_3)_{0.5}]\cdot 2.25H_2O$
Formula	$C_8H_{25}CaClN_2O_{10}P_4$	$C_{12}H_{44}CuN_2O_{16}P_4$	$C_6H_{20}CuN_{1.5}O_{8.75}P_2$
M_w	508.71	659.91	378.71
Colour	colourless	light blue	light blue-green
Shape	prism	prism	prism
Dimensions (mm)	0.105×0.203×0.261	0.287×0.405×0.421	0.265×0.276×0.379
Crystal system	monoclinic	monoclinic	monoclinic
Space group	*C*2/*c*	$P2_1/c$	*C*2/*c*
a (Å)	23.6965(11)	15.5110(2)	14.8708(3)
b (Å)	5.2028(2)	16.1990(2)	17.7541(4)
c (Å)	18.4274(8)	11.2788(2)	12.8882(4)
β (°)	119.639(2)	103.428(1)	124.8959(8)
V (Å^3)	1974.62(15)	2756.47(7)	2790.87(12)
Z	4	4	8
D_c (g cm^{-3})	1.711	1.590	1.803
μ (mm^{-1})	0.826	1.093	1.833
$F(000)$	1056	1388	1564
Diffractions; observed ($I_0 > 2\sigma(I_0)$)	2266; 2017	6338; 5660	3202; 2841
Parameters	130	328	190
G-o-f on F^2	1.078	1.053	1.110
R; R' (all data)	0.0297; 0.0346	0.0266; 0.0306	0.0342; 0.0379
wR; wR' (all data)	0.0790; 0.0823	0.0763; 0.0792	0.0968; 0.0995
Difference max; min (e Å^{-3})	0.534; –0.385	0.963; –0.493	0.854; –0.594

Supporting Information (see footnote on the first page of this article): Coordination polymer motive found in the crystal structure of $[Ca(H_2\mathbf{L}^2\text{-}O,O')(H\mathbf{L}^2\text{-}O,O')]Cl$; geometric parameters of phosphinate functions in the crystal structure of $[Ca(H_2\mathbf{L}^2\text{-}O,O')(H\mathbf{L}^2\text{-}O,O')]Cl$; Time course of decomposition of compounds $H_2\mathbf{L}^1$ (A) and $H_2\mathbf{L}^2$ (B) in acidic solution (1 M HCl, 80 °C); ^{31}P and ^1H NMR titration of compound $H_2\mathbf{L}^1$and $H_2\mathbf{L}^2$; Determined equilibrium constants ($\log\beta_{hlm}$); Distribution diagrams of the studied metal-ligand systems. Geometry of the Ca^{2+}-coordination sphere of the $[Ca(H_2\mathbf{L}^2\text{-}O,O')(H\mathbf{L}^2\text{-}O,O')]Cl$ complex. Structure of the hydrazide isolated as a side-product of the synthesis of compound $H_4\mathbf{L}^4$. Colored representation of Figures representing the solid-state structures of the complexes.

Acknowledgments

Support from the Grant Agency of the Czech Republic (No. P207/10/P153), from the Grant Agency of the Charles University (No. 310011) and from Long-Term Research Plan of the Ministry of Education of the Czech Republic (No. MSM0021620857) is acknowledged. This work was carried out in the framework of TD1004, TD1007 and CM1006 (MSMT no: LD 13012) COST Actions. We thank Dr. Jakub Hraníček for AAS measurements.

[1] E. Matczak-Jon, V. Videnova-Adrabinska, *Coord. Chem. Rev.* **2005**, *249*, 2458–2488.

[2] C. Queffélec, M. Petit, P. Janvier, D. A. Knight, B. Bujoli, *Chem. Rev.*, 2012, **112**, 3777–3807.

[3] G. Guerrero, J. G. Alauzun, M. Granier, D. Laurencin and P. H. Mutin, *Dalton Trans.*, 2013, **42**, 12569–12585.

[4] A. Mucha, P. Kafarski and L. Berlicki, *J. Med. Chem.*, 2011, **54**, 5955–5980.

[5] A. Vioux, J. Le Bideau, P. H. Mutin, D. Leclerq, *Top. Curr. Chem.* **2004**, *232*, 145–174.

[6] I. Řehoř, V. Kubíček, J. Kotek, P. Hermann, J. Száková, I. Lukes, *Eur. J. Inorg. Chem.* **2011**, 1981–1989.

[7] M. de los Reyes, P. J. Majewski, N. Scales, V. Luca, *ACS Appl. Mater. Interfaces*, **2013**, *5*, 4120–4128.

[8] D. Portet, B. Denizot, E. Rump, J.-J. Lejeune, P. Jallet, *J. Colloid Interf. Sci.* **2001**, *238*, 37–42.

[9] A. Panahifar, M. Mahmoudi, and M. R. Doschak, *ACS Appl. Mater. Interfaces* **2013**, *5*, 5219−5226.

[10] L. Sandiford, A. Phinikaridou, A. Protti, L. K. Meszaros, X. Cui, Y. Yan, G. Frodsham, P. A. Williamson, N. Gaddum, R. M. Botnar, P. J. Blower, M. A. Green, R. T. M. de Rosales, *ACS Nano*, **2013**, *7*, 500–512.

[11] Y. Lalatonne, C. Paris, J.-M. Serfaty, P. Weinmann, M. Lecouvey, L. Motte, *Chem. Commun.*, **2008**, 2553–2555.

[12] V. Kubíček, I. Lukeš, *Future Med. Chem.* **2010**, *2*, 521–531.

[13] E. Palma, J. D. G. Correia, M. P. C. Campello, I. Santos, *Mol. BioSyst.* **2011**, *7*, 2950.

[14] J. Galezowskaa, E. Gumienna-Konteckab, *Coord. Chem. Rev.*, **2012**, *256*, 105–124.

[15] E. V. Giger, B. Castagner, J.-C. Leroux, *J. Controlled Release*, **2013**, *167*, 175–188.

[16] (a) G. A. Rodan, H. A. Fleisch, *J. Clin. Invest.* **1996**, *97*, 2692–2696; (b) H. Fleisch, *Endocrine Rev.* **1998**, *19*, 80–100.

[17] S. P. Luckman, F. P. Coxon, F. H. Ebetino, R. G. G. Russell and M. J. Rogers, *J. Bone Miner. Res.*, 1998, **13**, 1668–1678.

[18] T. David, P. Křečková, J. Kotek, V. Kubíček and I. Lukeš, *Heteroatom Chem.*, 2012, **23**, 195–201.

[19] (a) S. Gouault-Bironneau, S. Deprele, A. Sutor and, J.-L. Montchamp, *Org. Lett.*, **2005**, *7*, 5909–5912; (b) M. I. Antczak and J.-L. Montchamp, *Tetrahedron Lett.*, **2008**, *49*, 5909–5913.

[20] B. Kaboudin, F. Saadati and T. Yokomatsu, *Synlett*, **2010**, 1837–1840.

[21] M. Bochno, Ł. Berlicki, *Tetrahedron Lett.*, **2014**, *55*, 219–22.

[22] (a) F. Gaizer, G. Haegele, S. Goudetsidis and H. Papadopoulos, *Z. Naturforsch., B: Chem. Sci.*, **1990**, *45*, 323–328; (b) L. P. Loginova, I. V. Levin, A. G. Matveeva, S. A. Pisareva, and E. E. Nifant'ev, *Russ. Chem. Bull.*, **2004**, *53*, 2000–2007.

[23] T. David, S. Procházková, J. Havlíčková, J. Kotek, V. Kubíček, P. Hermann, I. Lukeš, *Dalton Trans.* **2013**, *42*, 2414–2422.

[24] Prishchenko, A. A.; Livantsov, M. V.; Novikova, O. P.; Livantsova, L. I. Russ, *J. Gen. Chem.* **2010**, *80*, 1889–1890.

[25] K. Issleib, W. Moegelin and A. Balszuweit, *Z. Chem.*, 1985, **25**, 370–371.

[26] (a) E. K. Baylis, C. D. Campbell, J. G. Dingwall, *J. Chem. Soc., Perkin Trans. 1*, **1984**, 2845–2853; (b) J. Rohovec, I. Lukeš, P. Vojtíšek, I. Císařová, P. Hermann, *J. Chem. Soc., Dalton Trans.*, **1996**, 2685–2691.

[27] J. Kehler, B. Ebert, O. Dahl, P. Krogsgaard-Larsen, *Tetrahedron*, **1999**, *55*, 771–780.

[28] V. Kubíček, J. Kotek, P. Hermann, I. Lukeš, *Eur. J. Inorg. Chem.* **2007**, 333–344.

[29] I. Lukeš, J. Kotek, P. Vojtíšek, P. Hermann, *Coord. Chem. Rev.* **2001**, *216–217,* 287–312.

[30] S. Ciattini, F. Costantino, P. Lorenzo-Luis, S. Midollini, A. Orlandini and A. Vacca, *Inorg. Chem.*, 2005, **44**, 4008–4016.

[31] J. Šimeček, P. Hermann, J. Havlíčková, E. Herdtweck, T. G. Kapp, N. Engelbogen, H. Kessler, H.-J. Wester, J. Notni, *Chem. Eur. J.* **2013**, *19*, 7748 – 7757.

[32] J. Šimeček, O. Zemek, P. Hermann, J. Notni, H.-J. Wester, *Mol. Pharmaceutics*, DOI:10.1021/mp400642s

[33] J. Šimeček, M. Schulz, J. Notni, J. Plutnar, V. Kubíček, J. Havlíčková, P. Hermann, *Inorg. Chem.* **2012**, *51*, 577–590.

[34] (a) J. Beckmann, F. Costantino, D. Dakternieks, A. Duthie, A. Ienco, S. Midollini, C. Mitchell, A. Orlandini and L. Sorace, *Inorg. Chem.*, 2005, **44**, 9416–9423; (b) S. Midollini and A. Orlandini, *J. Coord. Chem.*, 2006, **59**, 1433–1442; (c) T. Bataille, F. Constantino, P. Lorenzo-Luis, S. Midollini, A. Orlandini *Inorg. Chim. Acta* **2008**, *361*, 9–15; (d) F. Constantino, A. Ienco, S. Midollini, A. Orlandini, L. Sorace, A. Vacca *Eur. J. Inorg. Chem.* **2008**, 3046–3055.

[35] (a) T. Glowiak and W. Sawka-Dobrowolska, *Acta Crystallogr., Sect. B*, 1977, **33**, 2648; (b) T. Glowiak and W. Sawka-Dobrowolska, *Acta Crystallogr., Sect. B*,1977, **33**, 2763–2766; (c) Z. Žák, J. Kožíšek and T. Glowiak, *Z. Anorg. Allg. Chem.*, 1981, **477**, 221–224; (d) W. Sawka-Dobrowolska and T. Glowiak, *Acta Crystallogr., Sect. C*, 1983, **39**, 345–347; (e) T. Glowiak, *Acta Crystallogr., Sect. C*, 1986, **42**, 62–64.

[36] D. Fernández, D. Vega, A. Goeta, *Acta Crystallogr.* **2002**, *C58*, m494–m497; D. Fernández, D. Vega, A. Goeta, *Acta Crystallogr.* **2003**, *C59*, m543–m545.

[37] E. Alvarez, A. G. Marquez, T.Devic, N.Steunou, Ch. Serre, Ch. Bonhomme, Ch. Gervais, I. Izquierdo-Barba, M. Vallet-Regi, D. Laurencin, F. Maurif, P. Horcajada, *CrystEngComm* **2013**, *15*, 9899–9905.

[38] τ is a coefficient reflecting shape of the coordination polyhedron – τ = 0 for tetragonal pyramid, τ = 1 for trigonal bipyramid. Based on: A. W. Addison, T. N. Rao, J. Reedijk, J. van Rijn, G. C. Verschoor *J. Chem. Soc. Dalton Trans.* **1984**, 1349–1356.

[39] J. Notni, P. Hermann, J. Havlíčková, J. Kotek, V. Kubíček, J. Plutnar, N. Loktionova, P. J. Riss, F. Rösch, I. Lukeš, *Chem. Eur. J.* **2010**, *16*, 7174–7185.

[40] V. Kubíček, P. Vojtíšek, J. Rudovský, P. Hermann and I. Lukeš, *Dalton Trans.*, **2003**, 3927–3938.

[41] C. F. Jr. Baes and R. E. Mesmer, *The Hydrolysis of Cations*, Wiley, New York, 1976.

[42] M. Kývala and I. Lukeš, *International Conference, Chemomotrics '95*, p. 63. Pardubice, Czech Republic, 1995; full version of *"OPIUM"* is available (free of charge) on http://www.natur.cuni.cz/~kyvala/opium.html.

[43] SAINT V8.32B (Bruker AXS Inc., 2013).

[44] SADABS V2012/1 (Bruker AXS Inc., 2012).

[45] G. M. Sheldrick. SHELXS97 – A Computer Program for Solution of Crystal Structures. University of Göttingen, 1997.

[46] G. M. Sheldrick. SHELXL97. Program for Crystal Structure Refinement from Diffraction Data: University of Göttingen, 1997.

[47] A. L. Spek. PLATON – A Multipurpose Crystallographic Tool. Utrecht University, Utrecht, The Netherlands, 2011. A. L. Spek, *Acta Crystallogr. D*, **2009**, *65*, 148–155.

Received: ((will be filled in by the editorial staff))
Published online: ((will be filled in by the editorial staff))

Cyclam derivatives with bis(phosphinate) and phosphinato-phosphonate pendant arms: fast and efficient Cu(II) complexation for radiomedical applications

Tomáš David,[a] Vojtěch Kubíček,[a*] Jan Kotek,[a] Petr Hermann,[a] Přemysl Lubal,[b] Ivan Lukeš[a]

[a] Department of Inorganic Chemistry, Faculty of Science, Charles University in Prague, Hlavova 2030, 128 40 Prague 2, Czech Republic
E-mail: kubicek@natur.cuni.cz; Tel.: +420 221921264; Fax: +420 221921253
[b] Department of Chemistry, Masaryk University, Kotlářská 2, 611 37, Brno, Czech Republic

Abstract

Cyclam derivatives bearing one geminal bis(phosphinate) or one geminal phosphino-phosphonate pendant arm were synthesized and studied as potential copper(II) chelators in radiomedical applications. The compounds were synthesized in excellent yields by highly efficient procedure. Acid-base and coordination properties were studied by potentiometric titrations. Copper(II) complexes of title ligands are formed at pH < 1 and they show high thermodynamic stability. Detailed study of kinetics revealed three-step mechanism of complex formation. Quantitative formation of "in-cage" complex is completed in milliseconds at pH ≈ 7. Four isomers differing in spectral properties and kinetic inertness (studied by acid-assisted assisted dissociation kinetics) of each complex were detected. Two of them were isolated and their interconversion in alkaline region was studied. Unlike structurally related geminal bis(phosphonates), studied compounds showed negligible adsorption onto hydroxyapatite, a commonly used model of bone tissue. Rare combination of simple ligand synthesis, very fast copper(II) complex formation, high thermodynamic stability, extraordinary kinetic inertness and low bone tissue affinity predestinates the use of such species in radiomedicine as chelators of ^{64}Cu and other copper isotopes.

Keywords: cyclam derivatives, bis(phosphinates), fast formation, kinetics, macrocyclic ligands, copper(II).

Introduction

Positron emission tomography (PET) is a powerful diagnostic tool of modern medicine. The method relies in the application of proton-rich isotopes that undergo β^+ decay. Collision of the emitted positron with an electron in the surrounding tissue results in a pair of collinear γ-photons. Position-sensitive detectors allow localization of the annihilation and, consequently, they show distribution of the radioisotope in tissues. PET requires isotopes with suitable half-life, low energy of emitted positrons and good availability. The requirements result in application of various non-metallic (^{18}F, ^{11}C) and metallic (^{68}Ga, ^{44}Sc, ^{110}In) isotopes.[1] Very promising metallic isotope is ^{64}Cu due to half-life of 12.8 hours and low positron energy that results in high image resolution. Besides that, other copper isotope ^{67}Cu can be used for radiotherapy.[2]

Copper cannot be applied in the form of free ion due to non-specific deposition in tissues. To reach desired biodistribution, metal ion must be bound in a thermodynamically stable and kinetically inert complex. The ligands that are perspective for copper(II) binding in medicine are mostly various macrocycle derivatives of cyclam (1,4,8,11-tetraazacyclotetradecane, Figure 1) family.[3]

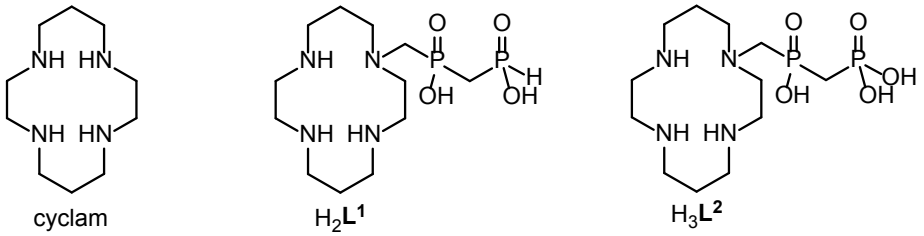

Figure 1. Structure of cyclam and of the title compounds H_2**L**^{1} and H_3**L**^{2}.

Due to the short half-life of PET isotopes, the major limitation of macrocycle derivatives is the low complex-formation rate. The rate can be improved by introducing various pedant arms – most typically carboxylates – leading to ligands like H_4**teta** (Figure 2). Recently, we have shown that cyclam derivatives with phosphonate pendants H_4**te2P**^{1,8} or H_2**teP** (Figure 2) show the highest reported complexation rates.[4,5,6] This could be explained by strong interaction between the metal ion and the phosphonate groups in the initial stage of complexation. Based on these findings we have suggested new type of pendant arms containing two phosphorus atoms – methylene-bis(phosphinate) and methylene-phosphinato-phosphonate – to further increase stability of the reaction intermediate and,

consequently, improve the Cu(II) complex formation rate. Here we present two cyclam derivatives bearing the above-mentioned bisphosphorus pendant arms – $H_2\mathbf{L}^1$ and $H_3\mathbf{L}^2$ (Figure 1), which are first reported examples of geminal bis(phosphinate) and geminal phosphinato-phosphonate fragment present on any macrocyclic ligand. Both compounds were prepared by elegant synthetic approaches, consisting of only one and two reaction steps, respectively. Detailed thermodynamic and kinetic coordination studies have shown high selectivity for Cu(II) ions and extremely high complex formation rate.

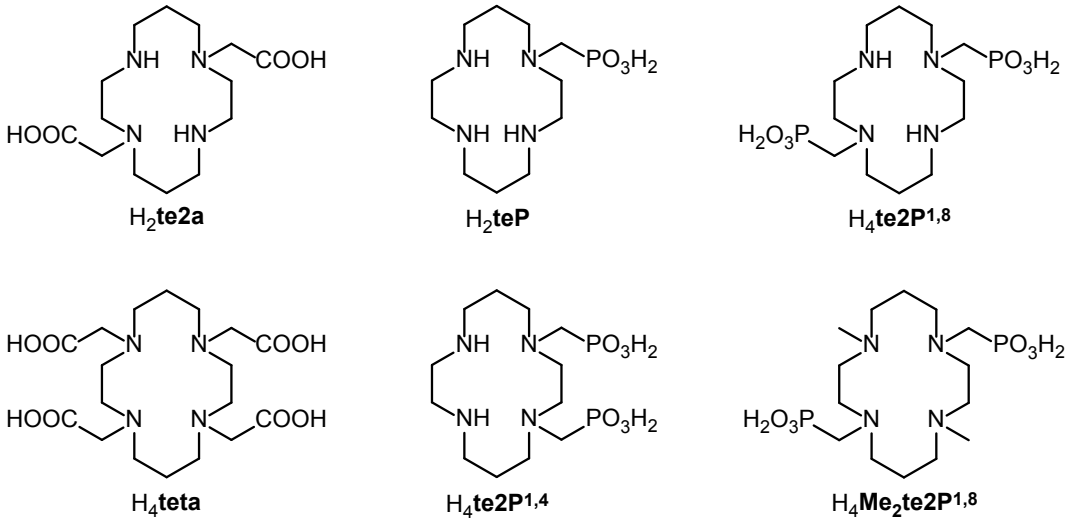

Figure 2. Structure of various cyclam derivatives discussed in the text.

Results and Discussion

Ligand synthesis

The title cyclam derivatives bearing one bis(phosphinate) ($H_2\mathbf{L}^1$) or one phosphinato-phosphonate ($H_3\mathbf{L}^2$) pendant arm were synthesized by highly efficient procedures in one and two reaction steps, respectively. The overall reaction scheme is described in Figure 3.

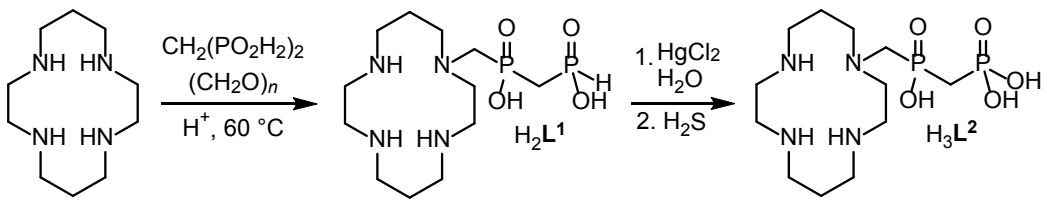

Figure 3. Overall synthetic scheme for preparation of ligands $H_2\mathbf{L}^1$ and $H_3\mathbf{L}^2$.

Direct Mannich-type reaction (no protection of cyclam was used) of methylene-bis(phosphinic) acids, paraformaldehyde and cyclam in acidic media (i.e. conc. HCl as a solvent) at 80 °C affords ligand $H_2\mathbf{L}^1$ in 70–75 % conversion (monitored by ^{31}P NMR). To avoid formation of di-substituted derivatives, excess of cyclam and methylene-bis(phosphinate) was used (no such species were observed under conditions described in Experimental section). Excess of both compounds, cyclam and methylene-bis(phosphinate), can be easily recovered during workup. The compound $H_2\mathbf{L}^1$ was isolated in the zwitterionic form as well as unstoichiometric hydrochloride. Oxidation of $H_2\mathbf{L}^1$ to $H_3\mathbf{L}^2$ was performed smoothly with $HgCl_2$ with subsequent removal of mercury ions using H_2S. No cleavage of N—C—P bond was observed by this treatment (as opposed to examined oxidation using H_2O_2). The reaction was performed under acidic conditions. The ligand $H_3\mathbf{L}^2$ was also isolated in the zwitterionic form as well as unstoichiometric hydrochloride.

Complexation of Cu(II) ions

Cyclam Cu(II) complexes adopt various geometries that are mainly given by configuration of the ring nitrogen atoms. Among them, *cis*-**I** isomer having all nitrogen substituents pointing to the same direction (Figure 4) and *trans*-**III** isomer having two pairs of nitrogen substituents pointing to opposite directions (Figure 4) are the most common.[7] For cyclam derivatives with phosphonate and phosphinate pendant arms the blue *cis*-**I** isomer represents the kinetic product of Cu(II) complexation that is formed at room temperature. At high temperature violet *trans*-**III** isomer is slowly formed as the thermodynamically most stable complex.[4,5,6]

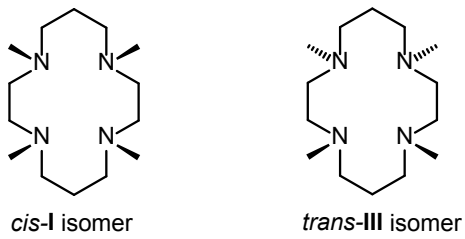

cis-**I** isomer *trans*-**III** isomer

Figure 4. Geometry of two notable isomers of the cyclam derivatives found in the Cu(II) complexes of such ligands.

Both title ligands $H_2\mathbf{L}^1$ and $H_3\mathbf{L}^2$ show similar coordination behavior. The suggested complexation mechanism is shown in Figure 5. Upon mixing with Cu(II) ions they form deep blue complexes. The complexes possess expected sharp charge-transfer (CT) adsorptions and broad d–d (an overlap of d_{xy}, d_{xz} and d_{x2-y2} transitions). Detailed spectral properties of the isomers can be found below (Table 1). However, the detailed kinetic study (see lower) has

shown that the complexation is not a simple process. The time dependence of the absorbance shows bi-exponential profile pointing to two consequent steps. However, there is just small difference in the shape of UV-Vis spectra indicating similar geometry of both species. Thus, we conclude that both of them are similar complexes differing just in the geometry on ring nitrogen atoms. The dependence of the pseudo-first order formation kinetic constant of the first step on concentration of copper(II) ions follows saturation growth (see lower). Similar behavior was previously reported for complexation of lanthanide (III) ions with DOTA-like ligands[8] and it indicates formation of an "out-of-cage" intermediate. In the intermediate the metal ion is coordinated only through pendant arms, whereas the ring nitrogen atoms are protonated. The "out-of-cage" complex is formed swiftly and it is slowly converted to the "in-cage" complex with metal ion coordinated by all ring nitrogen atoms. The conversion to the "in-cage" complex is usually the rate-determination step. In the case of title ligands, formation of the "out-of-cage" intermediate is expectable as geminal bis(phosphonates) and bis(phosphinates) are known to be efficient chelating agents for wide range of metal ions.[9] This is different from the results reported for structurally similar ligand H_4**te2P**[1,8] (Figure 2), where only one product was observed during formation (identified as isomer *cis*-**I**) and the "out-of-cage" reaction intermediate was not identified. This indicates that arrangement of phosphonate/phosphinate groups on cyclam backbone has significant influence on formation behavior of copper(II) complexes.

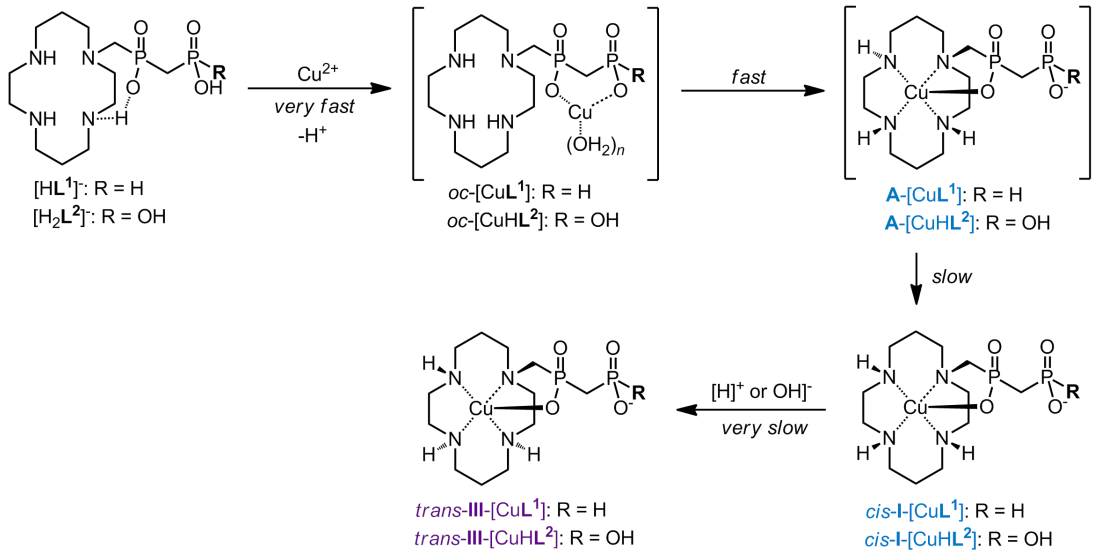

Figure 5. The suggested overall mechanism of complexation.

As mentioned above, the second step is probably isomerisation of the "in-cage" complex. Whereas, the first isomer (further denoted as **A**-isomer) cannot be identified, quantum mechanics shows (see lower) that the second isomer is more-like *cis*-**I** isomer. The isomerisation is slower than formation of **A**-isomer and characterizes change of chirality of one or more amine donor groups. The dependence of isomerisation rate on concentration of copper(II) ions is linear. This finding indicates that one of the isomerisation mechanisms might be an exchange of the metal ion between macrocycle cavity and surrounding solution.

Treatment of *cis*-**I** complexes at high temperature or in strongly alkaline solutions (pH > 12) at room temperature led to next isomerisation – the blue *cis*-**I** isomers are converted to violet *trans*-**III** isomers. However, the conversion is never quantitative. The resulting mixture of *cis*-**I** and *trans*-**III** complexes was efficiently separated by column chromatography. The *trans*-**III** complexes possess similar charge-transfer (CT) adsorption as isomer *cis*-**I**. The blue shift of the d–d transitions of the *trans*-**III** isomer corresponds to the increasing ligand field resulting from a change in the geometry of the coordination sphere (see Table 1). The isomerisation occurs also in strongly acidic solution but it is difficult to study in detail due to simultaneous dissociation of the complexes.

Table 1. Spectral properties of studied isomers.

Isomer	Adsorption	λ_{max} [nm]	ε [$mol^{-1}\,dm^3\,cm^{-1}$]	Color
cis-**I**-[Cu**L**^{1}]	CT	270	$5.6\cdot10^3$	deep blue
	d–d	590	$1.5\cdot10^2$	
cis-**I**-[Cu**L**^{2}]	CT	270	$5.6\cdot10^3$	deep blue
	d–d	590	$1.4\cdot10^2$	
trans-**III**-[Cu**L**^{1}]	CT	265	$6.3\cdot10^3$	violet
	d–d	535	$1.2\cdot10^2$	
trans-**III**-[Cu**L**^{2}]	CT	265	$6.1\cdot10^3$	violet
	d–d	535	$1.2\cdot10^2$	

Formation of cis-I complexes

As mentioned above, formation of cis-**I** complexes is a stepwise process including extremely fast formation of the “out-of-cage” complex, fast formation of the “in-cage” intermediate (**A**-isomer) and slow isomerisation resulting in the cis-**I** isomer. The complexation was studied in detail under pseudofirst order conditions (c_L = 0.1 mM, c_M = 1.0 – 5.0 mM) at the pH range 2 – 7.

Due to the formation of an "out-of-cage" intermediate the dependence of the pseudo-first order formation kinetic constant of the **A**-isomer ${}^{fCu}k_{obs,1}$ on concentration of copper(II) ions follows saturation growth (Figure 6). The overall reaction rate is given by contributions of "out-of-cage" species in differently protonated states (Equation 1):

$$v = {}^{f}k_{obs} * [ML_{tot}]^{oc} = {}^{f}k_0 * [ML]^{oc} + {}^{f}k_1 * [M(HL)]^{oc} + {}^{f}k_2 * [M(H_2L)]^{oc} + {}^{f}k_3 * [M(H_3L)]^{oc}, \quad (1)$$

upon including the mass balance and ligand protonation constants, ${}^{f}k_{obs}$ can be expressed as in Equation 2:

$${}^{f}k_{obs} = \frac{K_{ML} * [M] * ({}^{f}k_0 + {}^{f}k_1 * [H] / K_{a1} + {}^{f}k_2 * [H]^2 / (K_{a1} * K_{a2}) + {}^{f}k_3 * [H]^3)}{(1 + K_{ML} * [M]) * (1 + [H] / K_{a1} + [H]^2 / (K_{a1} * K_{a2}) + [H]^3 / (K_{a1} * K_{a2} * K_{a3}))}, \quad (2)$$

where ${}^{f}k_x$ are the rate constants describing isomerisation of the $[M(H_xL)]$ complexes, K_{ax} are corresponding stepwise protonation constants and K_{ML} is conditional stability constant of the "out-of-cage" complex. In the studied pH range, the equation could be further simplified. As ligand **L¹** does not change protonation state along the studied pH range, the resulting rate constant is given by Equation 3.

$${}^{f}k_{obs} = \frac{K_{ML} * [M] * ({}^{f}k_1 * K_{a2} + {}^{f}k_2 * [H])}{(1 + K_{ML} * [M]) * [H]}, \quad (3)$$

Dissociation of the second proton of the macrocycle (described by dissociation constant K_{a2}) proceeds at high pH and, so, it is not accessible from the kinetic measurements. However, in the "out-of-cage" complex metal ion is not coordinated to ring nitrogen atoms. So, one could expect that the dissociation constant is close to that of free ligand and, thus, these were used in the fitting of the data.

In the case of ligand **L²**, phosphonate group undergoes protonation in the studied pH range. It changes the mass balance and, thus, the conditional stability of the "out-of-cage" complex is not constant as is documented by different slopes of the curves obtained at different pH values (Figure 6B). Including the dissociation constant of free phosphonate group K_P, the rate constant could be expressed as in Equation 4.

$$ {}^{f}k_{obs} = \frac{K_{ML} * [M] * ({}^{f}k_1 * K_{a2} + {}^{f}k_2 * [H] + {}^{f}k_3 * [H]^2 / K_{a3}) / (1 + [H] / K_P)}{(1 + K_{ML} * [M] / (1 + [H] / K_P)) * ([H] + [H]^2 / K_{a3})}, \quad (4) $$

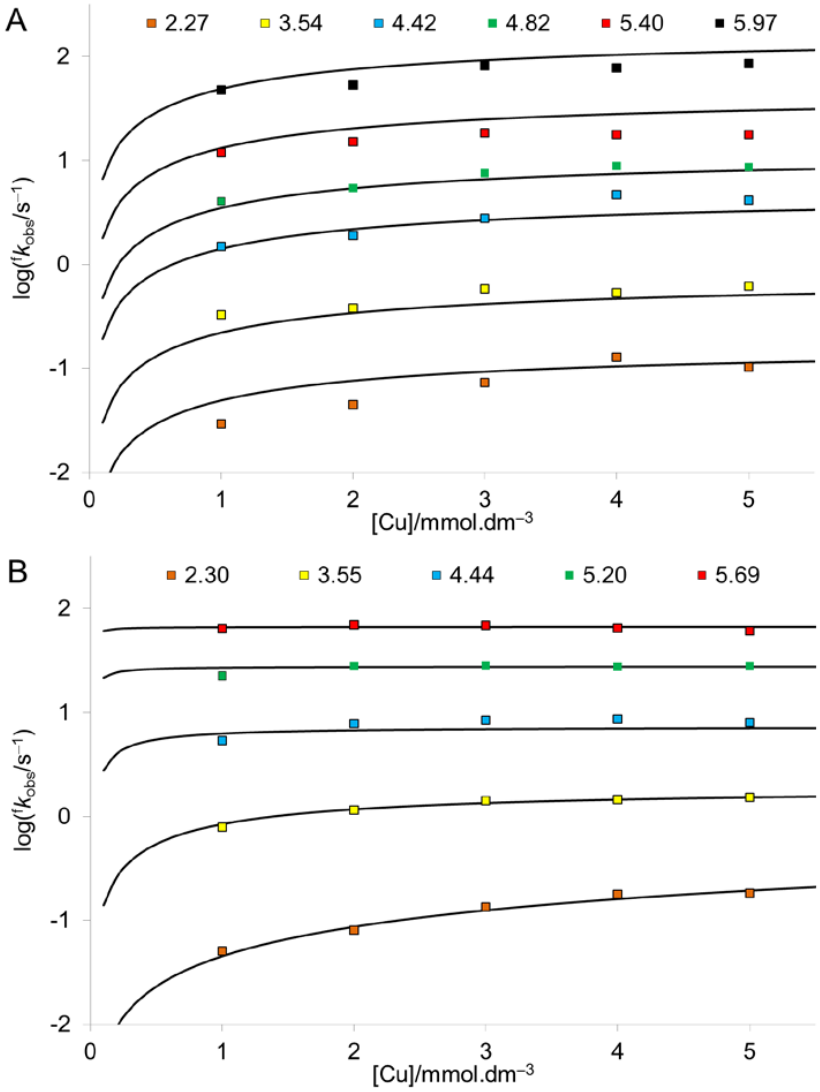

Figure 6. Formation of **A**-isomer. Dependence of the pseudo-first order formation kinetic constant ${}^{f}k_{obs}$ of ligand $H_2\mathbf{L}^1$ (A) and $H_3\mathbf{L}^2$ (B) on concentration of copper(II) ions measured at various pH.

Table 2. Kinetic parameters describing formation of **A**-isomers and *cis*-**I** isomer.

	Formation of **A**-isomer	
	L¹	**L²**
$^{f}k_1$	$(10 \pm 1)\cdot 10^{6}$	$(51 \pm 5)\cdot 10^{6}$
$^{f}k_2$	$(13 \pm 2)\cdot 10^{-2}$	29 ± 10
$^{f}k_3$	-	1.0 ± 0.2
K_{ML}	$(4 \pm 1)\cdot 10^{2}$	$(29 \pm 6)\cdot 10^{5}$
K_{a3}	-	$(9 \pm 3)\cdot 10^{-6}$

	Formation of *cis*-**I** isomer	
	L¹	**L²**
$^{is1}k_1$	$(15 \pm 1)\cdot 10^{8}$	$(17 \pm 1)\cdot 10^{8}$
$^{is1}k_{0Cu}$	38 ± 7	12 ± 5
$^{is1}k_{1Cu}$	$(83 \pm 9)\cdot 10^{10}$	$(4.9 \pm 1)\cdot 10^{10}$

The results are compiled in Table 2. Complexation of cooper(II) ions with **L¹** proceeds through monoprotonated and diprotonated species. Complexation with **L²** involves also the triprotonated specie due to presence of phosphonates group. The phosphonate group is protonated also upon coordination. The protonation constant of the phosphonate group in the "out-of-cage" complex was obtained from the kinetic data and it is in the expected range. However, for both ligands k_{obs} increases linearly with pH (Figure S1). It indicates major role of the monoprotonated species in the complexation mechanism. It is in accordance with the commonly accepted complexation mechanism in which transfer of the metal ion into the macrocyclic cavity is preceded by cleavage of one proton from macrocycle nitrogen atoms.

The two ligands significantly differ in stability of "out-of-cage" complex. **L²** shows significantly higher stability due to presence of phosphonate group showing significantly better coordination properties. The higher "out-of-cage" complex stability and higher values of rate constants result for **L²** in faster complex formation in comparison with **L¹**.

Despite the second step of complexation is isomerisation of **A**-isomer to *cis*-**I** isomer without change of the complex protonation state, it also shows faster rate with increasing pH (Figures 7 and S2). This is explained by catalytic effect of hydroxide ions forming hydroxide complexes. In the complex the coordinated hydroxide ions forms hydrogen bond to the amine group of the macrocycle and, consequently, enhances inversion of the nitrogen atom geometry. Further, the rate of the second step increases with increasing Cu^{2+} concentration. This might be rationalized by formation of dinuclear species. One metal ion is coordinated in the macrocyclic cavity, whereas the other is coordinated by the pendant phosphonate/phosphinate groups. Temporary interaction of the weakly coordinated Cu^{2+} ion accelerates the nitrogen geometry inversion. So, the behavior could be described by Equation 5:

$$^{is1}k_{obs} = {}^{is1}k_0 + {}^{is1}k_1 \cdot [OH^-] + {}^{is1}k_{0Cu} \cdot [OH^-] \cdot [Cu^{2+}] + {}^{is1}k_{1Cu} \cdot [Cu^{2+}], \quad (5)$$

where $^{is1}k_0$ is the rate constant describing the unassisted isomerisation, $^{is1}k_1$ is the rate constant describing the hydroxide assisted isomerisation, $^{is}k_{0Cu}$ is the rate constant describing the metal assisted isomerisation and $^{is}k_{1Cu}$ is the rate constant describing the pathway including both, metal and hydroxide assistance. However, spontaneous isomerisation plays negligible role. The results (Table 2) show that the major contribution to the overall reaction rate is given from both hydroxide assisted pathways.

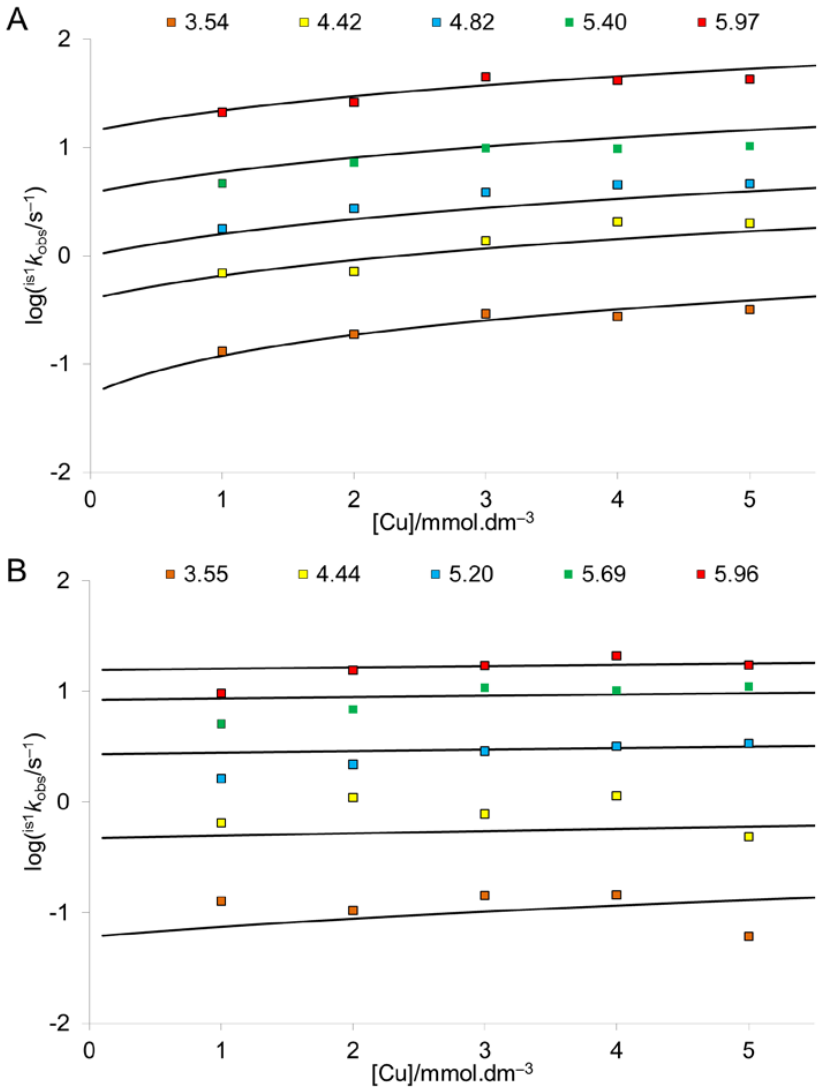

Figure 7. Formation of *cis*-**I** isomer. Dependence of the pseudo-first order formation kinetic constant $^{is1}k_{obs}$ of ligand $H_2\mathbf{L}^1$ (A) and $H_3\mathbf{L}^2$ (B) on concentration of copper(II) ions measured at various pH.

Direct comparison of the studied ligands with previously reported carboxylate and phosphonate cyclam derivatives is difficult due to different mechanisms of complexation. Direct comparison of reaction rates indicates that title ligands form "in-cage" complex (**A**-isomer) much faster than other cyclam derivatives. This is experimental prove of accelerated copper(II) complexation in the presence of bis(phosphinate) or phosphinato-phosphonate pendant arm.

Isomerisation *cis*-**I** – *trans*-**III** complexes

As mentioned above, *cis*-**I** complexes and *trans*-**III** isomers are in an equilibrium. Their interconversion is rather slow and, so, the two isomers were isolated in pure form. Thus, the isomerisation could be followed starting from both ends. Time-change of the spectra (Figure S3) shows that the same equilibrium mixture is reached in both cases. The ratio of species in equilibrium is approximately [*cis*-**I**]:[*trans*-**III**] = 17:83 and 27:73 for [Cu**L**^{1}] and [Cu**L**^{2}], respectively. The isomerisation was investigated in detail in the [OH^-] range 10 – 100 mM at constant ionic strength (K[OH, Cl]; I = 0.5 mM) and temperature (T = 25 ± 0.1°C). Isomerisation process is characterized by rate constants $^{is2}k_{obs1}$ and $^{is2}k_{obs-1}$ for the *cis*-**I** → *trans*-**III** process and for the reverse process, respectively. Both constants are included in the equations describing the kinetics resulting in an equilibrium mixture (see ESI) and, so, both constants could be determined from a single experiment. The measurements have been performed in both "directions" – starting with pure *cis*-**I** isomer or with pure *trans*-**III** isomer. The two sets of experiments give fully consistent results (Figure 8) that proofs correctness of the chosen model. The $^{is}k_{obs}$ values show nonlinear dependence on concentration of hydroxide ions. In the studied pH range complexes form hydroxide species. Stability constant of the [Cu**L**(OH)] species are known from potentiometry (see lower). However, analysis of the kinetic data has shown that the isomerisation is also assisted with other hydroxide anions. These anions might be coordinated to the metal center or bound to the complex through hydrogen bonds. The proposed isomerisation mechanism is depicted in Scheme 1 and the process is described by Equation 6.

$$^{is2}k_{obs} = {}^{is2}k_1 \cdot [ML(OH)] + {}^{is2}k_2 \cdot [ML(OH)] \cdot [OH^-] + {}^{is2}k_3 \cdot [ML(OH)] \cdot [OH^-]^2, \qquad (6)$$

where $^{is2}k_1 = k_1$, $^{is2}k_2 = k_2 \cdot K_2$ and $^{is2}k_3 = k_3 \cdot K_2 \cdot K_3$. The results are compiled in Table 3. Fitting of the data obtained for [Cu**L**^{2}] gave only constants $^{is2}k_2$ and $^{is2}k_3$. In the case of [Cu**L**^{1}] all three constants were found, however, isomerisation of [Cu**L**(OH)] specie is very slow and its contribution to the overall isomerisation rate is negligible. The isomerisation process is

faster for [Cu**L**[1]] then for [Cu**L**[2]]. This is in good agreement with the proposed mechanism involving catalysis by hydroxide ions as interaction of hydroxide ion with [Cu**L**[2]] is disfavored due to the double negative charge of the phosphonate group.

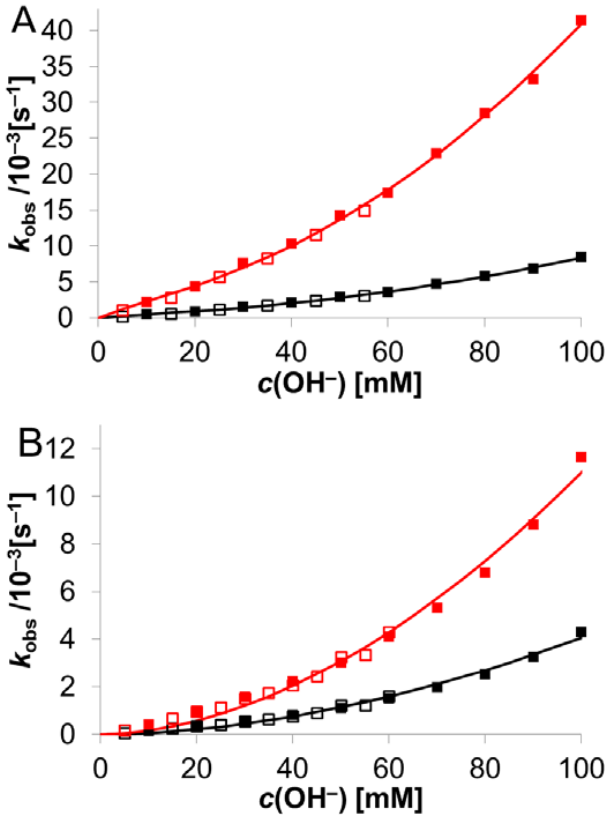

Figure 8. Isomerisation of [Cu**L**[1]] (A) and [Cu**L**[2]] (B) complexes. Isomerisation constants $^{is2}k_{obs1}$ (red) and $^{is2}k_{obs-1}$ (black) obtained for *cis*-**I** → *trans*-**III** process and for reverse process, respectively. The reaction was studied starting with pure *cis*-**I** isomer (full symbols) and *trans*-**III** isomer (empty symbols).

Table 3. Rate constants of the *cis*-**I** - *trans*-**III** isomerisation.

	[Cu**L**[1]]		[Cu**L**[2]]	
	cis-**I** → *trans*-**III**	*trans*-**III** → *cis*-**I**	*cis*-**I** → *trans*-**III**	*trans*-**III** → *cis*-**I**
$^{is2}k_1$	0.98 ± 0.18	0.20 ± 0.04	-	-
$^{is2}k_2$	22 ± 7	4.6 ± 1.3	14 ± 2	5.3 ± 0.6
$^{is2}k_3$	645 ± 56	132 ± 11	172 ± 22	63 ± 8

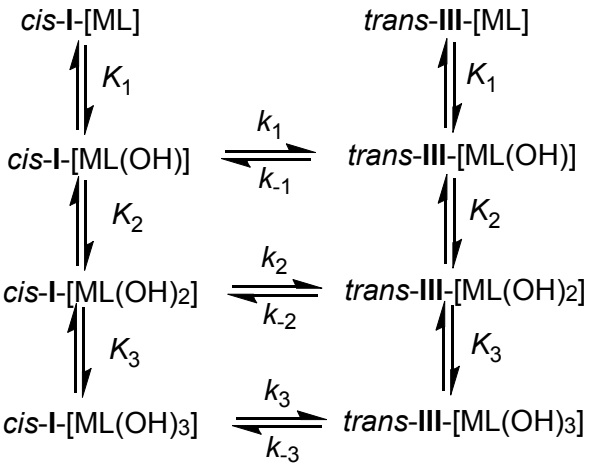

Scheme 1. Mechanism of *cis*-**I** → *trans*-**III** process.

Dissociation Kinetics

The kinetics of acid-assisted dissociation of complexes *cis*-**I**-[Cu**L**^{1}] and *cis*-**I**-[Cu**L**^{2}] were investigated in the 0.1–5.0 M $HClO_4$ at constant ionic strength (5 M (H, Na)ClO_4). According to TLC analysis, in the examined pH range, complex *cis*-**I**-[Cu**L**^{1}] was found to undergo slow oxidation leading to minor abundance of *cis*-**I**-[Cu**L**^{2}] that also undergoes dissociation. The oxidation process could not be easily quantified due to the very similar spectra of both complexes, which also disallowed quantification of dissociation process of *cis*-**I**-[Cu**L**^{1}]. However, overall rate of *cis*-**I**-[Cu**L**^{1}] dissociation (including minor contribution of the oxidation-dissociation pathway) is almost the same as in the case of *cis*-**I**-[Cu**L**^{2}] (Figure S4). This indicates similar dissociation resistant and mechanism for both complexes suggesting no significant contribution of the terminal P—H or P—OH bond to the overall kinetic inertness. Under the experimental conditions used in the dissociation study, traces of *trans*-**III** isomer are formed. However, the amount is negligible and, so it does not disable evaluation of the *cis*-**I**-[Cu**L**^{2}] dissociation kinetics.

Dissociation of *cis*-**I**-[Cu**L**^{2}] complex was studied at the temperature range 60 – 90 °C (Figure 9). The saturation shape of the curves indicates that the complex is present in two forms differing in number of bound protons. However, the number of protons is difficult to determine as the studied pH range is far from the range of titration data (see lower). Thus, the data were treated according to Equation 7,

$$^{d}k_{obs} = (^{d}k_0 + {}^{d}k_1 \cdot K \cdot [H^+]) / (1 + K \cdot [H^+]), \quad (7)$$

where $^{d}k_0$ is constant corresponding to dissociation of the less protonated complex, $^{d}k_1$ is constant corresponding to dissociation of the more protonated complex and K is the protonation constant). The results show negligible value of $^{d}k_0$ indicating that dissociation of the more protonated species is the dominant process. The obtained values of $^{d}k_1$ and K are summarized in. Analysis of the results provided activation thermodynamic parameters of the dissociation process (Table 5). Comparison with cyclam phosphonate derivatives shows similar values of the activation parameters (Table 5).[4,5] This indicates similar dissociation mechanism including protonation of the ring nitrogen atom, formation of hydrogen bond between the ring nitrogen and pendant arm oxygen atom followed by dissociation of the protonated intermediate.

Table 4. Kinetic parameters for acid-assisted decomplexation of cis-**I**-[Cu**L**^{2}]

Parameter	T = 60 °C	T = 70 °C	T = 80 °C	T = 90 °C
$^{d}k_1$ [s^{-1}]	$(2.59 \pm 0.04) \cdot 10^{-3}$	$(6.2 \pm 0.2) \cdot 10^{-3}$	$(1.42 \pm 0.03) \cdot 10^{-2}$	$(2.88 \pm 0.06) \cdot 10^{-2}$
K [M s^{-1}]	1.92 ± 0.07	1.6 ± 0.1	1.45 ± 0.06	1.5 ± 0.1

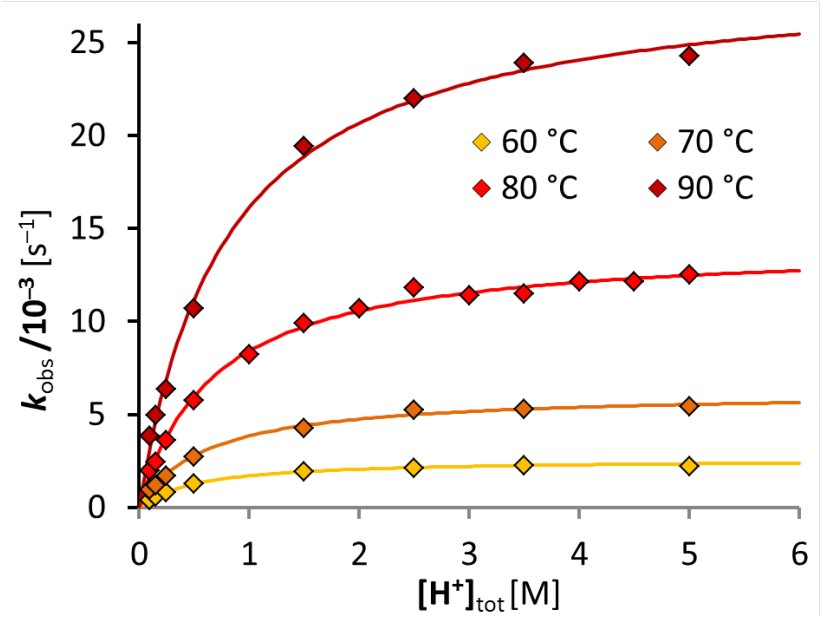

Figure 9. Acid-assisted dissociation of *cis*-**I**-[Cu**L**^{2}] dissociation rate (I = 5 M [H, Na]ClO$_4$).

Table 5. Activation thermodynamic parameters of the acid-assisted dissociation of *cis*-**I**-[CuH**L**^{2}] and related complexes.

Parameter	*cis*-**I**-[CuH**L**^{2}]	*cis*-**I**-[Cu**te2P**^{1,8}][5]	*cis*-**I**-[Cu**Me$_2$te2P**^{1,8}][4]
E_A [kJ mol^{-1}][a]	81 ± 1	72.0; 85[d]	60
$\Delta H^{\#}$ [kJ mol^{-1}][b]	78 ± 1	69.5; 82[d]	57
$\Delta S^{\#}$ [J K^{-1} mol^{-1}][b]	– 61 ± 2	– 71; – 52[d]	– 95
ΔH [kJ mol^{-1}][c]	– 13.6 ± 0.7	– 8.3	– 17
ΔS [J K^{-1} mol^{-1}][c]	– 36 ± 2	– 22.7	– 30

[a] Arrhenius model ln $^{d}k = -(E_A/RT) + \ln A$; [b] Eyring model ln $(^{d}k/T) = -(\Delta H^{\#}/RT) + \Delta S^{\#}/R) + \ln (k_B/h)$; [c] ln $K = -(\Delta H/RT) + \Delta S/R)$; [d] Data of two dissociation pathways.

To get direct comparison of kinetic inertness of both [Cu**L**^{2}] isomers (*cis*-**I** and *trans*-**III**) with related complexes dissociation was studied at 90 °C in 5.0 M $HClO_4$ or 5.0 M HCl and with initial complex concentration c_{ML} = 0.1 mM or 1.0 mM (Table 6). The results show negligible role of complex concentration and important role of the anions present in the solution. In the presents of chlorides dissociation is 5 – 20 times faster. This indicates coordination chlorides to the metal ion accelerating the dissociation process. The half-lives of *trans*-**III** isomer are almost two orders of magnitude longer than those found for *cis*-**I** isomer. It is necessary to mention that *trans*-**III** dissociation more-likely involves also the isomerisation step and consequent dissociation of *cis*-**I** isomer. The spectra obtained during isomerisation experiments at low H^+ concentration have shown shift of the absorption band maximum and presence of blue *cis*-**I** isomer was confirmed by TLC analysis. However, the simultaneously proceeding isomerisation and dissociation of both species disable detailed characterization of the mechanism.

The higher stability of *trans*-**III** isomer in comparison with *cis*-**I** isomer has been previously observed for **te2P** derivatives; however, their half-lives are significantly longer than those found for *trans*-**III**-[Cu**L**^{2}] complex. The lower kinetic inertness of the *trans*-**III**-[Cu**L**^{2}] complex is more likely result of coordination of the phosphinate group that shows lower negative charge and worse coordination abilities when compared with phosphonates. Furthermore, the studied trans-**III** isomers of **te2P** derivatives have octahedral coordination sphere formed by four ring-nitrogen atoms and two phosphonate pendants. Due to absence of one pendant arm, ligand H_3**L**^{2} cannot saturate octahedral coordination sphere in the trans-**III** isomer. This leads to a decreased kinetic inertness. However, kinetic inertness of the studied complexes is more than sufficient for potential application in molecular imaging.

Table 6. Dissociation half-lives of both [Cu**L**^{2}] isomers and related complexes in $HClO_4$ or HCl aq. solutions (c_{H+} = 5.0 M, 90 °C).

	c_{ML} [mM]	$t_{½}$ (in $HClO_4$)	$t_{½}$ (in HCl)
cis-**I**-[Cu**L**^{2}]	0.1	28.6 ± 0.3 s	7.1 ± 0.2 s
cis-**I**-[Cu**L**^{2}]	1.0	26.9 ± 0.8 s	6.4 ± 0.1 s
trans-**III**-[Cu**L**^{2}]	0.1	62.8 ± 0.4 min	3.92 ± 0.04 min
trans-**III**-[Cu**L**^{2}]	1.0	67 ± 5 min	3.84 ± 0.09 min
trans-**III**-[Cu**te2P**^{1,8}][5]	0.3	≈ 37 h	≈ 37 s

Thermodynamic Properties

Acid-base properties of ligands and thermodynamic stability of the complexes were studied by potentiometry. Both ligands show two basic protonation constants that correspond to the protonation of ring nitrogen atoms (Table 7 and S1). The third protonation constant of ligand H_3**L**^{2} describes the first protonation of the terminal phosphonate group. Remaining protonation constants are strongly acidic and they correspond to the protonation of phosphinates and phosphonates. Basicity of ring nitrogen atom is comparable to those found for carboxylate and phosphonate derivatives (Table 7).This is somewhat surprising, as presence of methylphosphinate pendant arm on the macrocycle mostly results in decreased nitrogen basicity. It indicates that the second (terminal) methylphosphinate or methylphosphonate group play important role in the electronic properties of the pendant arms.

Table 7. Protonation constants pK_a of the title compounds and related ligands (25 °C, I = 0.1 M KNO_3) and stability constants of their Cu(II) complexes.

Constant	**H_2L^1**	**H_3L^2**	**cyclam**[10]	**H_2teP** [6c]	**H_4te2P^{1,8}** [11]
pK_1	12.18	12.88	11.29	12.49	nd[a]
pK_2	10.75	11.68	10.19	11.76	*26.41*[b]
pK_3	2.94	7.12	1.61	6.05	6.78
pK_4	1.61	3.17	1.91	2.42	5.36
pK_5	–	1.84	–	*2.16*[b]	1.15
log$K_{[CuL]}$	25.83	27.66	27.20	27.34	25.40

[a] nd – not determined. [b] Values in italics correspond to the protonation over two steps.

Complexation of Cu(II) and Zn(II) ions is rather fast and, so, the in cell titration method could be performed for determination of the complex stability. This is not the case of Ni(II) ions, and, thus, the out of cell equilibrium method had to be used in this case. The results show that both ligands exhibit high stability of Cu(II) complexes and high selectivity when compared to Zn(II) and Ni(II) ions (Table 8 and S2). Due to high complex stability Cu(II) complex is formed already under acidic conditions and, so, around 80% of Cu(II) ions is complexed at the beginning of titration at pH = 1.5. The short time-range at low temperature indicate that the presented stability constant correspond to the complex with *cis*-**I** conformation. As the terminal phosphonate/ phosphinate group is not coordinated it can undergo protonation and, so, the protonation constants of the complexes are in the range typical for phosphonates and phosphinates. In the case of Cu(II) complexes, coordination of the pendant arm is somewhat weakened by Jahn-Teller distortion and, thus, hydroxido complexes are formed in strongly alkaline solutions. The value of the Cu(II) complex stability of cyclam derivatives is mainly given by basicity of ring nitrogen atoms. In the case of title ligands, the high nitrogen basicity results in high Cu(II) complex stability that is comparable with those found for other cyclam derivatives (Table 7).

Table 8. Stability constants log*K* of the studied complexes (25 °C, I = 0.1 M KNO_3).

	Cu^{2+}		Zn^{2+}		Ni^{2+}	
	H_2L^1	**H_3L^2**	**H_2L^1**	**H_3L^2**	**H_2L^1**	**H_3L^2**
M + L ↔ [ML]	25.83	27.66	18.12	19.84	21.94	24.01
[ML] + H ↔ [M(HL)]	–	6.97	3.74	7.17	2.04	6.61
[M(HL)] + H ↔ [M(H_2L)]	–	1.66	–	3.68	–	–
[ML] + OH ↔ [ML(OH)]	12.26	12.63	–	–	–	–

Adsorption Experiments

The limiting factor for the application of phosphonate complexes in molecular imaging is their binding to bone tissue. To evaluate binding properties of the studied complexes aqueous suspension of hydroxyapatite was used as a model of bone tissue. All complexes showed negligible adsorption under conditions that lead to complete adsorption of macrocyclic complexes of similar size bearing bis(phosphonate) group (Figure S5).[12] This indicates that both, bis(phosphinate) and phosphinato-phosphonate moiety might have negligible sorption on bones and, thus, they are suitable pendant arms for biomedical applications.

Experimental

General:

The commercially available chemicals had synthetic purity and were used as received. ^{1}H, ^{13}C, and 2D NMR (H,H-COSY, H,C-HSQC and H,C-HMBC) spectra were recorded on Bruker Avance III 600 MHz spectrometer equipped with the triple resonance cold probe and were referenced to literature.[13] The ^{31}P NMR spectra were recorded on Varian NMR System (Agilent, Santa Clara, CA, USA) operating at 300 MHz proton frequency with ASW probe and with 85% H_3PO_4 as an external reference (δ = 0.00 ppm). The NMR spectra were recorded at 25 °C. Chemical shifts δ are given in ppm scale and the coupling constants J in Hz. The ESI-MS spectra were recorded on Bruker Esquire 3000 spectrometer.

Electronic spectra: In UV-Vis characterization of the complexes, the adsorption peaks are presented in format λ_{max} (ε). The wavelengths λ_{max} are given in nm scale and molar absorption coefficients ε are given in $mol^{-1}\,dm^3\,cm^{-1}$ scale. The stock solutions of the complexes for this purpose were analyzed with AAS. The resulting copper abundance (obtained in $mg_{Cu}\ L^{-1}$) was used for precise determination of complex concentration in each solution sample. Spectra of UV and Vis region can be found in Figure S6. Classification of the cyclam ring conformation in complexes was adopted from the literature.[14,15]

Thin-layer chromatography: Merck aluminum foils with silica gel 60 F_{254} were used for TLC. For the analysis of the copper(II) complexes, 2D TLC techniques was used for determination of species stability in used mobile phase. Analysis was done on square-shaped TLC plate. After the first run, the mobile phase was carefully evaporated by flow of air and the analysis was repeated on the same plate 90° rotated (in the same mobile phase). In this setup, diagonal spots are stable in examined mobile phase.

Synthesis

Ligand H_2L^1: To an ice bath cooled flask with cyclam (11.2 g; 55.7 mmol) and methylene-bis(phosphinic) acids (4.00 g; 27.8 mmol) was slowly added cold 12 M aq. HCl (650 mL). After the end of exothermic reaction, paraformaldehyde (422 mg; 14.1 mmol) was added in one portion and the flask was quickly closed by stopper. The resulting suspension was then stirred at 80 °C overnight. After cooling to RT, the reaction mixture was evaporated to dryness and further co-evaporated several times with H_2O. The crude product was purified on strong anion exchange resin (DOWEX 1; ≈ 250 mL; OH^--form; H_2O → 10% aq. AcOH). Unreacted cyclam was eluted with H_2O and crude product was eluted with acetic acid. Acetate fraction

was evaporated to dryness and several times co-evaporated with H_2O and the residue was purrified on strong cation exchange resin (DOWEX 50; ≈ 250 mL; H^+-form; H_2O → 10% aq. pyridine). Unreacted methylene bis(phosphinic) acid was eluted with H_2O and the product was eluted with pyridine. Pyridine fraction was evaporated to dryness and co-evaporated several times with H_2O. Resulting colorless residue was then dried several days on vacuum pump at 80 °C and the solid was further dried in vacuum desiccator over P_2O_5. Product was obtained as fine white hygroscopic powder (3.95 g; 73 %). **Elem. anal.** Calcd. for $C_{12}H_{30}N_4O_4P_2 \cdot 1.5H_2O$ (M_r = 383.4): C, 37.6; H, 8.7; N, 14.6. Found: C, 37.9; H, 8.8; N, 14.3. NMR (LiOD, pD = 13): **^{1}H** δ 1.72 (CH_2—C*H*$_2$—CH_2, p, 2H, $^3J_{HH}$ = 5 Hz); 1.76 (CH_2—C*H*$_2$—CH_2, p, 2H, $^3J_{HH}$ = 5 Hz); 2.07 (C*H*$_2$—PH, t, 2H, $^2J_{HP}$ = 17 Hz); 2.65–2.80 (N—C*H*$_2$—P, cycle, 18H, m); 7.17 (*PH*, d, 1H, $^1J_{HP}$ = 530 Hz); **^{13}C**{^{1}H} δ 25.5 (CH_2—*C*H_2—CH_2, s); 27.0 (CH_2—*C*H_2—CH_2, s); 35.6 (C*H*$_2$—PH, t, $^1J_{CP}$ = 76 Hz); 46.2 (cycle, s); 46.3 (cycle, s); 46.8 (cycle, s); 47.0 (cycle, s); 48.9 (cycle, s); 54.5 (cycle, s); 54.6 (cycle, s); 55.2 (N—CH_2—P, d, $^1J_{CP}$ = 109 Hz); **^{31}P** δ 18.9 (*P*H, dtd, 1P, $^1J_{PH}$ = 530 Hz, $^2J_{PH}$ = 18 Hz, $^2J_{PP}$ = 5 Hz); 32.9 (*P*—CH_2—N, m, 1P). **ESI-MS** *m/z* **(–):** 355.6 $[M–H]^-$; **(+):** 357.9 $[M+H]^+$; 395.7 $[M+K]^+$. **TLC** (SiO_2, EtOH–NH_4OH 1:1)**:** R_f = 0.7.

Ligand H_3L^2: Hot solution of $HgCl_2$ (1.63 g; 6.00 mmol) in H_2O (30 mL) was added to the solution of $H_2\mathbf{L^1} \cdot 1.5H_2O$ (1.47 g; 3.83 mmol) in 1% aq. HCl (30 mL) and the mixture was stirred at 60 °C overnight. After cooling to RT, precipitated Hg_2Cl_2 was carefully removed by filtration and washed with H_2O. The filtrate was saturated with H_2S and the precipitated HgS was filtered off and washed with H_2O. The colorless filtrate was evaporated to dryness and the residue was purified on strong anion exchange resin (DOWEX 1; ≈ 100 mL; OH^--form; H_2O → 10% aq. AcOH). Acetate fraction was evaporated to dryness and several times co-evaporated with H_2O and the residue was purrified on strong cation exchange resin (DOWEX 50; ≈ 100 mL; H^+-form; H_2O → 10% aq. pyridine). Pyridine fraction was evaporated to dryness and co-evaporated several times with H_2O.Resulting colorless residue was then dried several days on vacuum pump at 80 °C and the solid was further dried in vacuum desiccator over P_2O_5. Product was obtained as fine white hygroscopic powder (1.34 g; 90 %). **Elem. anal.** Calcd for $C_{12}H_{30}N_4O_5P_2 \cdot H_2O$ (M_r = 390.4): C, 37.0; H, 8.3; N, 14.2. Found: C, 37.3; H, 8.6; N, 13.9. NMR (LiOD, pD = 13): **^{1}H** δ 1.74 (CH_2—C*H*$_2$—CH_2, p, 2H, $^3J_{HH}$ = 5 Hz); 1.87 (CH_2—C*H*$_2$—CH_2, p, 2H, $^3J_{HH}$ = 5 Hz); 1.92 (C*H*$_2$—PH, t, 2H, $^2J_{HP}$ = 17 Hz); 2.66 (cycle, m, 2H); 2.72–2.90 (N—C*H*$_2$—P, cycle, 16H, m); **^{13}C**{^{1}H} δ 24.4 (CH_2—*C*H_2—CH_2, s); 27.1 (CH_2—*C*H_2—CH_2, s); 33.1 (P —*C*H_2—P, dd, $^1J_{CP}$ = 116 Hz, $^1J_{CP}$ = 79 Hz); 45.3 (cycle, s); 46.1 (cycle, s); 46.6 (cycle, s); 46.9 (cycle, s); 49.2 (cycle, s); 49.7 (cycle, s); 54.1 (N—CH_2—P, d, $^1J_{CP}$ = 106 Hz); 54.8 (*C*H_2—N—CH_2—P, d, $^3J_{CP}$ = 11 Hz); 55.3 (cycle, s); **^{31}P**{^{1}H} δ 12.8 (HO—*P*—OH, d, 1P, $^2J_{PP}$ =

7 Hz); 36.2 (*P*—CH_2—N, d, 1P, $^2J_{PP}$ = 7 Hz). **ESI-MS** *m/z* **(+):** 373.3 $[M+H]^+$; 395.2 $[M+Na]^+$; 411.2 $[M+K]^+$. **TLC** (SiO_2, EtOH–NH_4OH 1:1)**:** R_f = 0.4.

Complex *cis*-I-[CuL¹]: To a solution of ligand H_2**L¹** (138 mg; 360 μmol) in H_2O (4 mL) was added solution of pyridine (10 %, 3 mL). Solid $Cu(OAc)_2 \cdot H_2O$ (104 mg; 521 μmol) was added and the mixture was carefully evaporated to dryness and further co-evaporated several times with H_2O (the temperature of bath was not raised above 35 °C). Residue was purrified on weak cationic exchange resin (Amberlite CG50; H^+-form; ≈ 20 mL; elution with H_2O). Fractions with product were combined and evaporated to dryness. The dark blue oily residue was and dissolved in H_2O (100 mL) and subsequently lyophilized. The resulting solid product was further dried in vacuum desiccator over P_2O_5. Product was obtained as dark blue hygroscopic powder (108 mg; 64 %). **Elem. anal.** Calcd for $C_{12}H_{28}N_4O_4P_2Cu \cdot 3H_2O$ (M_r = 471.9): C, 30.5; H, 7.3; N, 11.9. Found: C, 30.8; H, 7.0; N, 11.8. **2D TLC** (SiO_2, *i*-PrOH–NH_4OH–H_2O 7:3:3)**:** R_f = 0.6 (blue spot). **ESI-MS** *m/z* **(–):** 415.6 $[M-H]^-$; 451.6 $[M+Cl]^-$; **(+):** 417.8 $[M+H]^+$; 439.8 $[M+Na]^+$; 455.7 $[M+K]^+$. **UV/Vis** (H_2O, pH = 7.4)**:** 270 ($5.6 \cdot 10^3$); 590 ($1.5 \cdot 10^2$).

Complex *cis*-I-[CuL²]: To a solution of ligand H_3**L²** (216 mg; 553 μmol) in H_2O (6 mL) was added solution of pyridine (10 %, 4 mL). Solid $Cu(OAc)_2 \cdot H_2O$ (159 mg; 797 μmol) was added and the mixture was carefully evaporated to dryness and further co-evaporated several times with H_2O (the temperature of bath was not raised above 35 °C). Residue was purrified on weak cationic exchange resin (Amberlite CG50; H^+-form; ≈ 20 mL; elution with H_2O). Fractions with product were combined and evaporated to dryness. The dark blue oily residue was dried on vacuum pump for 1d at 35 °C and the resulting solid was further dried in vacuum desiccator over P_2O_5. The product was obtained as dark blue hygroscopic powder (195 mg; 78 %). **Elem. anal.** Calcd for $C_{12}H_{28}N_4O_5P_2Cu \cdot 2H_2O$ (M_r = 469.9): C, 30.7; H, 6.9; N, 11.9. Found: C, 30.5; H, 6.6; N, 11.9. **2D TLC** (SiO_2, *i*-PrOH–NH_4OH–H_2O 7:3:3)**:** R_f = 0.3 (blue spot). **ESI-MS** *m/z* **(–):** 431.6 $[M-H]^-$; 467.6 $[M+Cl]^-$; **(+):** 433.8 $[M+H]^+$; 455.8 $[M+Na]^+$; 471.7 $[M+K]^+$. **UV/Vis** (H_2O, pH = 7.4)**:** 270 ($5.6 \cdot 10^3$); 590 ($1.4 \cdot 10^2$).

Complex *trans*-III-[CuL¹]: Solution of $CuCl_2$ (101.8 mM; 6.29 mL; 640 μmol) was added to a ligand H_2**L¹** (246 mg; 642 μmol). Then, aq. solution of NaOH (2 M; 15 mL; to reach pH ≈ 12–13) was added and the mixture was stirred 1 h at RT. The resulting solution (containing mixture of *cis*-**I** Cu**L¹**] and *trans*-**III**-[Cu**L¹**] in ratio ≈ 4:1; monitored by TLC) was then evaporated to dryness and the residue was purrified by column chromatography SiO_2; ≈ 250 g; *i*-PrOH–NH_4OH–H_2O 7:3:3, R_f (*trans*-**III**-[Cu**L¹**]) = 0.5). Fraction with product were combined, carefully concentrated and purified on weak cationic exchange resin (Amberlite CG50; H^+-form; ≈ 100 mL; elution with H_2O). Fractions with product were combined,

carefully concentrated and lyophilized. The resulting solid was further dried in vacuum desiccator over P_2O_5. Product was obtained as dark violet hygroscopic powder (106 mg; 35 %). **Elem. anal.** Calcd for $C_{12}H_{28}N_4O_4P_2Cu{\cdot}0.5NH_3{\cdot}2.5H_2O$ (M_r = 471.4): C, 30.6; H, 7.4; N, 13.4. Found: C, 30.2; H, 7.1; N, 13.1. **2D TLC** (SiO_2, *i*-PrOH–NH_4OH–H_2O 7:3:3)**:** R_f = 0.5 (violet spot). **ESI-MS** *m/z* **(–):** 415.6 $[M–H]^-$; 451.6 $[M+Cl]^-$; **(+):** 417.8 $[M+H]^+$; 439.8 $[M+Na]^+$; 455.7 $[M+K]^+$. **UV/Vis** (H_2O, pH = 7.4)**:** 265 ($6.3{\cdot}10^3$); 535 ($1.2{\cdot}10^2$).

Complex *trans*-III-[CuL²]: Solution of $CuCl_2$ (101.8 mM, 5.72 mL; 582 μmol) was added to a ligand H_3**L²** (249 mg; 638 μmol). Then, aq. solution of NaOH (2 M; 15 mL; to reach pH ≈ 12–13) was added and the mixture was stirred 1 h at RT. The resulting solution (containing mixture of *cis*-**I** Cu**L²**] and *trans*-**III**-[Cu**L²**] in ratio ≈ 4:1; monitored by TLC) was then concentrated and purified by column chromatography (SiO_2; ≈ 200 g; *i*-PrOH–NH_4OH–H_2O 7:3:3, R_f (*trans*-**III**-[Cu**L²**]) = 0.2). Fraction containing the product was carefully concentrated and purified on strong cationic exchanger (DOWEX50; ≈ 50 mL; pyridine$^+$-form; H_2O). Resulting solution was carefully concentrated and purrified on weak cationic exchange resin (Amberlite CG50; H^+-form; ≈ 100 mL; elution with H_2O). Fractions with product were combined, carefully concentrated and lyophilized. The resulting solid was further dried in vacuum desiccator over P_2O_5. Product was obtained as dark violet hygroscopic powder (126 mg; 43 %). **Elem. anal.** Calcd for $C_{12}H_{28}N_4O_5P_2Cu{\cdot}3.5H_2O$ (M_r = 496.9): C, 29.0; H, 7.1; N, 11.3. Found: C, 28.6; H, 6.7; N, 11.1. **2D TLC** (SiO_2, *i*-PrOH–NH_4OH–H_2O 7:3:3)**:** R_f = 0.2 (violet spot). **ESI-MS** *m/z* **(–):** 431.6 $[M–H]^-$; 467.6 $[M+Cl]^-$; **(+):** 433.8 $[M+H]^+$; 455.8 $[M+Na]^+$; 471.7 $[M+K]^+$. **UV/Vis** (H_2O, pH = 7.4)**:** 265 ($6.1{\cdot}10^3$); 535 ($1.2{\cdot}10^2$).

Potentiometry

Methodology of the potentiometric titrations and processing of the experimental data were analogous to those previously reported.[16] Titrations were carried out in a vessel thermostatted at 25 ± 0.1 °C at ionic strength I = 0.1 M KNO_3. Ligand-to-metal ratio was 1:1 with c_L = 0.004 M, pH range was 1.7–12. Titrations were carried out at least three times, each consisting of about 40 points. The water ion product, pK_w = 13.78, and stability constants of M(II)–OH^- systems were taken from ref.[17] The protonation constants β_n calculated are concentration constants and are defined by $\beta_n = [H_nL] / ([H]^n \times [L])$ ($\log K_1 = \log\beta_1$; $\log K_n = \log\beta_n - \log\beta_{n-1}$). The stability constant are defined by $\beta_{hlm} = [M_mH_hL_l] / [M]^m \times [H]^h \times [L]^l$. The constants (with standard deviations) were calculated with program OPIUM.[18] Through the paper, pH means $-\log[H^+]$.

The stability constants of the Ni(II) complexes were obtained by the out-of-cell "equilibrium" method. The batches (starting volume 1 mL) were prepared under Ar stream in

tubes with ground joints from ligand, metal ion and HNO_3/KNO_3 stock solutions and water (M : L = 0.95 : 1 molar ratio, c_L = 0.004 M). Then a known amount of KOH standard solution was added under Ar. The tubes were firmly closed with stoppers and ampoules were flame-sealed and the solutions were equilibrated at room temperature for four weeks. Titrations were performed in the pH range 1.8–7 (final pH values) with around 20 data points per whole titration and three titrations per system.

Formation kinetics

Experiments were performed on Bio Sequential SX-20 Stopped Flow Spectrophotometer (Applied Photophysics, Leatherhead, UK) equipped with 150 W xenon lamp and with diode-array accessory. The measurements were done at T = 25 ± 0.1 °C, at ionic strength I = 0.1 M KCl and at the pH range 2.2–6.4. Fifty-fold molar excess of appropriate buffers were used (chloroacetate, acetate and MES) to buffer stock solutions of ligands. Aqueous solutions of $CuCl_2$ were used as source of copper(II) ions. The spectra were recorded in the in the range of λ = 200–800 nm. Experiments were run at c_L = 0.1 mM for measurements in UV region or at c_L = 0.1 mM for Vis region. Changes in the intensity of the CT band of the complexes at λ = 300 or 590 nm with time were used for fitting. Data were fitted by Pro-KII software (Applied Photophysics).

Dissociation kinetics

Experiments were run on diode-array spectrophotometer HP 8453A (Agilent, Santa Clara, CA, USA) equipped with thermoregulator. The measurements were done at ionic strength I = 5.0 M in either (H, Na)ClO_4 or (H, Na)Cl and in the temperature range T = 60–90 ± 0.1°C. For measurements in UV region, experiments were run at c_{ML} = 1.0 mM and the spectra were recorded in the range of λ = 250–350 nm. For measurements in Vis region experiments were run at c_{ML} = 5.0 mM and with range of λ = 300–1000 nm was used. Following wavelengths were used for fitting: *cis*-**I** isomers λ = 270 or 590 nm; *trans*-**III** isomer λ = 270 or 535 nm.

Isomerisation kinetics

Experiments were run on Varian Cary 50 UV-Vis Spectrophotometer (Agilent, Santa Clara, CA, USA), equipped with thermoregulator. The measurements were done at T = 25 ± 0.1 °C, initial concentration of complexes c_{ML} = 5.0 mM in the [OH^-] range 20–100 mM. If not stated otherwise, the experiments were done at ionic strength I = 0.5 M K(OH, Cl) or I = 0.5 M

K(OH, NO_3). The spectra were recorded in the range of λ = 500–700 nm. For the determination of isomerisation constants, changes in intensity of the d–d bands at 650 nm were used for fitting.

Adsorption Experiments

Hydroxyapatite was purchased from Fluka (catalogue number 55496; specific surface area 73 $m^2 \cdot g^{-1}$). In a four 4-mL glass vials, HA (0–50 mg) was suspended in the HEPES buffer solution (V = 3 mL, pH 7.4; c = 100 mM) containing the compound under study (c = 1.0 mM). The suspensions were gently shaken at 25 °C for 72 h and then filtered through a Millipore filter (Rotilabo®-syringe filter; PVDF; 0.22 μm). Amount of the complex remaining in the supernatant was determined by UV-Vis spectrometry at wavelength λ_{max} = 590 nm (*cis*-**I** isomers) or λ_{max} = 535 nm (*trans*-**III** isomer).

Conclusion

The studied cyclam derivatives bearing bis(phosphinate) or phosphinato-phosphonate pendant arms show high amine basicity, high stability of complexes with divalent transition metal ions and high selectivity for copper(II) ion. The ligands show significantly increased rate of copper(II) complexation when compared with non-substituted or acetate-substituted macrocycles. Further, none of the studied compounds was found to show measurable hydroxyapatite sorption and, so, negligible bone uptake *in vivo* could be expected. The extremely fast complex formation is result of the ligand coordination properties – presence of weakly coordinating bis(phosphinate) or phosphinato-phosphonate pendant arm forming an ”out-of cage” complex. All these facts indicate that the studied macrocyle derivatives are promising for complexation of copper isotopes and, consequent, utilization of complexes in nuclear medicine.

Acknowledgement

Support from the Grant Agency of the Czech Republic (P207/10/P153), from the Long Term Research Plan of the Ministry of Education of the Czech Republic (No. MSM0021620857) and Grant Agency of Charles University (No. 310011) is acknowledged. The work was conducted in the framework of the TD1004 and CM0802 COST Actions. We thank Laboratory of Molecular Structure Characterization (Academy of Science of the Czech Republic) for performing HMRS measurements.

References

[1] a) D. E. Reichert, J. S. Lewis, C. J. Anderson *Coord. Chem. Rev.* **1999**, *184*, 3–66; b) Wadas, T. J.; Wong, E. H.; Weisman, G. R.; Anderson, C. J.: *Chem. Rev.* **2010**, *110*, 2858–2902.

[2] P. J. Blower, J. S. Lewis, J. Zweit *Nucl. Med. Biol.* **1996**, *23*, 957–980.

[3] a) M. D. Bartolomä *Inorg. Chim. Acta* **2012**, *389*, 36–51; b) R. E. Mewis, S. J. Archibald *Coord. Chem. Rev.* **2010**, *254*, 1686–1712.

[4] I. Svobodová, J. Havlíčková, J. Plutnar, P. Lubal, J. Kotek, P. Hermann *Eur. J. Inorg. Chem.* **2009**, *24*, 3577–3592.

[5] J. Kotek, P. Lubal, P. Hermann, I. Císařová, I. Lukeš, T. Godula, I. Svobodová, P. Táborský, J. Havel, J. *Chem. Eur. J.* **2003**, *9*, 233–248.

[6] a) P. Lubal, J. Maleček, P. Hermann, J. Kotek, J. Havel *Polyhedron* **2006**, *25*, 1884–92; b) P. Lubal, M. Kývala, P. Hermann, J. Holubová, J. Rohovec, J. Havel, I. Lukeš *Polyhedron* **2001***, 20*, 47–55; c) S. Füzerová, J. Kotek, I. Císařová, P. Hermann, K. Binnemans, I. Lukeš *Dalton Trans.*, **2005**, 2908–15.

[7] M. Meyer, V. Dahaoui-Gindrey, Claude Lecomte, Roger Guilard *Coord. Chem. Rev.* **1998**, *178–180*, 1313–1405.

[8] (a) Wu, S.-L.; Horrocks, W.DeW. *Inorg. Chem.* **1995**, *3*, 3724–3732; (b) Moreau, J.; Guillon, E.; Pierrard, J.-C.; Rimbault, J.; Port, M.; Aplincourt, M. *Chem. Eur. J.* **2004**, *10*, 5218–5232.

[9] a) E. Matczak-Jon, V. Videnova-Adrabinska *Coord. Chem. Rev.* **2005**, *249*, 2458–2488; b) V. Kubíček, J. Kotek, P. Hermann, I. Lukeš *Eur. J. Inorg. Chem.* **2007**, 333–344; c) T. David, S. Procházková, J. Havlíčková, J. Kotek, V. Kubíček, P. Hermann, I. Lukeš *Dalton Trans.* **2013**, *42*, 2414–2422.

[10] R. D. Hancock, R. J. Motekaitis, J. Mashishi, I. Cukrowski, J. H. Reibenspies, A. E. Martell *J. Chem. Soc., Perkin Trans. 2* **1996**, 1925–1929.

[11] J. Kotek, P. Vojtíšek, I. Císařová, P. Hermann, P. Jurečka, J. Rohovec and I. Lukeš, *Collect. Czech. Chem. Commun.* **2000**, *65*, 1289.

[12] T. Vitha, V. Kubíček, P. Hermann, Z. I. Kolar, H. T. Wolterbeek, J. A. Peters, I. Lukeš *Langmuir* **2008,** *24,* 1952–1958.

[13] H. Gottlieb, V. Kotlyar, A. Nudelman *J. Org. Chem.* **1997**, *62*, 7512-7515.

[14] B. Bosnich, C. K. Poon, M. Tobe *Inorg. Chem.* **1965**, *4*, 1102–1108.

[15] X. Liang, P. J. Sadler *Chem. Soc. Rev.* **2004**, *33*, 246–266.

[16] a) P. Táborský, P. Lubal, J. Havel, J. Kotek, P. Hermann, I. Lukeš *Collect. Czech. Chem. Commun.* **2005**, *70*, 1909–1942; b) M. Försterová, I. Svobodová, P. Lubal, P. Táborský, J. Kotek, P. Hermann, I. Lukeš *Dalton Trans.* **2007**, 535–549; c) V. Kubíček, J. Havlíčková, J. Kotek, G. Tircsó, P. Hermann, É. Tóth, I. Lukeš *Inorg. Chem.* **2010,** *49*, 10960–10969.

[17] C. F. Jr. Baes, R. E. Mesmer, *The Hydrolysis of Cations*, Wiley, New York, 1976.

[18] M. Kývala, I. Lukeš, *International Conference, Chemomotrics '95*, p. 63. Pardubice, Czech Republic, 1995; full version of *"OPIUM"* is available (free of charge) on http://www.natur.cuni.cz/~kyvala/opium.html.